

ERCOFTAC

*Bulletin*

June 2012

91

---

# European Research Community on Flow, Turbulence and Combustion

---

ERCOFTAC is a leading European association of research, education and industry groups in the technology of flow, turbulence and combustion. The main objectives of ERCOFTAC are: To promote joint efforts of European research institutes and industries with the aim of **exchanging technical and scientific information**; to promote **Pilot Centres** for collaboration, stimulation and

application of research across Europe; to stimulate, through the creation of **Special Interest Groups**, well-coordinated European-wide research efforts on specific topics; to stimulate the creation of advanced training activities; and to be influential on funding agencies, governments, the European Commission and the European Parliament.

[www.ercoftac.org](http://www.ercoftac.org)

## Honorary Presidents

Mathieu, J.                      Spalding, D.B.

## Executive Committee

*Chairman*                      Hutton, A.G.  
Airbus UK  
Building 09B  
Bristol BS99 7AR  
United Kingdom  
Tel: +44 117 936 7519  
anthony.hutton@airbus.com

*Deputy Chairman*        Tomboulides, A.  
*Deputy Chairman*        Hirsch, C.  
*Treasurer*                    Duursma, R.P.J.  
*Deputy Treasurer*        Ooms, G.  
*SPC Chairman*              Geurts, B.J.  
*SPC Deputy Chairman*    Von Terzi, D.  
*IPC Chairman*                Geuzaine, P.  
*IPC Deputy Chairman*    Oliemans, R.V.A.  
*Horizon 10 Chairman*    Jakirlic, S.  
*Ind. Engagement Officer* Seoud, R.E.  
*Knowledge Base Editor* Rodi, W.  
*Bulletin Editor*              Elsner, W.  
*Observer*                    Hunt, J.  
*Observer*                    Jacquin, L.  
*Secretary*                    Borhani, N.

## ERCOFTAC Seat of the Organisation

*Director*                      Hirsch, C.  
Numeca International  
Chaussée de la Hulpe 189  
Terhulpesteenweg  
B-1170 Brussels  
Belgium

Tel: +32 2 643 3572  
Fax: +32 2 647 9398  
ado@ercoftac.be

*Secretaries*                    Bongaerts, S.  
stephane.bongaerts@ercoftac.be

Laurent, A.  
anne.laurent@ercoftac.be

## Scientific Programme Committee

*Chairman*                      Geurts, B.J.  
University of Twente  
Mathematical Sciences  
PO Box 217  
NL-7500 AE Enschede  
The Netherlands  
Tel: +31 53 489 4125  
b.j.geurts@utwente.nl

*Deputy Chairman*        Von Terzi, D.

## Industrial Programme Committee

*Chairman*                      Geuzaine, P.  
*Deputy Chairman*        Oliemans, R.V.A.  
*Engagement Officer*    Seoud, R.E.  
ERCOFTAC  
Crown House  
72 Hammersmith Road  
London W14 8TH  
United Kingdom  
Tel: +44 207 559 1430  
Fax: +44 207 559 1428  
richard.seoud-ieo@ercoftac.org

## ERCOFTAC Central Administration and Development Office

ERCOFTAC CADO  
Crown House  
72 Hammersmith Road  
London W14 8TH  
United Kingdom  
Tel: +44 207 559 1427  
Fax: +44 207 559 1428

*CADO Manager and Industrial Engagement Officer*  
Richard Seoud  
Tel: +44 207 559 1430  
Richard.Seoud-ieo@ercoftac.org

# ERCOFTAC Bulletin 91, June 2012

## TABLE OF CONTENTS

### WORKSHOP AND SUMMER SCHOOL REPORTS

<b>2nd UK-Japan Bilateral Workshop and 1st ERCOFTAC Workshop on Turbulent Flows Generated/Designed in Multiscale/fractal Ways: Fundamentals and Applications</b> <i>S. Laizet, Y. Sakai and J.C. Vassilicos</i>	3
<b>Morphology and Dynamics of Anisotropic Flows</b> <i>F. S. Godeferd, L. Danaila and J. Flor</i>	13
<b>New Challenges In Turbulence Research II</b> <i>A. Naso, M. Bourgoïn, A. Pumir and B. Rousset</i>	17
<b>Simulation of Multiphase Flows in Gasification and Combustion</b> <i>C. Hasse, D. Thévenin and L. Vervisch</i>	20
<b>Workshop 'ASTROFLU II' Organized by Henri Bénard. Pilot Center, SIG 4 and SIG 35</b> <i>C. Cambon, A. Pieri and F. S. Godeferd</i>	21

### PILOT CENTRE REPORTS

<b>The France West Pilot Center Report</b> <i>L. Danaila</i>	24
<b>The Germany South Pilot Center Report</b> <i>S. Becker</i>	58

<b>EDITOR</b>	Marek, M.
<b>TECHNICAL EDITOR</b>	Kuban, Ł.
<b>CHAIRMAN</b>	Elsner, W.
<b>EDITORIAL BOARD</b>	Armenio, V. Dick, E. Geurts, B.J.
<b>DESIGN &amp; LAYOUT</b>	Borhani, N. Nichita, B.A.
<b>COVER DESIGN</b>	Aniszewski, W.
<b>SUBMISSIONS</b>	
ERCOFTAC Bulletin Institute of Thermal Machinery Czestochowa University of Technology Al. Armii Krajowej 21 42-201 Czestochowa Poland	
Tel:	+48 34 3250 507
Fax:	+48 34 3250 507
Email:	ercoftac@imc.pcz.czest.pl

HOSTED, PRINTED & DISTRIBUTED BY



CZĘSTOCHOWA UNIVERSITY OF TECHNOLOGY

*The reader should note that the Editorial Board cannot accept responsibility for the accuracy of statements made by any contributing authors*

## NEXT ERCOFTAC EVENTS

### ERCOFTAC Autumn Festival

25<sup>th</sup> October 2012  
Trieste, Italy.

### ERCOFTAC SPC, IPC & MB-GA Meetings

26<sup>th</sup> October 2012  
Trieste, Italy.



# The ERCOFTAC Best Practice Guidelines for Industrial Computational Fluid Dynamics

The Best Practice Guidelines (BPG) were commissioned by ERCOFTAC following an extensive consultation with European industry which revealed an urgent demand for such a document. The first edition was completed in January 2000 and constitutes generic advice on how to carry out quality CFD calculations. The BPG therefore address mesh design; construction of numerical boundary conditions where problem data is uncertain; mesh and model sensitivity checks; distinction between numerical and turbulence model inadequacy; preliminary information regarding the limitations of turbulence models etc. The aim is to encourage a common best practice by virtue of which separate analyses of the same problem, using the same model physics, should produce consistent results. Input and advice was sought from a wide cross-section of CFD specialists, eminent academics, end-users and, (particularly important) the leading commercial code vendors established in Europe. Thus, the final document can be considered to represent the consensus view of the European CFD community.

Inevitably, the Guidelines cannot cover every aspect of CFD in detail. They are intended to offer roughly those 20% of the most important general rules of advice that cover roughly 80% of the problems likely to be encountered. As such, they constitute essential information for the novice user and provide a basis for quality management and regulation of safety submissions which rely on CFD. Experience has also shown that they can often provide useful advice for the more experienced user. The technical content is limited to single-phase, compressible and incompressible, steady and unsteady, turbulent and laminar flow with and without heat transfer. Versions which are customised to other aspects of CFD (the remaining 20% of problems) are planned for the future.

The seven principle chapters of the document address numerical, convergence and round-off errors; turbulence modelling; application uncertainties; user errors; code errors; validation and sensitivity tests for CFD models and finally examples of the BPG applied in practice. In the first six of these, each of the different sources of error and uncertainty are examined and discussed, including references to important books, articles and reviews. Following the discussion sections, short simple bullet-point statements of advice are listed which provide clear guidance and are easily understandable without elaborate mathematics. As an illustrative example, an extract dealing with the use of turbulent wall functions is given below:

- Check that the correct form of the wall function is being used to take into account the wall roughness. An equivalent roughness height and a modified multiplier in the law of the wall must be used.
- Check the upper limit on  $y^+$ . In the case of moderate Reynolds number, where the boundary layer only extends to  $y^+$  of 300 to 500, there is no chance of accurately resolving the boundary layer if the first integration point is placed at a location with the value of  $y^+$  of 100.

- Check the lower limit of  $y^+$ . In the commonly used applications of wall functions, the meshing should be arranged so that the values of  $y^+$  at all the wall-adjacent integration points is only slightly above the recommended lower limit given by the code developers, typically between 20 and 30 (the form usually assumed for the wall functions is not valid much below these values). This procedure offers the best chances to resolve the turbulent portion of the boundary layer. It should be noted that this criterion is impossible to satisfy close to separation or reattachment zones unless  $y^+$  is based upon  $y^*$ .
- Exercise care when calculating the flow using different schemes or different codes with wall functions on the same mesh. Cell centred schemes have their integration points at different locations in a mesh cell than cell vertex schemes. Thus the  $y^+$  value associated with a wall-adjacent cell differs according to which scheme is being used on the mesh.
- Check the resolution of the boundary layer. If boundary layer effects are important, it is recommended that the resolution of the boundary layer is checked after the computation. This can be achieved by a plot of the ratio between the turbulent to the molecular viscosity, which is high inside the boundary layer. Adequate boundary layer resolution requires at least 8-10 points in the layer.

All such statements of advice are gathered together at the end of the document to provide a 'Best Practice Checklist'. The examples chapter provides detailed expositions of eight test cases each one calculated by a code vendor (viz FLUENT, AEA Technology, Computational Dynamics, NUMECA) or code developer (viz Electricité de France, CEA, British Energy) and each of which highlights one or more specific points of advice arising in the BPG. These test cases range from natural convection in a cavity through to flow in a low speed centrifugal compressor and in an internal combustion engine valve.

Copies of the Best Practice Guidelines can be acquired from:

ERCOFTAC CADO  
Crown House  
72 Hammersmith Road  
London W14 8TH, United Kingdom  
Tel: +44 207 559 1429  
Fax: +44 207 559 1428  
Email: Richard.Seoud-ieo@ercoftac.org

The price per copy (not including postage) is:

ERCOFTAC members		
First copy		<i>Free</i>
Subsequent copies		45 Euros
Students		30 Euros
Non-ERCOFTAC academics		
		75 Euros
Non-ERCOFTAC industrial		
		150 Euros

# 2<sup>nd</sup> UK-JAPAN BILATERAL WORKSHOP AND 1<sup>st</sup> ERCOFTAC WORKSHOP ON TURBULENT FLOWS GENERATED/DESIGNED IN MULTISCALE/FRACTAL WAYS: FUNDAMENTALS AND APPLICATIONS

S. Laizet<sup>1</sup>, Y. Sakai<sup>2</sup> and J.C. Vassilicos<sup>1</sup>

<sup>1</sup> Imperial College London, UK

<sup>2</sup> University of Nagoya, Japan

26 and 27 March 2012,  
Department of Aeronautics, Imperial College London

## 1 Introduction

After more than a century of exhaustive research on the aerodynamics and hydrodynamics of geometrically simple shapes, whether streamlined as in wings or bluff as in spheres/cylinders, it is blindingly natural to expect much of the future in fluid mechanics to lie in the aerodynamics and hydrodynamics of geometrically complex, and thereby multiscale, shapes. There has of course been work over the past decades on how to model and simulate complex turbulent flows, but the emphasis here is on working out rules for the design of multiscale objects so as to obtain desired flow effects beneficial for particular applications. The simplest cases of multiscale shapes are fractal, which is why they have been a good start. These are multiscale shapes with complex appearance which can nevertheless be defined with only a few scaling parameters.

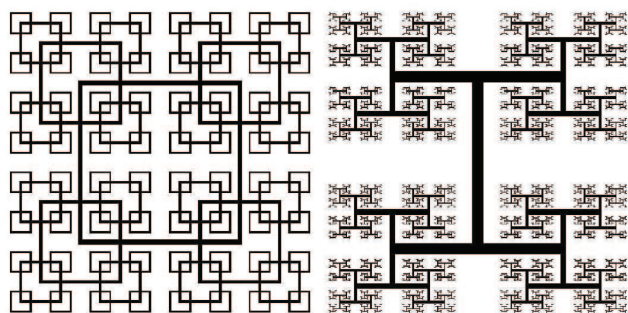


Figure 1: Diagrams of a fractal square grid (left) and a fractal I grid (right)

The primary idea is to interfere with the multiscale dynamics and inner geometry/topography of the turbulence and find out whether qualitatively different types of turbulence can be created. This is where well established research from the 1970s on the importance of initial/boundary conditions in various turbulent flows fits in and gives meaning to the endeavour. If turbulent flows keep some memory of the conditions which generate them then the possibility exists of designing bespoke turbulent flows tailor-made for particular applications. Multiscale/fractal generation/design is about using multiscale/fractal objects (grids, fences, profilers etc) to shape the nature of the resulting turbulent flow over

a broad range of scales for a broad range of applications, such as:

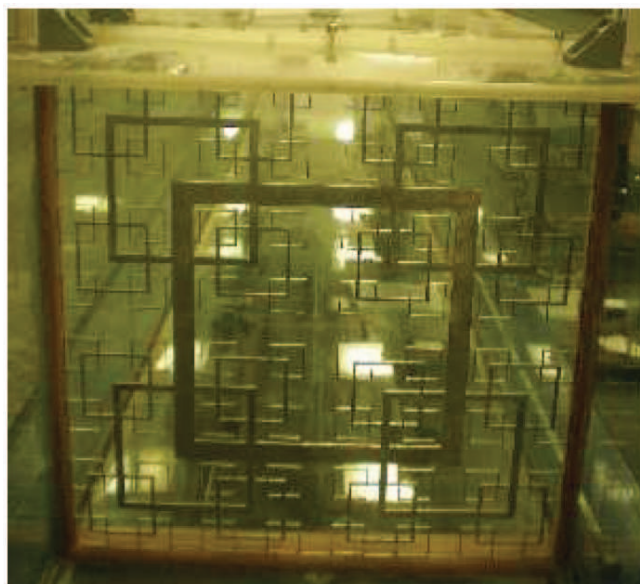


Figure 2: Image showing an experiment in a water tunnel to investigate the mixing and the turbulent properties of the flow generated by a fractal square grid

- Fractal mixers: fractal grids can be used to design turbulent flows with low power losses and high turbulence intensities for intense yet economic mixing over a region of designed length and location (see Figure 2).
- Fractal combustors: the fractal design of a long region of high turbulence intensity and its location are of great interest for premixed combustion and may pave the way for future fractal combustors particularly adept at operating at the lean premixed combustion regime where NO<sub>x</sub> emissions are the lowest. This is even more interesting if it can be achieved with reduced pressure drop and energy losses, as is indeed the case with fractal grids.
- Fractal spoilers and airbrakes can have significantly reduced sound pressure levels without degrading the

lift and drag characteristics of the wing system (see Figure 3).

- Fractal wind breakers and fractal fences: a fractal fence, for example, can have increased resistance because of all its empty areas, yet be an effective fence by modifying the momentum profiles in its lee and thereby forcing deposition of particulates, snow etc where desired.

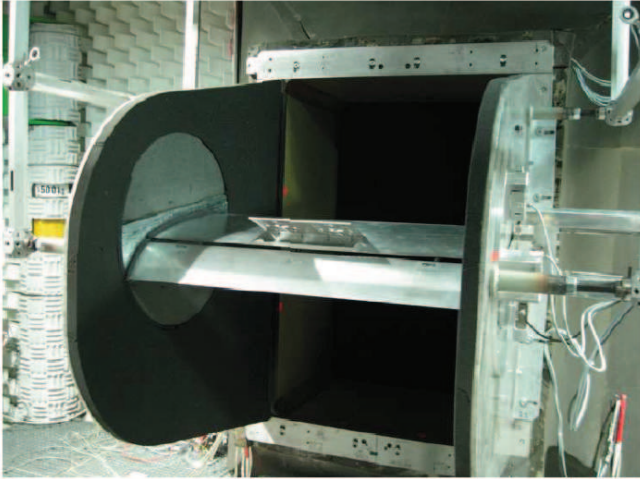


Figure 3: Image showing the back of the three-element wing system, connected at an exhaust nozzle, with one fractal square spoiler

This workshop follows from last year's 1<sup>st</sup> UK-Japan bilateral workshop on the same topic and is supported by the creation in October 2011 of a new ERCOFTAC Special Interest Group on multiscale-generated turbulent flows. The very significant progress in both fundamentals and applications since the 1<sup>st</sup> UK-Japan workshop a year ago was noted by many participants. One of them even said, while chairing a session, how impressed he was to see so many technological potentialities being seriously explored only 13 years after the first ever talk on this new subject. This talk, given by J.C. Vassilicos in June 1999 as part of the 1999 Isaac Newton Institute Turbulence Programme, was reporting fundamental turbulence experiments on fractal-generated turbulent flows which were subsequently published in Queiros-Conde & Vassilicos 2001 [1] and which were shortly followed by the first ever numerical simulations of fractal-generated turbulence by Mazzi et al 2002 [2], i.e. 10 years ago. More information about the 1st UK-Japan bilateral workshop can be found here: <http://www3.imperial.ac.uk/tmfc/conferences>

## 2 Summary

The workshop was divided in eight sessions. About 50 participants attended, some of them from industry.

## 2.1 PIV of grid-generated turbulence

### PIV study of fractal grid turbulence

S. Discetti<sup>1</sup>, I. B. Ziskin<sup>2</sup>, R. J. Adrian<sup>2</sup>, K. Prestridge<sup>3</sup>

<sup>1</sup> DIAS, University of Naples Federico II, Italy

<sup>2</sup> School for Engineering of Matter, Transport and Energy, Arizona State University, USA

<sup>3</sup> Los Alamos National Laboratory, Los Alamos, New Mexico, USA

An experimental investigation of the decay of the wind tunnel turbulence generated by space filling fractal square grids by means of Particle Image Velocimetry (PIV) is described. Measurements of power spectra are intrinsically challenging for PIV and they are particularly demanding in this flow owing to the low turbulence intensity. In addition, large numbers of frames are needed to achieve statistical convergence. Among the quantities obtained from the velocity fields are the Taylor micro-scale, streamwise twopoint correlation functions, measures of anisotropy and energy spectra as functions of position with respect to the inhomogeneous structure of the fractal grid. Three fractal grids have been used, with different thickness ratios (i.e. the ratio between of the largest to the smallest bar thicknesses)  $tr = 8.5, 13$  and  $17$ , respectively and only slightly different blockage ratio  $\sigma$  and effective mesh-length  $M_{eff}$ , calculated as in Hurst and Vassilicos (2007) [3]. The grids are tested in a low turbulence level open circuit wind tunnel, with a  $L = 1,524mm$  long and  $T = 152.4mm$  wide square test section. The residual level of turbulence in absence of the grid is lower than 0.5% along the centerline of the wind tunnel. The tests are conducted for two different Reynolds numbers (based on the mean velocity at the inlet of the test section, and the effective mesh length), namely about 3,500 and 12,000. The evolution of the generated structures is evaluated by placing the PIV system at different downstream positions, and measuring over 5,000 realizations at each location. The history of the statistical convergence shows faster convergence of the streamwise component of the velocity (the average value changes of less than 1% after 200 realizations), while the noise effect is much stronger on the mean squared fluctuation (more than 400 samples are needed to reduce the variations below 3%). The measured velocity fields are analysed to extract information about the turbulence statistics. The availability of two-dimensional two-component velocity data enables the possibility to perform a number of anisotropy tests, and the high resolution of the adopted PIV makes it possible to measure scales of the order of 10 Kolmogorov lengthscales. As observed by Mazellier and Vassilicos (2010) [4], quite surprisingly, even in absence of the dissipation anomaly, the 1D longitudinal energy spectrum is proportional to  $k^{-5/3}$  in a wide region of wavenumbers. Furthermore the spectra show an excellent collapse if the mean squared streamwise fluctuations and the Taylor lengthscale are considered as scaling parameters, in agreement with the single-length scale self-preserving energy spectra model by George (1992) [5].

## PIV study of turbulence generated by fractalgrids in a water tunnel

R. Gomes Fernandes<sup>1</sup>, B. Ganapathisubramani<sup>2</sup>,  
J.C. Vassilicos<sup>1</sup>

<sup>1</sup> Department of Aeronautics, Imperial College London, UK

<sup>2</sup> Department of Engineering Science, University of Southampton

An experimental investigation involving space-filling fractal square grids is presented. The flow is documented using Particle Image Velocimetry (PIV) in a water tunnel as opposed to previous experiments which mainly used hot-wire anemometry in wind tunnels. The experimental facility has the particularity of having a non-negligible incoming free-stream turbulence (with 2.8 and 4.4 % in the streamwise ( $u'/U$ ) and spanwise ( $v'/U$ ) directions, respectively) which presents a challenge in terms of comparison with previous wind tunnel results. An attempt to characterize the effects of the incoming free-stream turbulence in grid turbulence flow is made and an improved wake interaction length scale is proposed which enables the comparison of the present results with previous ones. This length scale also proves to be a good estimator of the turbulence intensity peak location. Furthermore, a new turbulence intensity normalisation capable of collapsing  $u'/U$  for various grids in various facilities is proposed. Comparison with previous experiments indicate good agreement in turbulence intensities, Taylor microscale as well as various other quantities, if the improved wake interaction length scale is used. Global and local isotropy of fractal-generated turbulence is assessed using the velocity gradients of the two-component (2C) 2D PIV and compared with regular grid results. Finally, the PIV data appears to confirm the new dissipation behaviour previously observed in hot-wire measurements.

## Scaling of turbulence statistics in the wake of conventional grids with different blockage ratios

J.I. Cardesa, J.R. Dawson

Engineering Department, Cambridge University, UK

We present measurements of grid turbulence using 2D particle image velocimetry (PIV) taken immediately downstream from the grid at a Reynolds number of  $Re_M = 16,500$  where  $M$  is the rod spacing. A long field of view of  $14M \times 4M$  in the downand cross-stream directions was achieved by stitching multiple cameras together. Two uniform biplanar grids were selected to have the same  $M$  and pressure drop but different rod diameter  $D$  and cross-section. A large data set (104 vector fields) was obtained to ensure good convergence of second order statistics. Estimations of the dissipation rate  $\epsilon$  of turbulent kinetic energy (TKE) were found to be sensitive to the number of mean-squared velocity gradient terms included and not whether the turbulence was assumed to adhere to isotropy or axisymmetry. The resolution dependency of different turbulence statistics was assessed with a procedure that does not rely on the dissipation scale. The streamwise evolution of the TKE components and were found to collapse across grids when the rod diameter was included in the normalisation. We argue that this should be the case between all regular grids when the other relevant dimensionless quantities are matched and the flow has become homogeneous across the stream. Two-point space correlation functions at  $x/M = 1$  show evidence of complex wake interactions which exhibit a strong Reynolds number dependence. However, these changes in initial conditions disappear indicating rapid cross-stream homogenisation.

On the other hand isotropy was, as expected, not found to be established by  $x/M = 12$  for any case studied.

## 2.2 Regular and Fractal/Multiscale grids

### Near field flow development behind two multi-scale grids and a conventional grid

P.A. Krogstad

Norwegian University of Science and Technology, NORWAY

A grid experiment in a wind tunnel sufficiently large to avoid interference from side walls has been performed using LDA and hot wire anemometry. A conventional square monoplane grid with  $\sigma = 44\%$  solidity is used for reference and the development in the near field is compared to two “cross” type multiscale grids. The first has the same solidity as the reference grid, while the second is geometrically similar, but with  $\sigma = 33\%$ . Initially the conventional grid produces the largest spanwise variations as the flow exits from a few, large jets. Therefore, the multiscale grids, with all its bars of variable size, produce the highest turbulence levels. However, further downstream, the conventional grid, which has the highest pressure drop coefficient, also produces the highest levels of turbulent energy. This is found after the jets have interacted strongly. The development of the near field characteristics depends on the path followed, but they all end up with same turbulence levels after about 50 integral length scales, or of the order of 30 mesh distances. We show that the peak energy level scales with the pressure drop coefficient,  $CP$ , and that the position of the peak scales with the hole size,  $H$ . For paths starting behind an intersection of bars it is shown that the bar width,  $t$ , successfully scale the development for the two multiscale grids down to  $x/t \approx 70$ . Due to the differences in geometry, the conventional grid data only follows the multiscale grids down to  $x/t \approx 20$ . As has been shown previously, it was found that the mesh size is not a suitable scaling length for the far field due to the complex geometry of multiscale grids. Most grid experiments been using hot wire anemometry, also in the highly turbulent near field. Having performed measurements with both LDA and HWA from the grids down to about  $250M$  it has been possible to sort out where the two measurement techniques have their advantages and shortcomings. Inspecting the pdf distributions in the homogeneous region for  $x > 50$  integral length scales, very good collapse between the two methods is found. However, the pdfs close to the peak in energy show considerable differences. These are due to the measurement errors in hot wire data when the turbulence level high. Since hot wires are unable to measure reverse flows, the negative velocities are folded over to the positive side, increasing the mean velocity and reducing the deduced kinetic energy. Additional errors are introduced by the fact that single hot wires has the same sensitivity to both the wire normal components. Finally we look at the question of exponential energy decay rate, which has been documented for certain multifractal grids. It is demonstrated that exponential decay may be found also for all three grids used here. But we also show that a power law fits the data equally well. In fact, the power law proves to be a better function unless the range used to fit the data is very short. By extending the region it is shown that the power fit produces a decay exponent which is almost unaffected by the range used, while the coefficient in the exponential fit strongly depends on the range.

## Towards a universal dissipation scaling for non-equilibrium turbulence?

P. C. Valente, J. C. Vassilicos

Department of Aeronautics, Imperial College London, UK

It is experimentally shown that the non-classical high Reynolds number energy dissipation behaviour,  $C_\epsilon \equiv \epsilon L/u^3 = f(Re_M)/Re_L$ , observed during the decay of fractal square grid-generated turbulence (where  $Re_M$  is a global inlet Reynolds number and  $Re_L$  is a local turbulence Reynolds number) is also manifested in decaying turbulence originating from various regular grids. For sufficiently high values of the global Reynolds numbers  $Re_M$ ,  $f(Re_M) \sim Re_M$ .

### Wind tunnel experiments on the spatial development of fractal-generated turbulence

K. Nagata<sup>1</sup>, Y. Sakai<sup>1</sup>, H. Suzuki<sup>1,2</sup>, and O. Terashima<sup>1</sup>

<sup>1</sup> Department of Mechanical Science and Engineering, Nagoya University, JAPAN

<sup>2</sup> Department of Engineering Physics, Mechanics and Electronics, Nagoya Institute of Technology, JAPAN

We investigated the spatial development of multi-scale/fractal generated turbulence originally investigated by Hurst & Vassilicos [3] (HV hereafter), Seoud & Vassilicos [6] (SV hereafter) and Mazellier & Vassilicos [4] (MV hereafter) using a wind tunnel. The test section of the wind tunnel is  $0.3 \times 0.3m$  and  $4m$  in length. The square-type fractal grid (blockage ratio  $\sigma = 0.25$ , thickness ratio  $t_r = 13.0$ , fractal dimension  $Df = 2$ ,  $L_0 = 163.8mm$ ,  $L_1 = 78.9mm$ ,  $L_2 = 38.1mm$ ,  $L_3 = 18.3mm$ ,  $t_0 = 11.7mm$ ,  $t_1 = 4.9mm$ ,  $t_2 = 2.1mm$ ,  $t_3 = 0.9mm$ , where  $L_i$  are the successive bar length and  $t_i$  are the successive bar thickness: see HV and SV for detail) was installed at  $0.15m$  downstream of the entrance of the test section. The Reynolds numbers  $Re_0$  based on  $t_0$  and mean flow velocities upstream of the grid are 5,900 and 11,400, which are the same as in the previous experiments. The instantaneous two-component velocities are measured using hot-wire anemometry with an inhouse X-probe. The diameter and length of the sensor are  $d = 5\mu m$  and  $l = 1mm$ , respectively. The results on the centerline statistics generally agree with the previous measurements despite the different size of the test section: the longitudinal integral length-scale  $Lu$  and the Taylor microscale  $\lambda$ , or their ratio  $Lu/\lambda$  were approximately constant during decay and independent of turbulent Reynolds number  $Re_\lambda$ . The results on the centerline support the finding of MV that the classical scaling law of  $Lu/\lambda \approx Re_\lambda$  and the Richardson-Kolmogorov cascade are not universal. It is found that  $Lu/\lambda$  in the whole cross section of the tunnel hardly changes in the decay region of the rms velocity, which implies that the turbulent field in the decay region is self-similar. The cross-sectional profiles of the production, turbulent diffusion, viscous diffusion, pressure diffusion and dissipation terms in the transport equation of turbulence kinetic energy  $k$  are also measured.

### Numerical simulation of turbulence generated by the multiscale grid

H. Suzuki<sup>1</sup>, K. Nagata<sup>1</sup>, Y. Sakai<sup>2</sup>, H. Toshiyuki<sup>1</sup> and Y. Hasegawa<sup>1</sup>

<sup>1</sup> Department of Engineering Physics, Mechanics and Electronics, Nagoya Institute of Technology, JAPAN

<sup>2</sup> Department of Mechanical Science and Engineering, Nagoya University, JAPAN

In recent years, the fractal generated turbulence (FGT

hereafter) [3,6] has drawn remarkable attention. Some previous experimental studies [3,6] revealed that the fluctuating velocities of square-type FGT decay exponentially along the centre line. This is one of the most important characteristics of square-type FGT, because it means this FGT is not consistent with the classical Richardson-Taylor-Kolmogorov theory. In this study, to seek the essential characteristics of square-type FGT, the streamwise variation of turbulence intensities of fluctuating velocity and static pressure along the centre line have been investigated by the direct numerical simulation. Specifically, we focused on whether the exponential decay of fluctuating static pressure along the centre line can be found or not. Here it should be noted that the fluctuating static pressure is one of the key quantities to understand the dynamics of turbulent field, but its measurement in decaying grid turbulence is difficult. Either the square-type fractal grid (blockage ratio  $\sigma = 0.36$ , thickness ratio  $t_r = 8.5$ , and fractal dimension  $Df = 2$ : see the previous experiment [3] for detail) for FGT or a classical biplane square grid for the classical grid turbulence (CGT hereafter) was installed at  $5M$  downstream of the entrance to the test section, where  $M$  is the mesh size. The Reynolds numbers based on the mesh size are the same for both grid turbulences, which is 2,500. Direct numerical simulation based on finite difference method holding the conservation law obtained by Morinishi et al. [7] has been performed. The results show that both turbulent kinetic energy and turbulence intensity of fluctuating static pressure in the case of FGT decay exponentially. On the other hand, in the case of CGT both decay under power law.

## 2.3 Active, rotating and non-rotating grids

### Stirring turbulence with turbulence

W. van de Water

Eindhoven University of Technology, NETHERLANDS

We stir wind-tunnel turbulence with an active grid that consists of rods with attached vanes. The grid is driven through the time-varying angles of these rods. These angles can vary completely randomly, or tuned to impose gradients onto the mean flow. In this way we stir anisotropic turbulence and wonder about the degree of randomness needed to drive the grid. In the case of homogeneous shear, the simplest thinkable anisotropic turbulence, we study the return to isotropy at the smallest scales in high-order statistical moments. These challenging experiments employ the ability of the grid to quickly switch the degree of anisotropy of the stirred flow. We interpret measured structure functions, involving various mixed velocity components and various arrangements of our array of 10 x-probes, in terms of the SO(3) description of turbulence anisotropy. Ideally, turbulence in a windtunnel should be initiated by providing the detailed space-time dependent inflow velocity field, much as it is done in numerical simulations. This is clearly not feasible and an active grid only provides a crude approximation where only the large length scales and the slow time scales are accessible. Our closest approximation of this ideal is to drive the grid with random numbers generated by the Gledzer-Ohkitani-Yamada (GOY) shell model. The GOY model is a simple dynamic model of turbulence that produces a velocity field displaying inertial-range scaling behaviour. Thus we are stirring turbulence with

turbulence. The range of stirring scales can be adjusted by selection of shells in the model. We find that the largest energy input and the smallest anisotropy are reached when the time scale of the random numbers matches that of the large eddies in the wind-tunnel turbulence. A large mismatch of these times creates a flow with interesting statistics, but it is not turbulence.

### Wind tunnel experiments of decay characteristics in large-scale isotropic turbulence

N. Sekishita

Toyohashi University of Technology, JAPAN

The present study aimed to obtain experimental data with respect to basic turbulence quantities in homogeneous quasi-isotropic turbulence fields with  $Re_\lambda = 80 \sim 393$  artificially excited by installing an active turbulence generator in a laboratory wind tunnel. Velocity fluctuations were measured by conducting hot-wire measurements. Then, the turbulence quantities such as turbulence energy, energy dissipation rate, scales and energy spectra, were calculated from them. The present homogeneous turbulence field initially had a large anisotropy. It decayed downstream into quasi-isotropic turbulence through two stages characterized by the relation between turbulence energy  $q^2$  and invariant II of anisotropic tensor. Return to isotropy proceeded in the first stage and the viscous dissipation became dominant in the second stage. Even for  $Re_\lambda > 200$ , the turbulence field still maintained weak anisotropy in the second stage, though the degree of anisotropy was about the same as the values of conventional grid turbulence. A new power law for the decay of turbulence energy was derived from the turbulence energy equation by employing the Rotta's model to take the effect of the return to isotropy into account. As the result, almost the same decay rates were obtained between the first and the second stages. The decay rate decreased with increasing  $Re_\lambda$  for  $Re_\lambda > 110$  and gradually approached to the theoretically and numerically estimated value of about 1.4, when  $Re_\lambda \rightarrow \infty$ .

### Understanding rotating and nonrotating grid turbulence

P. Orlandi

Dipartimento di Ingegneria Meccanica e Aerospaziale,  
Universita La Sapienza, ITALY

Direct numerical simulations (DNS) are presented to understand the effects of the initial conditions on the turbulent energy decay rate. An accurate second order finite difference scheme has been used as the basic numerical method. The control of the inlet conditions is difficult for realistic simulations reproducing the solid grid, then analytical anisotropic velocity distributions were assigned for single and multiple scale disturbances. For the single scale three simulations varying the size  $f$  of the disturbances show a scaling of the turbulent energy  $q$  when it is plotted versus  $x_1/M$  with  $M = f/(2\pi)$ . The decay rate reduces in presence of multiple scale disturbances. The transition to isotropic turbulence was analysed through the evolution of the statistics, and in particular those linked to the flow structures. Flow visualizations of the vorticity field and joint pdf contributing to the velocity correlations coefficients at different distances from the inlet, allowed to understand the reasons of the different behaviour between single and multiscale disturbances. For the latter the reduction of the decay rate of the turbulent kinetic energy may help to generate high  $Re_\lambda$  isotropic turbulence. To increase the  $Re_\lambda$  simulations with differ-

ent rates of solid rotation were also performed for the flow with multiple scale and  $f = 8$  disturbances. For the latter variations of the rotation rate  $N_\Omega$  allowed to investigate the modifications of the vortical structures. The energy spectra at different distances from the inlet allow to understand when the effects of the inlet disturbances disappear. The agreement with the spectra available in literature were corroborating the quality of the numerical method to reproduce the different behaviours in the inertial and in the exponential ranges.

## 3 Theory, flow structure and interfaces

### Kolmogorov and non-Kolmogorov scalings

C. Cambon<sup>1</sup>, S. Laizet<sup>2</sup> and J.C. Vassilicos<sup>3</sup>

<sup>1</sup> Ecole Centrale Lyon, France

Nagoya Institute of Technology, JAPAN

<sup>2</sup> Department of Aeronautics, Imperial College London, UK

When describing Kolmogorov's universal equilibrium hypotheses in his landmark turbulence book, Batchelor [8] stresses their clear implication that "all turbulent motions - decaying homogeneous turbulence, flow in a pipe under pressure, flow in a boundary layer, turbulent wakes, flow in a fluid with density stratification, etc - are such that at sufficiently large Reynolds number the motions associated with the small-scales have a common statistical form". In particular, the closely related Reynolds number-independent scaling  $\epsilon = K^{3/2}/L$  is indeed customarily used in the modelling of many different turbulent flows including wakes, jets and shear layers (Townsend [9]), decaying homogeneous turbulence (Batchelor [8]), stratified turbulence (Hopfinger & Toly [10]) and even models of the intermediate inertial layer in wall turbulence (e.g. Pope [11]). However, Seoud & Vassilicos [6], Mazellier & Vassilicos [4], Valente & Vassilicos [12], as well as Valente & Vassilicos, Discetti et al, Gomes et al and Nagata et al (all of which are presented in this workshop) all found a significant region of turbulent flow where  $C_\epsilon = L_\epsilon/K^{3/2} \approx Re_\lambda^{-\alpha}$  with  $\alpha$  close to 1 even though  $Re_\lambda$  is high and the turbulence energy spectrum is a broad power-law with exponent close to  $-5/3$ . We first present an analysis of the Lin equation for decaying turbulence which rigorously leads to the well known Kolmogorov scaling of the third order structure function provided that  $\alpha < 1$ . We then present Direct Numerical Simulations (DNS) of turbulence generated by a fractal square grid and by a regular grid and discuss the mechanism(s) of interscale transfer, vorticity and strain amplification and their relation to Kolmogorov and/or non-Kolmogorov scalings of energy spectra and dissipation rate.

### Simultaneous measurement of the velocity and pressure near the turbulent/nonturbulent interface

O. Terashima, Y. Sakai and K. Nagata

Department of Mechanical Science and Engineering,  
Nagoya University, Aichi, JAPAN

The interface between the turbulent and non-turbulent region in a plane turbulent jet is investigated by the simultaneous measurement of two velocity components and pressure near the interface of the turbulent and non-turbulent region. The measurement is performed by means of a combined probe comprising an X-type hot-wire and a static pressure tube. The measurement data are analyzed by the conditional sampling technique

and an ensemble averaging technique on the basis of the intermittency function for the turbulent/non-turbulent decision. The measurement results at the interface of the turbulent region show that there is a thin layer associated with a large shift of physical quantities such as mean streamwise velocity, streamwise velocity fluctuation, cross-streamwise velocity fluctuation, Reynolds stress, the irregularity of the streamwise velocity fluctuation and pressure fluctuation. Further, the thickness of the layer is found to be  $0.08b$ . It is also found that the thickness corresponds to about 10-12 times the Taylor micro-scale at the measurement position. Moreover, the possibility that there are small vortices in the middle of the layer is shown.

### Roles of sheared interfaces in turbulent flows

J. Hunt<sup>1</sup>, T. Ishihara<sup>2</sup>, Y. Kaneda<sup>2</sup>, M. Braza<sup>3</sup>, A. Mahalov<sup>3</sup>, M. Mostaoui<sup>4</sup>, J. Westerweel<sup>5</sup>

<sup>1</sup> University College London, UK

<sup>2</sup> CSE Nagoya, JAPAN

<sup>3</sup> IMFT Toulouse, FRANCE

<sup>4</sup> Arizona State University, USA

<sup>5</sup> TU Delft, NETHERLANDS

Randomly moving sheared interfaces are key mechanisms that greatly influence the structure of both simple and complex turbulent flows at very high Reynolds number. Conditional sampling measurements and local analysis leads to useful new models (or interpretations/adaptations of standard statistical models), explanations and perhaps technologies. Some general ideas and recent developments are reviewed in this presentation, including:

- Dynamics within and outside thin layers in homogeneous turbulence using DNS and rapid distortion theory
- Different interface dynamics and entrainment processes for the edges of different types of turbulent shear layers
- Reinforcement and breakdown of interfaces by internal and external forcing.

## 3.1 Mixing and combustion

### Development of scalar mixing layer in regular/fractal grid turbulence

Y. Sakai<sup>1</sup>, K. Nagata<sup>1</sup>, H. Suzuki<sup>2</sup>, K. Hoshino<sup>1</sup> and O. Terashima<sup>1</sup>

<sup>1</sup> Department of Mechanical Science and Engineering, Nagoya University, Japan

<sup>2</sup> Department of Engineering Physics, Mechanics and Electronics, Nagoya Institute of Technology, JAPAN

Turbulent mixing of high-Schmidt-number passive scalar in the regular and fractal grid turbulence is experimentally investigated using a water channel. A turbulence generating grid is installed at the entrance to the test section, which is  $1.5m$  in length and  $0.1m \times 0.1m$  in the cross section. Two types of grids are used: one is a regular grid of the square-mesh and biplane construction, and another is a square type fractal grid, which was first investigated by Hurst & Vassilicos [3] and Seoud & Vassilicos [6]. Both grids have the same solidity of 0.36. The Reynolds number based on the mesh size,  $Re_M = U_\infty M_{eff} / \nu$  is 2,500 in both flows, where  $U_\infty$  is the cross-sectionally averaged mean velocity,  $M_{eff}$  is the effective mesh size and  $\nu$  is the kinematic viscosity. A fluorescent dye (Rhodamine B) is homogeneously premixed only in the lower half

stream, and therefore, the scalar mixing layers with an initial step profile develop downstream of the grids. The Schmidt number of the dye is  $\mathcal{O}(10^3)$ . The time-resolved particle image velocimetry (PIV) and the planar laser induced fluorescence (PLIF) technique are used to measure the velocity and concentration field [13]. The results show that the turbulent mixing in the fractal grid turbulence is strongly enhanced compared with in the regular grid turbulence at the same  $Re_M$ . It is also found that the scalar dissipation takes place locally even in the far downstream region at  $x/M_{eff} = 120$  in the fractal grid turbulence. The instantaneous scalar variance  $k_c = 0.5c^2$  and the instantaneous two-dimensional scalar dissipation  $\epsilon_c = (\partial_x c)^2 + (\partial_y c)^2 / Re_M Sc$  in fractal grid turbulence are also investigated. The  $\epsilon_c$  profiles show that the scalar dissipation takes place locally even in the far downstream region at  $x/M_{eff} = 120$ , since the Schmidt number is very large. Further, we investigated the fractal geometries of the mixing interfaces in the regular and fractal grid turbulence. The fractal dimensions are calculated by using the box-counting method. The results show that the fractal dimensions in the fractal grid turbulence is larger than that in the regular grid turbulence. In addition, the fractal dimension in the fractal grid turbulence monotonically increased with time (or with the downstream direction), whereas that in the regular grid turbulence is almost constant with time. The investigation of the number of counted boxes in a unit area, together with the above results, suggests that turbulent mixing is more enhanced in the fractal grid turbulence from the viewpoint of fractal geometry and expansion of mixing interface too. We are now trying to make the simultaneous measurements of velocity and concentration by the combination of PIV and PLIF. In the workshop, it is expected that the results of simultaneous measurements will be shown. The Direct Numerical Simulation of the scalar mixing layer in the regular/fractal grid turbulence is also in progress. In the workshop, the DNS data will be shown to investigate the three-dimensional mixing process in the fractal grid turbulence.

### DNS of passive scalar mixing and transfers by gridgenerated turbulence

S. Laizet, J.C. Vassilicos

Department of Aeronautics, Imperial College London, UK

We develop Direct Numerical Simulations (DNS) of 3D turbulent flows generated by static regular and fractal square grids which include passive scalar calculations at Prandtl number equal to 0.1. The initial condition for the passive scalar is a linear scalar profile and our DNS demonstrate that this profile remains approximately constant in time, and therefore linear, in the mean throughout our computational domain. We study scalar transfers and scalar variances and the detailed balance between variance producing, variance destroying and inhomogeneity transfer mechanisms. Compared to static regular grids, static fractal square grids can enhance scalar transfer and turbulent diffusion by at least one order of magnitude while at the same time reducing pressure drop by half. These two different effects have a common cause which is the fractal space-scale unfolding (SSU) mechanism. Our computations suggest that fractal engineering based on novel mechanisms such as SSU may hold the power to set entirely new standards in the many industries where effective yet efficient mixing and cooling are required.

## Conditional statistics in reacting flows with fractal generated turbulence

P. Geipel, K.H.H. Goh, F. Hampf and R.P. Lindstedt  
Department of Mechanical Engineering, Imperial College London,  
UK

The opposed jet configuration presents an attractive geometry for the evaluation of the impact of strain on burning properties of laminar and turbulent flames through good optical access and comparatively simple boundary conditions. Disadvantages include potential low frequency flow instabilities at high nozzle separations and, for turbulent flames, relatively low turbulence levels causing bulk strain to exceed the turbulent contribution at small nozzle separations. Fractal generated turbulence was used to ameliorate the latter problem by significantly increasing turbulent strain with the turbulent Reynolds number range moved from 50-120 to 130-318 as compared to conventional perforated plate generators. The resulting flow structures were analysed using a Proper Orthogonal Decomposition technique with velocity and reaction progress variable statistics, including conditional velocities and scalar fluxes, reported for fuel lean methane, ethylene and propane flames approaching extinction. The instrumentation comprised particle image velocimetry with the flows to both nozzles seeded with  $1\mu\text{m}$  silicon oil droplets or  $3\mu\text{m}$   $\text{Al}_2\text{O}_3$  particles. Probability density functions were determined for the instantaneous location of the stagnation point and the impact of rejecting low frequency bulk motion on velocity statistics was also assessed. Probability density functions of flame curvature were determined using a developed multi-step flame front detection algorithm along with estimates of the turbulent burning velocity obtained using a range of alternative determination methods. The data sets present an opportunity for a systematic evaluation of calculation methods for premixed turbulent flames approaching extinction.

### On the structure of turbulent flames in fractal-grid generated turbulence

T. Sponfeldner<sup>1</sup>, S. Henkel<sup>1</sup>, N. Soulopoulos<sup>1</sup>, F. Beyrau<sup>1</sup>, Y. Hardalupas<sup>1</sup>, A.M.K.P. Vassilicos<sup>2</sup> and J.C.

<sup>1</sup> Department of Mechanical Engineering, Imperial College London, UK

<sup>2</sup> Department of Aeronautics, Imperial College London, UK

Fractal or multiscale turbulence-generating grids produce bespoke turbulent flows designed for the particular application at hand [3]. They allow more design and optimisation flexibility than conventional turbulence generators like perforated plates, for example, and generate high turbulence intensity at some distance away from the grid and over an extended region downstream at a low cost in terms of pressure drop. The possibility to design the parameters of this extended region of high turbulence intensity is of great interest for premixed combustion and may pave the way for future fractal combustors particularly adept at operating at the lean premixed combustion regime where NOX-emissions are the lowest. The high turbulence intensity, in particular, has the potential to increase the turbulent burning velocity and the power density of the flame. In previous work we observed a significant increase of turbulent burning velocity when using a fractal instead of a regular grid[14]. In this work we further investigate the influence of fractal-grid generated turbulence on the structure of premixed V-shaped methane-air flames. For a parametric study, a set of different space-filling fractal

square grids is designed and several design parameters such as the blockage ratio, the ratio between the sizes of the largest and the smallest structures of the fractal grids and the number of fractal iterations are varied. A regular square mesh grid that, at a given downstream position, produces the same velocity fluctuations as one of the fractal grids acts as reference case. The velocity fields for the different grids are characterized based on hot wire measurements and the structure of the generated flames is investigated using the Conditioned Particle Image Velocimetry (CPIV) technique [15]. Quantities like the flame brush thickness, flame surface density and the turbulent burning velocity as well as the flow field characteristics are compared. Preliminary results show significantly higher corrugation of the flames and larger flame brush thicknesses for all fractal grids. High-speed CPIV measurements are performed in order to resolve the turbulent behaviour of the flames.

## 3.2 Fractal orifices, plates and tetrahedron

### Return to axi-symmetry for pipe flows generated after a fractal orifice

F.C.G.A Nicolleau  
SFMG, University of Sheffield, UK

Pipe flows generated by fractal orifices were introduced in [17]. In this contribution, we compare the merits of the different orifices for the two reference types, orificelike and perforated-like. An objective assessment of how disruptive the orifice can be to the flow in view of flowmetering techniques, is to measure its return to axisymmetry. The flow is forced through a fractal orifice and we study the effect of this opening on the velocity (mean and rms) profiles. A practical application is to use such shapes as optimal flowmeters or flow mixers. Fractal shapes have been considered as an alternative to the classical circular orifice used for flowmetering. Fractal orifices have been shown to decrease pressure drops by as much as 10% when compared to the classical circular orifice [16,17]. They also improve the measurement quality when used as flowmeter conditioners [18]. The wind tunnel and its experimental conditions are reported in details in [17], The 5mm thick polycarbonate wind-pipe has a length of 4400mm and an inner diameter  $D=140.8\text{mm}$ . The different orifices have the same initial conditions. They all have the same flow area. The inlet velocity is  $U_0 = 5\text{ms}^{-1}$ . The bulk Reynolds number is 40,000. Measurements are taken at different locations downstream the orifice location. Hot-wire velocity measurements profiles are obtained as functions of the distance from the wall and at the different locations. For flows in pipes and ducts an important feature to consider is the interaction of the object with the wall. We introduce a new parameter  $\delta_g^*$  which measures the smallest gap between the flow area and the wall. The results presented here are also important for CFD validations. There is a need for validations of complex subgrid models dealing in particular with rough surfaces and fractal-forced flows could provide a systematic way to generate data for such validations. In particular, it is easy to see that such flows pose a real challenge to grid-dependent method as Detached Eddy Simulation.

## Simulation of turbulent flow through a fractal orifice in a pipe

B. Geurts

Twente University, NETHERLANDS

The flow through a cylindrical pipe equipped with a fractal orifice is simulated. A volume penalization immersed boundary method is used to simulate turbulent flow. We investigate the influence on the mixing efficiency arising from the mounted fractal orifice. We employ direct numerical discretization and include various shapes of fractal orifices. Basic shapes such as circles, squares and triangles are adopted, as well as several levels of shapes approximating the Koch snowflake. The flow is analyzed in detail, both at modest Reynolds numbers as well as under turbulent conditions. Mixing efficiency is quantified by tracking Lagrangian particles in the flow and analyzing their dispersion rates.

## Drag and wake characteristics of flat plates with fractal edge geometries

J. Nedic<sup>1</sup>, B. Ganapathisubramani<sup>2</sup>, J.C. Vassilicos<sup>1</sup>

<sup>1</sup> Department of Aeronautics, Imperial College London, UK

<sup>2</sup> Department of Engineering Science, University of Southampton, UK

Past results have suggested that the coefficient of drag and shedding frequencies of flat plates with various degrees of axi-symmetry, such as circular disks, squares and triangles, all fall within a very narrow band of values. In this study, we introduce a variety of length-scales into the perimeter of a plate facing a laminar free-stream, and study the effects of this multiscale/fractal perimeter on the wake characteristics and overall drag on the plate. The perimeter of the plate can be made as long as allowed by practical constraints with as many length-scales as desired under these constraints without changing the area of the plate. A total of eight fractal-perimeter plates were developed, split into two families of different fractal dimension, and their wakes and drag properties were compared to a square and cross plate, all of which had the same frontal area. It is found that by increasing the number of fractal iterations, thus the perimeter, the mean drag coefficient increases by roughly 10% whilst the drag fluctuation amplitude decreases. For the family of fractal plates with the higher dimension, it is also found that when the perimeter increases above a certain threshold the mean drag coefficient drops back again. Our results also suggest that the shedding frequency remains the same, however the intensity of the shedding decreases with each fractal iteration. In an attempt to explain these results, we consider both the large scale turbulent properties that exist in the shear layer (via turbulent entrainment) and the small scale properties in the wake itself (via turbulent dissipation).

## Development of turbulence properties of wake behind the Sierpinski tetrahedron

T. Ushijima and H. Suzuki

Department of Engineering Physics, Electronics and Mechanics, Graduate School of Engineering, Nagoya Institute of Technology, JAPAN

In some flat plain areas of Japan where seasonal winds are strong, the forests are planted to protect the farm houses from the strong wind. The windbreak forests not only protect the houses but provide shade to moderate the temperature variation of residential area. It is reported that the wind drag against trees increase linearly

with the wind speed. This seems strongly relevant to the structure of their crown tree. Tree leaves are sparsely distributed and provides comfortable shade effectively. In botany, it is known that the fractal dimension of foliage distribution lies in the range from 2 to 2.4. It is suggested that the Sierpinski tetrahedron, whose fractal dimension is exactly two, can be used as a model of the crown tree structure. Self-similarity means that there is no characteristic scale within the range where the self-similarity holds. We set the thrice iterated Sierpinski tetrahedron at the inlet of small wind tunnel whose dimension is  $13 \times 13 \text{ cm}^2$  in cross-section and 2 m in length, and measured the turbulence produced by passing through the Sierpinski structure for two wind speeds (5 and 10 m/s). The turbulence intensity peaks around twice tunnel height in the streamwise direction and starts to decay. The turbulence decay obeys the power law at the beginning and changed to the exponential decay downstream. In the power law region, the mean velocity distribution of the cross-section is still quite inhomogeneous due to the proximity of the fractal structure and strong shear is a source of turbulence. In the exponential decay region, the mean velocity distribution gets more homogeneous and shear becomes milder. Exponential decay has been observed by the precursor experiment of space-filling fractal grids. Exponential decay in our case is, however, possibly due to the small geometry of the wind tunnel which limits the growth of the size of the energy containing eddy at the downstream region of the test section. Finally, the dissipation coefficients are evaluated and the inverse-proportional relationship between the coefficients and Reynolds number observed by Vassilicos and co-workers appears to serve as an envelop of our results.

## 3.3 Decompositions

### On the impact of massive use of decompositions on paradigmatic issues in turbulence

A. Tsinober

Tel Aviv University, Israel

The first part is devoted to a brief overview of the reductionist approaches, i.e. various decompositions from formal to heuristic ones and a discussion on how useful they were (and are) for the analysis of flow states and processes and whether studying turbulence via (some) decompositions is aiding understanding its fundamental physics. In the second part examples will be given as to how decompositions may obscure the physics. This includes the problem of ill-posedness of the concept of the inertial range and some of the consequences supported by an experiment at high Reynolds number with the access to the field of velocity derivatives including dissipation. Anomalous scaling, nonlinear interactions in the "IR" are not purely inertial ones (PI) and consist of PI and the inertial-viscous interactions as well. The 4/5 law is not a purely inertial relation.

### A critique of the application of Fourier analysis to finite domain measurements and numerical simulations

W. K. George<sup>1</sup>, G. Mallouppas<sup>2</sup>, B. Van Wachem<sup>2</sup>

<sup>1</sup> Department of Aeronautics, Imperial College London, UK

<sup>2</sup> Department of Mechanical Engineering, Imperial College London, UK

An alternative to the linear forcing of Lundgren [19] has been implemented by Malloupas et al. [20] for sustaining homogeneous and isotropic turbulence. The

method depends on a random pseudo-velocity field produced initially from an arbitrary spectrum. Energy can be fed into a variety of different wavenumbers or at all wavenumbers so that the resulting total turbulent kinetic energy remains constant. The overall goal is to evaluate the effect of initial conditions (i.e. triggering at different wavenumbers) on the statistics, especially spectra and correlation functions, with a particular view toward understanding the variety of spectra generated by experiment [20,21]. This talk will first introduce the methodology used and examine the degree to which the results for the sustained turbulence satisfy the homogeneous and isotropic relations. Particular attention will be paid to the isotropic derivative and spectral relations. Further, effects of window functions on 1D spectra and correlations will be also addressed. The time-resolved statistics behave in a manner consistent with a finite sample of an infinitely long stationary random process. Analysis treating the time records instead as a part of a period signal leads to a different result. By contrast, the spatial statistics reflect directly the underlying periodicity imposed by the boundary conditions. When the spatial symmetry is broken, then the spatial statistics behave as a finite piece of a homogeneous process. The results raise interesting (and apparently unresolved) questions about exactly what is the relation between a theoretically homogeneous turbulence and that we create in a computer by periodic boundary conditions or a finite number of Fourier modes.

### 3.4 Drag, Noise and Wind

#### Representing subgrid-scale drag forces in high Re number flow over fractal objects using RNS

J. Graham

John Hopkins University, USA

In this talk we will discuss a downscaling strategy for modelling subgrid-scale drag forces on fractal objects. This downscaling strategy is called Renormalized numerical simulation (RNS) as introduced by Chester [22] for flow over scaleinvariant objects. In this work we extend RNS to a generalized framework and present several formulations of the methodology. These formulations now include a local description for modeling parameters and temporal filtering to better enforce complete similarity assumed by RNS. We will discuss the application of these RNS formulations to a fractal tree canopy along with results from their implementation.

#### Acoustic signature of fractal-generated turbulence

V. Fortuné<sup>1</sup>, S. Laizet<sup>2</sup>, E. Lamballais<sup>1</sup>  
and J.C. Vassilicos<sup>2</sup>

<sup>1</sup> Institut P<sup>2</sup>, CNRS-ENSMA, Université de Poitiers, FRANCE

<sup>2</sup> Department of Aeronautics, Imperial College London, UK

Identifying the mechanisms responsible for the production of sound by turbulent flows remains to date an extremely difficult task, even for very extensively studied problems, like jet noise. Experimental studies are generally not sufficient when knowledge about the physical mechanisms of noise production is required. DNS allow the calculation of all unsteady flow quantities and can help to investigate the aerodynamically generated sound. The direct computation of sound by solving the compressible Navier-Stokes equations provides both the aerodynamic field and the acoustic field simultaneously but the very high cost of this

direct approach remains a limiting factor. As a result, flow-generated acoustic fields are often predicted via a hybrid approach using acoustic analogies or wave extrapolation methods. In this work, DNS of turbulent flows generated by a regular and a fractal grid are carried out (see Laizet & Vassilicos (2011) [23]), thanks to the parallel version of the Incompact3d code which solves the incompressible Navier-Stokes equations. More information about the numerical methods can be found in Laizet & Lamballais (2009) [24] and in Laizet & Li (2011) [25]. The acoustic radiation from the flow across the grids is then evaluated thanks to a hybrid approach based on the Lighthill acoustic analogy. To take the solid boundaries into account in the integral solution, we use the formulation due to Curle and Ffowcs-Williams and Hawkings. Our results show that the sound levels corresponding to a fractal square grid of three fractal iterations are significantly reduced by comparison to a regular grid of same porosity and mesh-based Reynolds number. We also find a well-defined peak at a Strouhal number between 0.2 and 0.3 in the acoustic spectrum of the fractal square grid which is absent in the case of the regular grid. We explain this effect in terms of a new criterion for quasi-periodic vortex shedding from a regular or fractal grid.

#### Multi-scale generation of turbulence and its relevance for wind energy applications

N. Reinke<sup>1</sup>, S. Weitemeyer<sup>1,2</sup>, M. Holling<sup>1</sup> and J. Peinke<sup>1</sup>

<sup>1</sup> ForWind - Institute of Physics, University of Oldenburg, GERMANY

<sup>2</sup> NEXT ENERGY - EWE-Forschungszentrum Energietechnologie e.V., Oldenburg, GERMANY

Wind energy converters (WEC) work in a highly turbulent wind field, the atmospheric boundary layer (ABL). It is well known that turbulence has a serious influence on WEC power production and consequently the loads raise tremendously, thus the WEC fatigues fast. Wind tunnel experiments help to understand the interaction between a turbulent wind field and a WEC. However, realistic wind conditions are difficult to realize in a wind tunnel, especially in terms of intermittent velocity fluctuations on a wide range time scales and in terms of the repeatability of such wind fields. The presentation will show two wind tunnel investigations with the fractal and the active grid. The measurements were realized with hot wire probes. The static fractal grid generates vortices on a range of scales. The grid creates a flow which is very turbulent and intermittent in a specific region behind the grid. Compared to a classical grid the wind field has a completely different decay of the turbulent field. It was investigated how these turbulent properties alter when changing the small scales of the grid. Furthermore, it was investigated how the flow properties change when the experiments are conducted without the wall of a tunnel being present. The results indicate that the evolution of the flow is invariant to the investigated boundary conditions. The active grid modulates turbulent flows in a new manner. The active grid is a grid which can change the blockage in space and time, and also force the flow. Special driving protocols of the active grid generate heavy intermittent flows on a wide range of time scales. The great benefit of the active grid is that it is possible to repeat turbulent wind fields. The investigations reveal limits of the repeatability and some misunderstood effects. Hence we are searching for a proper characterization and present here first results.

## Acknowledgment

We are very grateful to the Japanese Society for the Promotion of Science for its generous support which allowed so many Japanese scientists to participate in the workshop and to Jovan Nedic for his kind, expert and indefatigable help with the workshop's organisation and the production of the book of abstracts

## References

- [1] Queiros-Conde & Vassilicos (2001) Turbulent wakes of 3D fractal grids - Intermittency in turbulent flows, Cambridge University Book.
- [2] Mazzi, B., Okkels, F. & Vassilicos, J. C. (2002) A shell model approach to fractal-induced turbulence - *Europ. Phys. J. B* 28(2), 243-251
- [3] Hurst D. & Vassilicos J.C. (2007) Scalings and decay of fractal-generated turbulence - *Physics of Fluids*, 19, 035103.
- [4] Mazellier N. & Vassilicos J.C. (2010) Turbulence without Richardson-Kolmogorov cascade - *Physics of Fluids*, 22, 075101.
- [5] George W.K. (1992) The decay of homogeneous isotropic turbulence - *Physics of Fluids A*, 4, 1492-1509.
- [6] Seoud, R. E. & Vassilicos, J. C. (2007) Dissipation and decay of fractal-generated turbulence - *Physics of Fluids*, Vol. 19, 105108.
- [7] Morinishi, Y., Lund, T. S., Vasilyev, O. V. & Moin, P. J. (1998) Fully conservative higher order finite difference schemes for incompressible flow - *Comput. Phys.*, 143, 90- 124.
- [8] Batchelor, G.K. (1953) *The Theory of Homogenous Turbulence* - Cambridge University Press.
- [9] Townsend, A.A. (1956) *The Structure of Turbulent Shear Flow* - Cambridge University Press.
- [10] Hopfinger, E.J. & Toly, J.A. (1976) Spatially decaying turbulence and its relation to mixing across density interfaces - *J. Fluid Mech.* (1976), 78(1), 155-175.
- [11] Pope, S. B. (2000) *Turbulent Flows* - Cambridge University Press
- [12] Valente P. & Vassilicos J.C. (2011) The decay of turbulence generated by a class of multi-scale grids - *J. Fluid Mech.*, 687, 300-340
- [13] Suzuki, H. et al., (2009) DNS of Passive Scalar Field with Mean Gradient in Fractal-Generated Turbulence - *Proc. 6th Int. Symp. on Turbulence and Shear Flow Phenomena*, 1, 55-60
- [14] Sponfeldner, T. et al. (2011) A parametric study of the effect of fractal-grid generated turbulence on the structure of premixed flames - Presented at the 1st UK-Japan bilateral Workshop, Imperial College London, UK
- [15] Pfadler, S., Beyrau, F. & Leipertz, A. (2007) Flame front detection and characterization using conditioned particle image velocimetry (CPIV) - *Opt. Express* 15, 15444
- [16] Abou-El-Azm, A., Chong, C., Nicolleau, F. & Beck, S. (2010) *Experimental Thermal and Fluid Sc.* 34, 104
- [17] Nicolleau, F., Salim, S. & Nowakowski, A. (2011) Experimental study of a turbulent pipe flow through a fractal plate - *J. of Turbulence* 12(1).
- [18] Manshoor, B., Nicolleau, F. & Beck, S. (2011) The fractal flow conditioner for orifice plate flow meters - *Flow Measurement and Instrumentation* 22, 208.
- [19] Lundgren, T. S. (2003) *Ann. Res. Briefs*, CTR, Stanford.
- [20] Mallouppas, G, George, W.K. & VanWachem, B. (2011) Alternative Forcing for Homogeneous Isotropic Turbulence in Real Space - *APS/DFD Meeting*, Baltimore, USA.
- [21] Comte-Bellot, G. & Corrsin, S. (1971) Simple Eulerian time correlation of full- and narrow-band velocity signals in grid-generated, 'isotropic' turbulence - *J. Fluid Mech*, 48(2), 273-337.
- [22] Chester et al. (2007) Modeling turbulent flow over fractal trees with renormalized numerical simulation - *J. Comp. Phys.* 225, 427-448.
- [23] Laizet & Vassilicos (2011) DNS of fractal-generated turbulence - *Flow, Turbulence and Combustion*, 87(4), 673-705
- [24] Laizet & Lamballais (2009) High-order compact schemes for incompressible flows: a simple and efficient method with the quasi-spectral accuracy - *J. Comp. Phys.*, 228(15), 5989-6015.
- [25] Laizet & Li (2011) Incompact3d, a powerful tool to tackle turbulence problems with up to 0(105) computational cores - *Int. J. of Numerical Methods in Fluids*, 67 (11), 1735-1757

# MORPHOLOGY AND DYNAMICS OF ANISOTROPIC FLOWS

F. S. Godeferd<sup>1</sup>, L. Danaïla<sup>2</sup> and J. Flor<sup>3</sup>

<sup>1</sup> LMFA CNRS UMR 5509, École Centrale de Lyon, Université de Lyon, France

<sup>2</sup> CORIA CNRS UMR 6614, Université de Rouen, France

<sup>3</sup> LEGI CNRS UMR 5519, Université Joseph Fourier, Grenoble, France

Summerschool ANISO, 18–30 July 2011

## 1 Motivations and organization

The summer school “ANISO 2011” was organized in the context of a three-year long project funded by the Agence Nationale de la Recherche to study the anisotropy arising in turbulent flows due to the presence of external rotation. The goal is to reach beyond the mere isotropic description of turbulence, since anisotropy is present throughout most turbulent flows, in relation with external distortions or with internal inhomogeneities, and to improve the statistical description and modelling of anisotropic turbulence. Applications are found in contexts in which anisotropy modifies the classical point of view about the dynamics of turbulence, its Eulerian structure and its Lagrangian properties; that is, most realistic flows, in geophysics, in industry, etc., are impacted.

The summer school was then organized not only as an enlarged, two-week long, meeting place for exchanges between experts in fluid dynamics and related areas, but also as a training session aimed at doctoral students, in order to provide them with adequate tools to tackle the issue of anisotropy in turbulence. From July 18th to 30th, the programme included a succession of specialized courses and conferences, presentation sessions by attendants, round tables and discussions, both organized and free, thanks to the venue in Cargèse[3], which permits optimal interactions. An evening conference was also offered to the local inhabitants and tourists, in order to explain how the challenges in the understanding of flows and turbulence are also crucial for industrial and economic development, as well as for environmental issues. In addition, a basic turbulence course was proposed during the week-end to participants who did not come from the turbulence community. Seventeen invited speakers came from European countries and overseas (USA, Japan), and 40 students and researchers were registered to attend the school, amounting to a total of 57 participants overall, who interacted during the eleven days extent of the school. The program gathered 29 talks, each of about 1h30, and was organized around three axes:

- Statistical tools for describing anisotropic turbulence, including physical and spectral space descriptors.
- Morphology of anisotropic flows.
- The statistics and dynamics of coupled fields. Mixing. Particles transport. Variable viscosity flows. Combustion. Quantum turbulence.

A web site was set up for registration and providing information to participants [1], and a book of abstracts was compiled, available upon request [2].

## 2 Contents of the talks

We give hereafter a short summary of the topics developed by the invited speakers

**C. Cambon (LMFA, École Centrale de Lyon, France)** presented two talks devoted to anisotropy in homogeneous turbulence, characterized essentially by spectral statistics. Different models of the influence of external distortions were presented. To start with, the linear response of turbulence to body forces and to large-scale mean gradients constitutes a

first interesting approach that provides valuable information on short time evolution of turbulent statistical quantities, assuming that nonlinearities act over a longer time scale. Then, a more complete nonlinear approach was presented, using Direct Numerical Simulations (DNS) and a two-point statistical model (EDQNM). It is important to point out that, in the latter, the linear effects are still included exactly, so that the closure is original with respect to similar models for isotropic turbulence developed in the 70s. This second presentation by C. Cambon dealt with energy and anisotropy cascades, with a spectral characterization.

**F. Godeferd (LMFA, École Centrale de Lyon, France)** followed with an extended comparison of the previously exposed theories and models applied to relevant flows: rotating, stably stratified turbulence, and flows of conducting fluid in the presence of a magnetic field. In this presentation, the refined dynamics of energy transfer using modal decompositions – toroidal/poloidal, wave/vortex, etc. – permitted to accurately characterize the dynamical properties of each flow, and the reason why structural effects are different, though they may be similar at first glance. This especially applies to the anisotropy of rotating and magnetohydrodynamic (MHD) turbulence, which exhibit an extension of the scales along the axis bearing the rotation or external magnetic vector, but produce very different secular anisotropies.

**K. Schneider (M2P2-CNRS & CMI Université de Provence, Marseille, France)** gave a talk about orthogonal wavelets used to characterize the anisotropy properties of turbulence and its geometrical scale-dependent statistics. This tool extends the spectral analysis to a location-dependent decomposition, that permits a separate analysis of the spectral contents of a turbulent field, and of its localization in space, thus introducing the possibility to consider statistically inhomogeneous flows. In addition, wavelets are also a very efficient signal processing tool that permits the optimal compression of velocity fields, keeping almost

all its interesting features, in terms of vorticity and structure contents. The presentation by K. Schneider included illustrations to rotating, stratified and magnetohydrodynamic (MHD) turbulence).

**F. Moisy (FAST, Université Paris-Sud, France)**, proposed a very pedagogical presentation of the influence of solid body rotation on the dynamics of fluid flows, as well as the latest experimental results of rotating homogeneous turbulence, performed on the Giroflow experimental facility in Paris. Rotation triggers an additional way of transporting energy in turbulence, due to the presence of inertial waves. These waves propagate with a dispersion relation linking the time frequency to the angle of propagation, so that, depending on the initial conditions of isotropic turbulence, the activation of the Coriolis force generates a strong anisotropy in the flow: elongated structures appear along the axis of rotation. The highly debated dynamics of rotating turbulence, and its explanation, was presented in all its aspects, clearly showing that the debate is not yet settled.

**C. Vassilicos (Imperial College, London, United Kingdom)**, presented in a first talk fundamental alternative approaches of homogeneous turbulence, revisiting the existing dogma about the decay laws of turbulence in relation with its spectral scalings. This work is based on new recent experiments in wind tunnels, in which the mode of generation of grid turbulence may produce long lasting effects in the energy transfers, throughout all turbulent scales. The influence of the geometry and shape of the grid is thus demonstrated to be important, and it seems that very long wind tunnels would be required if one wanted to separate all the production effects of classical, fractal, or active grids. In his second talk, Vassilicos discussed the topological aspects of small-scale anisotropy in turbulence channel flows, as well as the mean flow profile near walls.

**A. Llor (CEA Paris, France)** also devoted his talk to fundamental aspects of free turbulence decay, focused on Landau's big scale invariants, first revisited, then producing new ideas for the modelling of the kinetic energy dissipation  $\epsilon$ . Complex theoretical considerations are shown to prevail when one needs to obtain the exponent  $n$  of decay of kinetic energy, as  $k \propto t^{-n}$ . The work by Landau (1944) about the self-similar decay of homogeneous isotropic turbulence was presented, and related to more recent experimental results, not without relations with the previously mentioned talk by Vassilicos. Based upon these founding studies, the anisotropic cases were discussed, to extend the results to turbulence in a slab geometry, a tube, or in the inhomogeneous case for localized turbulent spots.

**R. Antonia (University of Newcastle, Australia)** proposed two talks about theoretical multiscale characterization of turbulence, through the statistics of structure functions in physical space, tested against an extensive experimental database. The first talk was devoted to grid turbulence isotropy, or lack thereof, and reviewed several previous experimental measurements in grid turbulence, with various geometries, and tunnel shapes. Very accurate metrology was used, in order to minimize the experimental bias, so that very subtle anisotropy levels may be evaluated. The second talk by Antonia extended this work to the geometry of turbulence in a channel flow, especially focusing on small-scale

anisotropy. In that case, DNS data are used, since it permits the computation of statistics not attainable by currently available experimental techniques or probes. The speaker identified zones in the channel in which isotropic relationships do apply, in terms of kinetic energy and dissipation, whereas an extension towards the axisymmetric description is required in other parts. The effect of surface roughness, of different shapes and height, was also described.

**F. Anselmet (IRPHE UMR 6594, Marseille, France)** discussed the anisotropy of turbulence in a boundary layer with vegetation. The atmospheric flow is considered in its lowest layer, in which it interacts with vegetation covers. If the latter are dense, the mixing layer analogy is a known result, but when they become sparse, the boundary layer is disturbed in a more complex way. It is therefore important to characterize this boundary layer depending on the characteristic scales of the cover, tree height, leaf area index, ground arrangement, etc., by means of various indicators, among which the invariants of the velocity gradient tensor, in the "anisotropy invariant map" introduced years ago by Lumley.

**G. Matheou (Jet Propulsion Laboratory, California Institute of Technology, USA)** presented a talk about various aspects of stratified turbulence, in the context of turbulence and cloud formation in the atmospheric boundary layer (ABL). With respect to the previous talk by Anselmet, devoted to the lowest levels of the ABL, the layer discussed in Matheou's talk ranges between 1km to 4km in height. Several physical processes are at play at these altitudes, and the formation of clouds in the boundary layer involves a balance of these generating phenomena, interacting with more global circulation phenomena over a planetary level. The Boussinesq approximation is used in DNS of homogeneous stratified turbulence, which exhibit different behaviors in the morphology of turbulence, depending on the value of the relevant non dimensional parameters, including the Froude and the Reynolds numbers.

**S. Tardu (LEGI, Université Joseph Fourier, Grenoble, France)** is a specialist of wall turbulence, and presented very original points of view of the structure and response of a generic boundary layer, including its modelling with dynamical systems theory. Basic concepts were first introduced, in a progressive introduction suitable to doctoral students or non specialists. Then, the regeneration process of self-maintaining coherent structures close to the wall was discussed, analyzing the interaction between two localized disturbances. DNS results were presented in support of this. The link between turbulence and dynamical systems was then illustrated by means of a synchronization phenomenon, identifying a quasi-periodicity in the near-wall structures. Important perspectives of this work concern the control of boundary layer turbulence, and thus the improvement of several industrial devices efficiency, both for internal dynamics, and for external aerodynamics.

**B.J. Boersma (Energy Technology, Delft University of Technology, Delft, The Netherlands)** considered wall turbulence in pipe flows, with a focus on the scaling effects in high Reynolds number turbulent pipe flows. The laminar-turbulent transition in the pipe flow was first introduced, as well as traditional scalings in the turbulent regime. DNS and experimental data

were used to show the performance of a proposed new scaling. Finally, the reduction of turbulent drag in the pipe flow was achieved by the addition of polymer or fiber in the fluid.

**N. Peters (RWTH Aachen University, Institute for Combustion Technology, Germany)** presented two talks, studying first passive scalars in turbulence, then active scalars. His first talk dealt with a new way of analyzing the geometry of turbulence, based on conditional statistics of turbulent vector and scalar fields. The lack of locality of complex flows, that prevents classical homogeneous statistical characterization, is overcome by considering small pieces of the flow amenable to statistical treatment. This leads to the definition of "dissipation elements", and to the identification of principal directions of gradient trajectories, computed in Direct Numerical Simulations. Peters then extended the context in his second talk to more complex situations of turbulent combustion, localizing flamelets on gradient trajectories in scalar fields in turbulence combustion. The context of non premixed conditions is considered, and time scales are duly introduced, characterizing the turbulent mixing one against chemistry ones. The previously exposed gradient trajectories analysis proves to be an invaluable tool to connect dissipation elements in passive scalar fields to the flamelet concept.

**B. Renou (CORIA UMR 6614, Rouen, France)** not only gave the general audience talk, but also presented a talk about stratified combustion, dealing with mixing processes and flame propagation phenomena when high fuel concentration fluctuations are identified. This is observed in real combustion systems in which reaction zones occur mostly in areas in which perfect mixing between fuel and oxidant is not achieved. The lecture concerned both fundamental scientific issues and industrial ones, and extended towards the study of isotropization between the two fluids, oxidant and fuel, exhibit different viscosities.

**M. Gorohkovski (LMFA, École Centrale de Lyon, France)** proposed a subject not unrelated to combustion, in terms of fragmentation: using scaling symmetries, fragmentation was discussed, with background topics presented first in a pedagogical way, then moving to the application of the concepts of fragmentation to the computation of turbulent flow. Theoretically obtained scalings are compared with results of Large Eddy Simulations (LES) using specifically constructed stochastic Subgrid-Scale (SGS) models.

**F.-X. Demoulin (CORIA UMR 6614, Rouen, France)** also proposed a lecture devoted to liquid-gas flows, focusing on the turbulence therein with interface deformation. The density and viscosity jump at the interface plays a role in the evolution of turbulence, for which the theory has to be adapted, also to account for the surface tension. Liquid-gas turbulence is therefore compared, in simulations, with the case of single-phase turbulence, thus extending previous studies in which the density and viscosity contrasts were low, particularly in experiments almost impossible to set up properly. The late P. Comte (Institut PPrime Poitiers, France) was a specialist of LES, especially in compressible flows. He presented an analysis of the effects of anisotropy in coherent structures and of compressibility effects in numerical simulations of turbulent shear flows.

He examined the role of the pressure field generated by subsonic jets and mixing layers in the generating of noise, relating rather subtle indirect mechanisms, unveiled by acoustic analogies and wave packet models, to noisy events. This also helps to grasp the disparity of scales between the turbulence and acoustic fields. Another interesting case presented by Comte, in which the acoustic/turbulence coupling is a strong driving mechanism, is that of a cavity opening in the wall of a turbulent channel. The effect of the Mach number is of course of utmost importance in all cases, although numerical simulations are limited in terms of value of the Reynolds number. The final case of a supersonic boundary layer was finally presented, and permitted to reach a quite high Reynolds number, higher than that in the previously mentioned cases. DNS was also shown to be a valuable tool for investigating different cases hardly reachable in experiments, such as different boundary conditions at the walls, adiabatic or not.

**M. Cazalens (SNECMA, Paris, France)** provided a very nice and appreciated link between the previously mentioned complex phenomena, compressibility, combustion, fragmentation, multiscale turbulent aspects, viewed mostly from an academic point of view, and modelling issues in actual flows, such as combustion chambers in jet engines. This lecture presented all the questions engineers are faced with when designing turbo-props or turbo-engines, and was particularly clear in identifying the key issues, in terms of models or understanding of phenomena, separate from purely technological ones. It provided all the academic attendants with food for thought in how to better orient their researches, in view of application, or even simply on how to communicate about them and present them in an way adapted to a broader audience.

**A. Naso (LMFA, École Centrale de Lyon, France)** extended statistical mechanics, classically used in physics, to the analysis of the axisymmetric Euler equation, with a comparison in the case of a Von Karman flow. The 2D Euler equations was presented as an introduction of the concepts of statistical mechanics applied to fluids, then Naso generalized the application of the theory to the 3D axisymmetric Euler equation. Steady Beltrami flows are calculated in a cylindrical box, and it is shown that the total imposed helicity and angular momentum in the fluid are crucial parameters. The bifurcation of the flow structure from a one-cell distribution to a two-cell one, either symmetric or asymmetric, is shown to result from a switch between steady states predicted by the theory. The talk eventually enlarged the point of view to the study of inhomogeneous and anisotropic turbulent flows.

Two talks were joint presentations devoted to Lagrangian aspects of turbulence. First, small scale anisotropy in Lagrangian turbulence was presented by **M. Bourgoïn & R. Volk (Laboratoire de Physique, ENS Lyon, France)**. The Lagrangian characterization of turbulence is done using advanced measurement techniques in high intensity closed turbulence, using the same Von Karman context as previously presented by Naso. Among other statistics, both second-order Lagrangian structure function and the Lagrangian velocity spectrum provided impressive results about the asymmetries of the large-scales, reflected in the smallscale statistics. The authors demonstrated the implication to stochastic modelling of turbulence and turbulent dispersion, which are important for e.g. environmental studies.

The second joint lecture was given by **M.-P. Rast (Laboratory for Atmospheric and Space Physics, Department of Astrophysical and Planetary Sciences, University of Colorado, Boulder, USA) & J.-F. Pinton (Laboratoire de Physique, ENS Lyon, France)**. The lecturers investigated the pair dispersion in turbulence, first, in terms of scalings, second, in terms of distributions. The approach is original in that a model flow is used to support the trajectography of fluid particles. The dynamics is shown to be dominated by the very wide distribution of the duration for which particle pairs behave as a single particle, until they eventually exhibit a signi-

cant separation. Probability distributions are used to characterize the distribution of the particles, depending on their initial separation. The modification of shape of this distribution at large initial separation suggests a different way of modelling the structure of real 3D turbulence.

**C.M. Casciola (Dipartimento di Ingegneria Meccanica e Aerospaziale Università di Roma La Sapienza, Roma, Italy)** divided his two talks in three topics. The first one was devoted to energy fluxes in anisotropic turbulence in wall-turbulent flows. Two dynamical processes are identified as driving mechanisms for the fluxes, one in the near wall region and a second further away from the wall. The second talk was devoted to particle clustering in anisotropic turbulent flows, with a characterization of the statistics of particle pair relative velocity in homogeneous shear flow, and also considering inertial particles. The third and last part extended the analysis of particle clustering to the case of turbulent jet flames. It is shown that, in reacting flows, the abrupt acceleration of the fluids across the thin flame front due to combustion adds new and unexpected features with respect to the previous cold flow turbulence analysis. A particularly striking result, and difficult to explain, is the enhanced clustering that occurs in the flame brush region. The role of the inertia of the particles is also investigated in relation to their distribution.

The last part of the school touched upon a most specific context, that of quantum turbulence, with two talks devoted to it.

**I. Danaïla (Université Pierre et Marie Curie, Laboratoire Jacques-Louis Lions, Paris, France)** started with vortex configurations in rotating Bose-Einstein condensates. After an experimental observation of these condensates, with pictures impressive but rather fuzzy, the 3D numerical simulations of the Gross-Pitaevskii equations by Danaïla provide a strikingly clear picture of how the quantization of vortices produces given shapes, in rotating Bose-Einstein condensates. The experimental-DNS agreement is quite impressive in view of the involved scales, which are much smaller than what a turbulence dynamicist is used to.

**M. Tsubota (Department of Physics, Osaka City University, Japan)**, provided a review on quantum turbulence, observed in superfluid helium and in atomic Bose-Einstein condensates also presented by Danaïla. Surprisingly, the recent theories about quantized vortices provide a picture of quantum turbulence which is simpler than conventional turbulence. Of course, models for the two cases are much different, but it is sometimes important to try to cross-breed between different disciplines.

### 3 Final comments

This school was a preliminary attempt at providing a common emphasized effort devoted to the characterization of anisotropy in turbulent flows. It has first demonstrated that all classes of flows are concerned: geophysical and astrophysical flows, industrial flows, environmental flows, reacting flows, MHD turbulence, etc. Even in academic flows, such as freely decaying grid turbulence in wind tunnels, or the Von Karman experiment, which were at first thought to provide to some extent a good approximation of isotropic turbulence in some regions, careful experimental measurements and refined statistics show that the level of observed isotropy depends on the characterization technique. Indeed, anisotropy may appear at different scales and in different regions, so that a universal characterization is hard to come by. The link between the Eulerian aspects and the Lagrangian ones is also a complexifying factor in the global study. The summer school “ANISO” nonetheless demonstrated that serious advances have been done during the recent years, towards characterizing some anisotropic features of turbulence in specific contexts. It seems, however, that an integrated effort of the community is still missing, whose objective would be the exhaustive compilation of all these attempts, and the extraction of generic phenomena. The goal is of course to reach a universal theory, much as what was proposed by Kolmogorov sixty years ago. A quantum step of progress is certainly not in view, but intermediate ones are within reach, starting with axisymmetric flows, and progressively introducing additional complex effects, with coupling with body forces, internal or external sources, and the all important question of the influence of initial conditions onto the short and long-term evolution of anisotropic turbulence.

### Acknowledgements

The organizers wish to thank the Agence Nationale de la Recherche for the funding of the ANISO project number 340803, which helped organize the summer school. Other sponsors also provided the necessary support without which the school could not have been organized. We are therefore thankful to the following institutions:

- Centre National de la Recherche Scientifique
- Association Française de Mécanique
- ERFOCTAC
- SNECMA, SAFRAN group, an industrial sponsor
- Laboratoire de Mécanique des Fluides et d’Acoustique UMR 5509
- CORIA Laboratory, UMR 6614
- Laboratoire des Écoulements Géophysiques et Industriels UMR 5519

### References

- [1] <http://www.coria.fr/spip.php?article636>
- [2] ANISO 2011 summer school, book of abstracts
- [3] <http://www.iesc.univ-corse.fr/>

# NEW CHALLENGES IN TURBULENCE RESEARCH II

A. Naso<sup>1</sup>, M. Bourgoïn<sup>2</sup>, A. Pumir<sup>3</sup> and B. Rousset<sup>4</sup>

<sup>1</sup> LMFA, CNRS (UMR 5509) & Ecole Centrale de Lyon, 36 avenue Guy de Collongue,  
69134 Ecully Cedex, France

<sup>2</sup> LEGI, CNRS (UMR 5519) & Université Joseph Fourier, 1025 rue de la piscine - BP 53,  
38041 Grenoble Cedex 9, France

<sup>3</sup> Laboratoire de Physique, CNRS (UMR 5672) & Ecole Normale Supérieure de Lyon, 46 allée d'Italie,  
69364 Lyon cedex 7, France

<sup>4</sup> SBT, CEA/DSM/INAC/SBT/GRTH, 17 rue des Martyrs,  
38054 Grenoble Cedex 9, France

Report on the Spring School

## 1 Motivations and organization

The school “New challenges in turbulence research II” aimed at conveying the core knowledge of the advanced understanding of turbulence to researchers in different fields. For this, a series of comprehensive courses has been given by invited speakers. The expected audience included PhD students, postdocs, as well as junior and senior researchers from different communities. Courses have been given in the following four axes:

- anisotropic and/or inhomogeneous turbulence
- transport of material particles
- cryogenic turbulence
- theories and models

The five-day school took place at the Ecole de Physique, in Les Houches. The audience was made of 55 participants: 20 PhD students, 9 postdocs and 26 junior and senior researchers. 12 lectures (one and half-hour, including questions) and 11 short presentations (half an hour) were given. All the talks have been recorded (audio files). The speakers’ voices are currently synchronized with their slides. The resulting files will be available on the school’s website.

## 2 Content of the talks

The programme of the school can be found in Figure 1. We give here the titles and abstracts of the lectures.

**Marc Brachet: Interplay between the Beale-Kato-Majda theorem and the analyticity-strip method to investigate numerically the incompressible Euler singularity problem**

The lecture starts by a review of the 3D incompressible Euler singularity problem and then follows the preprint <http://arxiv.org/abs/1112.1571>. Numerical simulations of the incompressible Euler equations are performed using the Taylor-Green vortex initial conditions and resolutions up to 4096<sup>3</sup>. The results are analyzed in terms of the classical analyticity strip method and Beale, Kato and Majda (BKM) theorem. The BKM criterium on the growth of supremum of the vorticity, applied on the same time-interval, does not rule out the occurrence of a singularity around  $t \approx 4$ .

These new findings lead us to investigate how fast the analyticity strip width needs to decrease to zero in order to sustain a finite-time singularity consistent with the BKM theorem. A new simple bound of the supremum norm of vorticity in terms of the energy spectrum is introduced and used to combine the BKM theorem with the analyticity-strip method. It is shown that a finite-time blowup can exist only if  $\delta(t)$  vanishes sufficiently fast at the singularity time. Our main conclusion is that the numerical results are not inconsistent with a singularity but that higher-resolution studies are needed to extend the time-interval on which a well-resolved power-law behavior of  $\delta(t)$  takes place, and check whether the new regime is genuine and not simply a crossover to a faster exponential decay.

**Bernard Castaing: Superfluids and turbulence**

Concerning turbulence, superfluids present differences with classical fluids, but also similar behaviours. This talk proposes to introduce, in the simplest possible way, the relevant characteristics of the physics of superfluids.

**Laurent Chevillard: Vorticity stretching mechanism in turbulence**

We review in this talk experimental and numerical facts about the Lagrangian dynamics of the velocity gradient tensor in homogeneous and isotropic turbulence. Consequences for the vorticity production mechanism are given. We finally discuss the implications of these facts for turbulence modeling. Francesca Chilla: Turbulent thermal convection: old and new issues The Rayleigh-Bénard convection is in principle one of the simplest convective systems to be studied. Turbulent thermal convection is often present in common geophysical or industrial situations, at the same time the turbulent state of Rayleigh Bénard convection is less understood and more difficult to achieve in controlled laboratory conditions. To study turbulent state is necessary to explore Rayleigh numbers larger than 10<sup>6</sup> and several orders of magnitude in Ra are necessary. In the last 20 years improvements have been done thanks to new experimental techniques (as PIV measurements) and the use of exotic fluids as gases near the critical point that allows to reach  $Ra = 10^{16}$ . Improvements in computation power also allow presently to run numerical simulations till  $Ra = 10^{12}$ . Nevertheless lot of points remain unclear, the behaviours of Nusselt number as function of Rayleigh number is not

completely elucidated, particularly for  $Ra > 10^{12}$ . A situation of multistability seems to appear, but the mechanism of selection of every particular state is not clear. A point will be done on the recent results and present axes of research. Particularly they will be presented new kinds of convective flow as asymmetric Rayleigh-Bénard convection and convective channel flow.

**Luminita Danaila: Turbulent mixing in isotropic and anisotropic (axisymmetric) flows**

A remarkable property of turbulence is its ability to enhance the mixing of scalar contaminants, either passive or active. Consequently, the accurate prediction and/or control of these phenomena requires a thorough understanding of scalar mixing in turbulent flows and its dependence on (or, interconnection with) the dynamic field which transports it. This talk is focused on turbulent, passive and active scalar mixing, characterized by using analytical and experimental tools. Three issues will be addressed:

1. One-point characterisation of gaseous (Schmidt number,  $Sc=1$ ) mixing, via e.g. the scalar probability density function (Pdf)
2. Two-point characterisation of gaseous ( $Sc=1$ ) mixing. The question is: Can we predict mixing from velocity field statistics?
3. One and two-point characterisation of gaseous, variable viscosity mixing.

**Davide Duri: High Reynolds cryogenic turbulence experiments: challenges and hurdles**

The objective of this lecture is to make the audience feel the challenges, hurdles and difficulties involved in performing turbulence experiments at cryogenic temperatures. After a brief introduction about the current experimental needs in term of high Re numbers controlled turbulent flows and the different ways to achieve this ultimate goal I will focus on the advantages and disadvantages of using cryogenic gaseous and liquid  $^4He$  as a working fluid. The superfluid nature of the liquid phase He II at temperatures lower than 2.17 K will be briefly discussed with respect to the classical framework of developed turbulence [7]. In the second part I will focus on the different mechanical, thermal and hydraulic problems that intervene in the design of a cryogenic wind tunnel along with the solutions adopted. As example I will use a newly developed cryogenic liquid  $^4He$  facility specifically designed to perform high Re numbers classical and quantum turbulence experiments [8]. The third part is devoted to the cryogenic sensors. I will briefly describe the available state-of-the-art sensor capable to work at cryogenic temperatures before focusing on the recent developments in hot-wire anemometry and vorticity scattering measurements. Preliminary results obtained in an axisymmetric jet at  $Re_\lambda$  between 1000 and 2000 will be also presented. I will conclude with a perspective on the future experimental challenges.

**Rudolf Friedrich: Kinetic equations for turbulent cascades**

The talk intends to provide an introduction to the application of kinetic equations for the statistics of turbulent flows. We will focus both on the inverse cascade in two dimensional flows as well as the direct cascade in homogeneous isotropic three dimensional turbulence. Furthermore, we discuss kinetic equations for the temperature statistics of Rayleigh-Bénard convection. Direct cascades in three dimensions will

be analyzed by the statistics of the vorticity field, which is characterized by the presence of Burgers-like vortices. We will explicitly show that the statistics of the vorticity field is strongly non-Gaussian and we will trace this nonnormality back to the presence of strong vorticity events. We shall discuss how the wings of the vorticity probability distribution can be related to the properties of these coherent structures. Two dimensional cascades will be investigated on the basis of a generalized Onsager vortex model explicitly showing that the energy transfer from small to large scales arises due to a clustering of like-signed vortices [1, 2, 3, 4, 5, 6].

**Fabien S. Godeferd: Multiscale characterization of anisotropy in axisymmetric turbulence**

Several questions can be raised when one tackles the problem of anisotropy in turbulence, related to: its link with inhomogeneity; the statistical tools to be used; the multiscale character of anisotropy; the link between Eulerian and Lagrangian anisotropy; the modified dynamics of turbulence; long lasting effects of non isotropic initial conditions; the role of forcing; etc. We mainly consider the case of axisymmetric turbulence, for which a series of experiments, simulations, and natural contexts, are available, and we illustrate instances of flows with mean velocity gradients, rotating turbulence, stably stratified turbulence, and conducting flows with an imposed external magnetic field, to start with. We review a few of the statistical tools that have been introduced to characterize anisotropic turbulence, using both tensorial decomposition in physical space (e.g. by Reynolds & Kassinos) or in spectral space. In the latter case, modal decompositions can be proposed, to yield simplifications linked with the linear operators that trigger anisotropy. We also propose a comparison of the statistics of turbulence obtained for the above-mentioned axisymmetric turbulent flows with those of isotropic turbulence, in terms of scaling of the two-point velocity correlation spectra, as well as its implication on the dynamics, with a more complex energy transfer than the standard downscale one.

**Mikhael Gorokhovski: Eddy-fragmentation under scaling symmetry**

We discuss here the eddy-fragmentation process under scaling symmetry, and its application to a high Reynolds number channel flow.

**Michel Lance: Bubbles, Turbulence, and Bubbulence...**

Two-phase bubbly flows can be found in a variety of natural phenomena and industrial processes, such as air entrainment in ocean, cavitation, boiling, chemical plants, or bioreactors. The main interest is to predict the size and spatial distribution of the gas bubbles, and their effect on mass, heat and momentum transfer in the liquid phase. In most applications, the bubble mean diameter is not small compared to turbulence length scales, and gravity effect are significant. The dynamics of bubbles in a turbulent field mostly escapes from the passive scalar range and belongs to the domain of the so-called inertial particles. Moreover, the velocity field induced in the liquid by the random motions of the bubbles and the vorticity produced in their wake give rise to pseudo-turbulent fluctuations, which one could nickname bubbulence. Interaction between turbulence and bubbulence is still debated. The aim of this course is to provide an introduction of this field, starting from the

bubble dynamics, to the question of the energy spectra in bubbly flows, with some detour to the modeling for practical applications.

**Sergey Nazarenko: Superfluid Turbulence - focus on small scales**

Superfluid Turbulence at large scales is believed to be similar to the classical Kolmogorov turbulence. The main differences with the latter arise when the energy cascade reaches scales of the order of the intervortex separation. At such small scales the quantum discrete nature of the superfluid vortices becomes crucial. This is where most interesting albeit least understood processes occur. Currently, this range of scales is not directly accessible in experiments, and is difficult to access even in numerical experiments. I will outline various theoretical ideas and approaches for describing the small-scale turbulence near and below the inter-vortex scale, review the possible roles of the vortex line reconnections and Kelvin wave turbulence. We will also examine recent numerical results and ideas on how to refine the numerical experiment for testing the existing theories.

**Philippe-Emmanuel Roche: Turbulence of superfluid  $^4\text{He}$ : a tour of 6 experiments & 1 simulation**

Following the preceding introductory course on superfluid turbulence (B. Castaing), this lecture will present 6 experiments and 1 simulation of  $^4\text{He}$  turbulence at finite temperature. Phenomenological and quantitative aspects of “the two-fluid cascade“ will be introduced step by step, to interpret the outcome of each experiment, or to illustrate present challenges in our understanding of superfluid turbulence.

We give here the titles of the short presentations:

**Wouter Bos:** Depletion of nonlinearity and self-organization in turbulence and mixing

**Claude Cambon:** Cascade in strongly anisotropic turbulence and related alteration of cubic correlations dynamics

**Ionut Danaila:** High order numerical methods for the simulation of Bose-Einstein condensates

**Lionel Fiabane:** Do finite size inertially buoyant particles cluster?

**Rainer Grauer:** Three short stories in turbu-

lence and singularities

**Eric Herbert:** Phase transition in turbulent flows

**Clément Jause-Labert:** Confined turbulent flows submitted to rotation effects

**Oliver Kamps:** Relating Eulerian and Lagrangian statistics in turbulent flows

**Robert Kerr:** Fully developed hydrodynamic turbulence from a chain reaction of reconnection events

**Emmanuel Lévêque:** Probing large-scale unsteadiness of turbulent flows by means of adaptive Kalman filtering – Application to the large-eddy simulation of turbulent engineering flows

**Robert Zimmermann:** Dynamics of an inertial-scale particle in turbulence

## References

- [1] M. Wilczek and R. Friedrich, Dynamical Origins for Non-Gaussian Vorticity Distributions in Turbulent Flows, *Phys. Rev. E* 80, 016316 (2009)
- [2] M. Wilczek, A. Daitche and R. Friedrich, Theory for the single-point velocity statistics of fully developed turbulence, *EPL*, 93 34003 (2011)
- [3] M. Wilczek, A. Daitche and R. Friedrich, On the velocity distribution in homogeneous isotropic turbulence, *J. Fluid Mech.*, first view article (2011)
- [4] J. Lulff, M. Wilczek and R. Friedrich, Temperature Statistics in Turbulent Rayleigh Bénard Convection, *New J. Phys.* 13, 015002 (2011)
- [5] R. Friedrich, M. Vosskuhle, O. Kamps and M. Wilczek, Two-Point Vorticity in the Inverse Turbulent Cascade, arXiv:1012.3356 (2010)
- [6] J. Friedrich and R. Friedrich, Vortex model for the inverse cascade of 2d-turbulence, arXiv:1111.5808
- [7] W.F. Vinen and J.J. Niemela, Quantum turbulence, *J. Low Temp. Phys.* 128, 167 (2002)
- [8] D. Duri, C. Baudet, P. Charvin, J. Virone, B. Rousset, J.M. Poncet and P. Diribarne, Liquid helium inertial jet for comparative study of classical and quantum turbulence, *Rev. Sci. Instrum.* 82,115109 (2011)

# SIMULATION OF MULTIPHASE FLOWS IN GASIFICATION AND COMBUSTION

Christian Hasse, Dominique Thévenin, Luc Vervisch

*September 18-20, 2011, Dresden, Germany*

## 1 Introduction

The first Ercoftac Conference on Simulation of Multiphase Flows in Gasification and Combustion took place in the Hilton Hotel in Dresden from September 18-20, 2011. It was organized by the Virtuhcon centre of the University of Technology Freiberg. The organizing committee responsible for the scientific program was Christian Hasse (University of Freiberg), Dominique Thévenin (University of Magdeburg), Luc Vervisch (INSA Rouen & CNRS CORIA).

The original idea for the conference was to bring together experts from the two scientific disciplines gasification and combustion with a special focus on modeling. Many gasification processes are a combination of combustion in the near nozzle region and a reforming zone under fuel rich conditions in the post flame region. Despite the apparent overlap between gasification and combustion, as of now, there is only limited direct interaction between the two communities. However, it has been recognized recently that both disciplines have much in common and sharing models and tools can be quite beneficial. They are both multi-scale and multi-physics high temperature conversion processes. Based on this, some of the models developed over the last decade, e.g. models for pyrolysis and heterogeneous reactions of coal or models for turbulence-chemistry interaction, could be used and adapted for either physical problem with appropriate care. The regime, e.g. defined by the chemical and turbulent time scales, as well as the boundary conditions, e.g. the overall stoichiometry, are different, but this opens up excellent opportunities for further model development and validation.

## 2 Participants

Despite the fact that this was the first conference focussing on modeling of both gasification and combustion, the organizers were happy to welcome 113 participants from 19 countries including USA, South Africa, Canada, South Korea, China as well as 14 European countries.

## 3 Event description

Based on the submitted contributions, the scientific program was split into 28 oral and 7 poster presentations. The oral presentations were organized by topics into 7 sessions. Extended abstracts of all accepted contributions were collected in a booklet.

In additions, four invited lectures were given by

- Henning Bockhorn (KIT Karlsruhe, Germany): Simulation of soot in combustion systems: black magic or knowledge-based modeling?
- Julien Réveillon (University of Rouen, France): Towards fully coupled modeling of liquid atomization and dispersed spray.
- Ashwani Gupta (University of Maryland, USA): Benchmark experiments for gasification modeling.
- Perrine Pepiot (Cornell University, USA): Biomass gasification for biofuel synthesis: a modeling approach to the tar problem.

The presentations were followed by a discussion covering all contributions for one session. A major point of interest was the availability of suitable validation data for gasification processes. As in combustion, such high quality data (generated out of workshops such as TNF) would support model development for oxyfuel combustion and gasification (gasification usually operates with pure oxygen as oxidizer) significantly. Furthermore, the need for reference data of laboratory flames with solid feedstocks, e.g. biomass and coal, was discussed.

Due to scientific quality of the contributions, a special track gasification-01 for a special issue of Flow Turbulence and Combustion was created by Springer. Authors of accepted contributions were invited to submit full length articles until end of February 2012.

## Acknowledgements

The organizers gratefully acknowledge the financial support from the Federal Ministry of Education and Research of Germany and the Saxon Ministry of Science and Fine Arts in the framework of Virtuhcon. Furthermore, special thanks are addressed to ERCOFTAC for financial support and the promotion of the event.

# WORKSHOP 'ASTROFLU II' ORGANIZED BY HENRI BÉNARD PILOT CENTER, SIG 4 AND SIG 35

Claude Cambon, Alexandre Pieri and Fabien S. Godefert

*Laboratoire de Mécanique des Fluides et d'Acoustique, UMR 5509,  
École Centrale de Lyon, 69134 Ecully cedex, France*

*December 15, 2011, Ecole Centrale de Lyon, France*

## 1 Motivations and objectives

Based on the success of our first event 'ASTROFLU', principally organised by the Henri Bénard pilot center in Lyon [November 12-13, 2008] the aim of this new workshop 'ASTROFLU II' was to once again gather researchers specialized in fluid dynamics, coming from various communities physics, engineering, astrophysics, and mathematics –, in order to exchange ideas and collaborate on common interests. ERCOFTAC scholarships were used to support three young, doctoral and post-doctoral, students.

The first ASTROFLU workshop was devoted to pulsating stars, justified by shared interests on *highly compressible flows*, theory, computation and modelling, and with particular emphasis on shock/turbulence interactions. During ASTROFLU II, we focused on the quite wide theme *rotating shear flows*, which was only partially covered; we therefore plan to expand further this research area in a coming workshop.

There is a strong parallel between accretion discs, which include rotation, in the astrophysical applications, and rotating shear flows in geophysics (ocean, atmosphere), and in engineering (turbomachinery). The models we use are often very similar, but with variable terminologies often published in separate journals. For instance, in astrophysics, the linear spectral method is known as the 'shearing box' approximation, but is called 'Rapid Distortion Theory' in fluid mechanics (e.g. [12].) Its nonlinear extension by direct numerical simulation (DNS) in astrophysics is also very similar to the pseudo-spectral DNS (Orszag/Patterson) using coordinates following the mean shear (Rogallo). These various terminologies come naturally from the different sources of shear in astrophysics and geophysics. In the first case, differential rotation is the origin of high velocity gradients in the plane parallel to the rotation axis, while in the second case shear results from strong winds and is considered parallel to the rotation axis. There is a large scientific network of astrophysicists engaged in the study of rotating accretion disks, with or without the effects of stratification and MHD: François Rincon and Carlo Cossu (Toulouse), Gordon Ogilvie, Michael Proctor (DAMTP, Cambridge), to cite but a few, and also in other countries. Exchanges between fluid dynamicists and astrophysicists are essential to the development of these research fields. More generally, these themes, in astrophysics, can be broadened towards topics including the interstellar medium, the formation and evolution of stars, and more specifically on solar physics.

## 2 Round table and proposals

It was decided to give to Jean-Paul Dussauge (IUSTI, Marseille) the responsibility for the SIG 4, 'Turbulence in compressible flows', at least temporarily, to replace the late Pierre Comte.

We initially planned to involve the Centre Blaise Pascal in Lyon, a structure devoted to the extension of numerical modelling and formation of scientists in high performance computing. By want of time during the workshop, this is left for future activities that will also form part of the project portfolio of the Centre Blaise Pascal. Our aim is to improve the communication between different groups or individuals disseminated in the Lyon-Grenoble area but also at a wider scale. At the national scale, this is an opportunity to involve all the French Pilot Centres, as well as SIG 4 and SIG 35 'Multipoint turbulence structure and modelling'. More generally, all activities of SIGs, 4, 39 'aeroacoustics', and 35 were discussed in both 'hydro' and 'astro' contexts, from highly compressible flows to quasi-incompressible ones.

Another more technical discussion dealt with the analogies of the numerical method of Rogallo, popular in engineering and geophysics, and the most recent one of Lesur (from his Ph. D. in 2007, 'Snoopy' code), increasingly used in astrophysics, following the 'shearing sheet approximation' for accretion discs with differential rotation as turbulent flows subjected to both constant space-uniform shear and constant angular velocity.

## 3 Contents of the talks

**Denis Gillet (Observatoire de Haute Provence, France)** presented the 'Effects of compressibility in gases with shock-waves'. He gave a large overview of shock-wave configurations, from engineering to astrophysics [6]. In addition to the case of reentry of aeronefs in the high Earth's atmosphere, astrophysical cases show the specificity of radiative shocks. With respect to engineering cases, dramatic changes concern the thickness of the shock waves, including precursors, and the relationship of Mach number with total compression rate (or volumetric ratio) across the shock-wave [5]. Compression rates are found to be much larger than the usual non-radiative Hugoniot limit  $(\gamma - 1)/(\gamma + 1)$ .

**Lionel Larchevêque (IUSTI, Marseille, France)** presented 'Large scale organization in shock wave/turbulent boundary layer interaction' [1]. Analyses of the experimental and computational database on shock/boundary layer interaction from IUSTI reveal that all the interactions under consideration result in a similar normalized space/frequency distribution, even

for incipient separations. Moreover, the mixing layer developing over the interaction region has some canonical features. Vortical structures associated with the mixing layer drive most of the kinematics of the reflected shock. Other vortical structures with lower frequencies are nonetheless found within the interaction region. They produce a strong modulation of the flow in the spanwise direction and could be related to centrifugal instabilities.

**Christophe Bailly (LMFA, Ecole Centrale de Lyon, Ecully, France)** presented 'Jet noise: from laboratory to infrasonic scales.' Numerical results are obtained from a unique LES approach [3] to both the radiated noise (far field) and to the near field, even at low and moderate Mach number. The case of the noise of a subsonic round jet is presented, with very good agreement of calculation with experimental data. Underexpanded jets with Mach discs are then considered to illustrate interactions with shock waves [2]. Finally, the propagation of the sonic boom, with infrasonic scales, is shown and calculated in the atmosphere.

**Geoffroy Lesur (Institut de Planétologie et d'Astrophysique, Grenoble, France)** presented 'The baroclinic instability in accretion discs: vortex amplification and evolution' [9, 10]. The baroclinic effect results from a misalignment of the entropy gradient with the gravitational acceleration, but is different from the one in the atmospheric case, given its coupling with the dominant shear. Differential rotation with radial variation of angular velocity  $\tilde{\Omega}(r) \sim r^{-q}$  yields a radial shear rate  $S$  and a constant rotation parameter  $S/(2\Omega) = -2/q$ . The important case of the Keplerian disc, with self-gravity balanced by the centrifugal force, corresponds to  $q = 3/2$ , so that  $S/(2\Omega) = -4/3$ , and stability is found according to the Rayleigh criterium, consistently with criteria of Bradshaw and Tritton for rotating shear in engineering. Various effects of additional growth rate for transition to turbulence are discussed, including stratification, MHD coupling and compressibility. In particular, the analysis may account for a differential rotation, which is corrected by the radial stratification, possibly rendering sub-Keplerian the distribution of angular velocity.

**Thierry Lehner (LUTH, Observatoire de Paris/Meudon, Meudon, France)** presented a large survey of studies in rotating and precessing shear flows, both experimental and theoretical [14, 15]. Experiments with and without MHD use water or liquid metal (gallium, sodium), and different geometries of tanks, cylinders (Meudon, IRPHE Marseille, Dresden) as well as spheres. The role of centrifugal and elliptic instabilities was discussed independently of geometry – in the volume, far from boundaries – using mainly classical modal hydrodynamic stability and extended Rapid Distortion Theory. Additional MHD effects, with the important case of MRI (MagnetoRotational Instability), was shown to alter classical instabilities, either elliptical, in the precessing flow case [15], or centrifugal with additional stratification in the classical shearing sheet approximation [16].

**Alexandre Pieri (LMFA, Ecole Centrale de Lyon, Ecully, France)** presented 'Numerical study of turbulence within a baroclinic context.' Combined effects of rotation, stratification and shear are a common feature of geophysical fluid dynamics. The misalignment of vertical system rotation and spanwise

mean-shear-vorticity induces a mean vorticity component in the streamwise direction, and this is exactly balanced by an additional buoyancy gradient in the horizontal direction. This is similar to the 'geostrophic front adjustment' in geophysical flows. Accordingly, combination of both vertical and additional horizontal mean stratification results in tilting the isopycnal lines, triggering the baroclinic instability. The linear stability analysis of Salhi & Cambon [13] in the above context is continued here using a stochastic RDT-based Kinematic Simulation model, whose results are compared to DNS ones. From the three basic frequencies,  $2\Omega$  (system vorticity),  $S$  (vertical shear rate) and  $N$  (Brünt-Väisälä frequency for vertical stratification), are defined the Richardson number  $Ri = N^2/S^2$  and the baroclinicity parameter  $\epsilon = S\Omega/N^2$ , which control the instability. New results show the kinetic energy growth rate and the development of Reynolds stress tensor anisotropy, as well as a detailed budget and a diagram in the parameter's space. With respect to the stratified shear case without Coriolis effect, the limit for instability is shifted from  $Ri \sim 0.1$  to  $Ri = 1$ . Finally, a dramatic transient growth is studied for  $Ri$  slightly larger than  $Ri = 1$ , in connection with bypass transition, using a generalized 'vortex-wave' decomposition [4].

**Jacques Masson (Ecole Normale Supérieure de Lyon, France)** presented 'Non-ideal MHD effects on low-mass star formation.' Our knowledge of star formation is, in broad lines, complete, but both theoretical and observational details are yet to be accurately understood. The physics of star formation is based on fluid mechanics [8], and therefore have a lot to share with this area. Magnetic fields have become in the last years a key point of star formation too [7], and it is only in the very last years that we have started to add non-ideal effects, which are of great importance to explain what is seen by observers (for example, the absence of very massive disks around low mass stars).

**Nicolas Plihon (Ecole Normale Supérieure de Lyon, France)** talked on the transition from hydrodynamic turbulence to MHD turbulence in von-Kármán (VK) flows [11]. The influence of an externally applied magnetic field on flow turbulence is investigated in liquid-gallium VK swirling flows. Time-resolved measurements of global variables (such as the flow power consumption) and local recordings of the induced magnetic field are made. From these measurements, an effective Reynolds number is introduced as  $Rm_{eff} = 3DRm(1 - \alpha\sqrt{N})$ , so as to take into account the influence of the interaction parameter  $N$ . This effective magnetic Reynolds number leads to unified scalings for both global variables and the locally induced magnetic field. In addition, when the flow rotation axis is perpendicular to the direction of the applied magnetic field, significant flow and induced magnetic field fluctuations are observed at low interaction parameter values, but corresponding to an Alfvén speed  $v_A$  of the order of the fluid velocity fluctuations  $u_{rms}$ . This strong increase in the flow fluctuations is attributed to chaotic changes between hydrodynamic and magnetohydrodynamic velocity profiles.

## References

- [1] L. Agostini, L. Larcheveque, P. Dupont, J.-F. Debieve and J.-P. Dussauge. *Zones of influence and shock motion in a shock-boundary layer interaction*. AIAA Journal to appear, 2011.
- [2] C. Bogey, N. de Cacqueray and C. Bailly. *A shock-capturing methodology based on adaptative spatial filtering for high-order nonlinear computations*. J. of Comput. Phys. 228(5), 1447-1465, 2009
- [3] C. Bogey, O. Marsden and C. Bailly. *Large-Eddy Simulation of the flow and acoustic fields of a Reynolds number 105 subsonic jet with tripped exit boundary layers*. Phys. Fluids 23, 035104, 1-20, 2011
- [4] D. Chagelishvili, A. G. Tevzadze, G. Bodo and S. S. Moiseev. *Linear mechanism of wave emergence from vortices in smooth shear flows*. Phys. Rev. Lett. 79, 3178., 1997
- [5] Y. A. Fadeyev and D. Gillet. A& A, 420, 423, 2004
- [6] Gillet, J. -F. Debieve, A. B. Fokin and S. Mazaauric. A & A, 332, 235.1998
- [7] P. Hennebelle and R. Teyssier. *Magnetic processes in a collapsing dense core. II. Fragmentation. Is there a fragmentation crisis ?* A & A, 477, 25-34. 2008
- [8] R. B. Larson. *Numerical calculations of the dynamics of collapsing proto-star*. Mon. Not. R. Astr. Soc., 145, 271, 1969
- [9] G. Lesur and J. C. B. Papaloizou. *On the stability of elliptical vortices in accretion discs*. A & A, 498, 1, 2009
- [10] G. Lesur and J. C. B. Papaloizou. *The subcritical baroclinic instability in local accretion disc models*. A & A, 513, 60, 2010
- [11] G. Verhille, R. Khalilov, N. Plihon, P. Frick and J.-F. Pinton. *Transition from hydrodynamic turbulence to magnetohydrodynamic turbulence in von-Kármán flows*. J.Fluid Mech. DOI:10.1017/jfm.2011.522, 2011
- [12] P. Sagaut and C. Cambon. *Homogeneous Turbulence Dynamics*. Camb. U. Press, New York, 2008
- [13] A. Salhi and C. Cambon. *Advances in RDT, from rotating shear flows to the baroclinic instability*. J. Appl. Mech., 73, 449-460, 2006
- [14] A. Salhi and C. Cambon. *Precessing rotating flows with additional shear: Stability analysis*. Phys. Rev. E, 79, 036303, 2009
- [15] A. Salhi, T. Lehner and C. Cambon. *Magnetohydrodynamic instabilities in rotating and precessing sheared flows: An asymptotic analysis*. Phys. Rev. E, 82, 016315, 2010
- [16] A. Salhi, T. Lehner, F. S. Godeferd and C. Cambon. *Magnetized stratified rotating shear waves*. Phys. Rev. E 85, 026301, 2011

# THE FRANCE WEST PILOT CENTER REPORT

L. Danaila

*CORIA, UMR 6614, University of Rouen, Saint Etienne du Rouvray, FRANCE*

## 1 Introduction

The France West Pilot Centre was formed by Dr. Jean-Paul Bonnet (PPRIME Laboratory, Poitiers), with the objective of promoting exchanges between academic institutions and industry, within the subject area of ERCOFTAC. After 2006, Pr. Pierre Comte became the chair of the France West Pilot Center, and several meetings have been organised since then, at least one per year. Some of them are common with the biennial meetings of the French Research Group GdR 'Turbulence' (French 'Groupement de Recherche'), where most of the laboratories members of France west PC are active.

The active members are the following laboratories and institutions:

- PPRIME (Recherche et Ingénierie en Matériaux Mécanique et Energétique pour les Transports, l'Energie et l'Environnement), Poitiers.
- CORIA (COMplexe de Recherche Interprofessionnel et Aérothermochimique), Rouen.
- CEA (Commissariat à l'Energie Atomique et aux énergies alternatives, DAM Ile-de-France Center).
- LaSIE (Laboratory of Engineering Science for Environment), Université La Rochelle, La Rochelle.
- PRISME (Pluridisciplinaire de Recherche en Ingénierie des Systèmes, Mécanique et Energétique), Orléans.
- LOMC (Laboratoire Ondes et Milieux Complexes), Le Havre.

Some of the summer schools and workshops recently organized by members of France West PC are the following (note that separated reports have been provided and published for each of these events):

- Summer School 'Small-scale turbulence. Phenomenology and theory', Cargèse, Corsica, 13-21 August 2007. This school was coorganized by L. Danaila (CORIA, Rouen), P. Petitjeans (PMMH, Paris) and A. Noullez (Observatoire de la Côte d'Azur, Nice).
- The summer school 'Turbulence and Mixing in Compressible Flows III', held from Sunday 29th August to Saturday 4th September 2010 on Oléron island. A description of the activities developed during this event is provided hereafter.
- Workshop on 'Highly resolved experimental and numerical diagnostics for turbulent combustion', organized by CORIA and ERCOFTAC SIG28 on 'REACTIVE FLOWS', May 25-26, 2011, in Rouen, FRANCE. The co-chairs were: P. Domingo and V. Moureau.

- Summer School 'Morphology and dynamics of anisotropic turbulence', Cargèse, Corsica, 18-30 July 2011. This school was coorganized by L. Danaila (CORIA, Rouen), F. Godefert (LMFA, Lyon) and J.B. Flor (LEGI, Grenoble).
- 15th ERCOFTAC SIG-15 workshop on refined turbulence modelling, co-organized by R. Manceau (PPRIME, Poitiers), S. Benhamadouche (EDF) and the SIG-15 committee, October 17-18, 2011, in Chateau (Paris).

In the following, we illustrate some of the activities developed in the laboratories members of France West PC.

-Section 2 is a report on the summer school 'Turbulence and Mixing in Compressible Flows III'.

-Section 3 represents an overview of the activities developed by CEA, DAM Ile-de-France Center.

-Section 4 illustrates some simulation and modelling activities at the Institute PPRIME (Poitiers).

-Section 5 is an overview of some experiments on compressible flows at PPRIME (Poitiers).

-Section 6 represents an example of the numerical studies performed in CORIA (Rouen).

-Sections 7 and 8 are activities developed in LOMC (Le Havre).

-Section 9 is an overview of the research performed in PRISME (Orléans).

-Section 10 represents some of the activities of the group 'Mathematical and Numerical Modelling of Transfer Phenomena', LaSIE, University La Rochelle.

-Section 11 is an example of the experimental activities in CORIA (Rouen).

## 2 Report on the summer school 'Turbulence and Mixing in Compressible Flows III' (Penelope Moffatt)

The summer school 'Turbulence and Mixing in Compressible Flows III', held from Sunday 29th August to Saturday 4th September 2010 on Oléron island, was the third summer school to be organised by ERCOFTAC's Special Interest Group n<sup>o</sup> 4 (after one in Strasbourg in 2005 and another in Marseille in 2008). Its attested aim was to offer an up-to-date introduction to different aspects of turbulence and mixing in compressible flows as encountered in a wide range of situations and disciplines, including aerodynamics, aeroacoustics, combustion and astrophysics, and to cover theoretical, experimental and numerical aspects. It was globally successful in fulfilling its aims.

The summer school brought together 40 different scientists, attracting students from India and China as well as Germany, Italy, and the Netherlands among other European countries. The location ('La Vieille Pérotine', a

CAES holiday and research centre on Oléron island in the Charente-Maritime region of west France) lent itself perfectly to thought-provoking discussions between participants over meal-times and in the bar after supper. The atmosphere was excellent, despite the perhaps slightly over-ambitious program, which some students suggested could have allowed more quality time off in which to decompress and explore the island.

The lectures opened on the Monday morning with a superb introduction to turbulence modelling for compressible flows by Bertrand Aupoix from Onera, Toulouse. With his inimitable style, he guided the students through the underlying equations before leading into an impressive overview of the physics of compressible turbulent flows and turbulence models for compressible flows. Professor Dussauge followed suit (after a delicious lunch out on the terrace), with a lecture explaining 'a classical view' (the mode theory and associated taxonomy) before posing the daring question of whether turbulence can be compressible. His first lecture ended with a global view for inhomogeneous equilibrium in supersonic flows (Morkovin's 1961 hypothesis and the Strong Reynolds Analogy.) Tom Gatski gave the last lecture of the day, filling in the students as to more recent developments in the modeling of compressible turbulence. The day's work ended six ten-minute student presentations. (Oana Petrache from the Netherlands in particular stood out for her results and style, leading to her winning a modest bottle of Pineau de Charente at the end of the week.)

On the Tuesday, Prof Dussauge's second contribution (on compressible mixing layers) was then complemented by a discussion on the structure of supersonic turbulent boundary layers with and without strong distortions by Alexander J. Smits from Princeton University, co-author with Dussauge of the well-known reference book 'Turbulent Shear Layers in Supersonic Flows' of which a second edition was published by Springer Verlag in 2005. After lunch (outside in the sunshine again), Tom Gatski and Alexander Smits gave their follow-up lectures, enabling the students to penetrate deeper into the mysteries of turbulent flow with an international perspective. Smit's pleadings about the need for basic experiments in his discussion on hypersonic turbulent boundary layers was particularly eye-opening. More student presentations followed, leading to some fascinating discussions over supper and in the bar afterwards.

The Wednesday afternoon having been mercifully kept free for some recreational activities, the morning had three lectures crammed into it. Claude Cambon began (at 8.30am) with some conceptual aspects and a dynamic approach to quasi-homogeneous compressible turbulence. Dussauge took over for some insights into interactions between shock waves and boundary layers before giving the floor to José Redondo. After getting out to the beach, exploring the forêt des Saumonards or being initiated into the joys of sailing, the students looked somewhat fresher, even sun-kissed, at that evening's six student ten-minute pre-dinner talks.

The Thursday saw an interesting follow-up lecture from Cambon and a dynamic performance from Jorn Sesterhenn in the morning, followed by an appearance by Peter Jordan and a round table ('Whither compressible turbulence? Vortices, shock and sound waves at the crossroads') animated by Prof. Jean-Paul Bonnet from Poitiers. A seminar by T. Lehner took the last slot of the day, instead of the usual student presentations.

The Friday's lectures (by Sesterhenn, Denis Gillet, Denis Veynante and Arnaud Mura) led the discussions from turbulence to combustion, turbulent combustion



Figure 1: Summer school 'Turbulence and Mixing in Compressible Flows III', September 2010

and high-speed combustion. A. Llor's most professional seminar ended the day, but not the conference; the final lectures by Veynante and Redondo were given on the Saturday morning.

Feedback from students was positive, with a majority considering that such summer schools should be held on a regular basis. The location was much appreciated as was the food and atmosphere; the work program was judged useful and of a high level, though maybe somewhat too intensive. Several students recommended holding a future summer school over a longer period, or being slightly less ambitious in scope.

Nevertheless and in conclusion, the week was a great success, with students from different backgrounds and universities striking up (hopefully lasting) friendships and initiating (hopefully fruitful) research collaborations. The students appreciated the chance to discuss in depth with the lecturers, researchers and professionals present, and to get to know some of the people who, before then, were mere names on books and articles for them.

The organisers thank all the speakers for their valuable contributions, and of course the CNRS and ERCOFTAC for their invaluable support.

### 3 CEA/DIF (Jean-François Haas and Antoine Llor)

The CEA/DIF (Commissariat à l'énergie atomique et aux énergies alternatives, DAM-Ile-de-France center), located in Bruyères-le-Châtel, is active in the field of compressible turbulent mixing induced by interface instabilities, one aspect of the scientific domain covered by SIG 4. This activity is organized around the development of Reynolds stress models aimed to simulate mixing zones involved in Inertial Confinement Fusion (ICF) flows.

The peculiarities of these finite thickness zones are as follows. They are generated on the interfaces between materials by hydrodynamic instabilities (Rayleigh-Taylor instability, ablation front instability, Richtmyer-Meshkov instability). The mean flows that feed them are non stationary, compressible with strong shock waves passing through, and are dependent on radiative and combustion processes.

The validation of our models goes through comparisons with direct numerical simulations of simplified

flows such as rarefaction wave / mixing zone interaction, Rayleigh-Taylor turbulence, ... To this end, we have developed two 3D codes computing either the compressible Navier-Stokes equations (the TRICLADE code) or the incompressible Navier-Stokes equations (the TurMix3d code, in collaboration with CMLA at ENS-Cachan).

GSG, one of the Reynolds stress model we are working on, is now based on a PDF formulation in order to ensure realisability [1]. The lessons of the pseudo-compressible approximation on turbulence modeling have been recently explored [2].

The consequences of pseudo-compressible approximations on statistical turbulence models have been studied in detail in many fields. However, it seems that no analysis has been dedicated to variable density turbulent mixing flows encountered in shock tubes. The primary reason for this absence of investigation comes from some specificities of shock tube flows which are unaccounted for in usual pseudo-compressible approximations. In particular, the mean field is highly compressible, fluids are not necessarily perfect gases and rapid distortions of the turbulent field can occur. To study these aspects, a pseudo-compressible approximation relevant for turbulent mixing flows encountered in shock tubes is derived. The asymptotic analysis used for this purpose puts forward the role played by four dimensionless numbers on the flow compressibility: namely, the turbulent, deformation, stratification and buoyancy force Mach numbers. The existence of rapid distortion and diffusion/dissipation regimes is also accounted for in the analysis. Then, some consequences of the derived pseudo-compressible approximation on statistical turbulence models are discussed. In particular, the evolutions of the density variance and flux are examined, as well as the turbulent transport of energy. The different aspects of this study are assessed by performing a direct numerical simulation of a shock tube flow configuration.

On the experimental level, we finance the realization of experiments in shock tube facilities by IUSTI and ISAE to get conclusive data in order to validate the behavior of the models in the presence of shock wave: Richtmyer-Meshkov instability (RMI) and shock / mixing zone interaction.

Shock tube experiments have been performed on the site of CEA/DIF until 2005 and are being continued in the aerodynamics department of ISAE (Institut Supérieur de l'Aéronautique et de l'Espace) in Toulouse [3, 4]. In a typical shock tube mixing experiment, two gases, air and SF<sub>6</sub>, are initially separated by a thin membrane between two grids which impose the small scale dominant wavelength of the perturbation. When a Mach 1.2 shock propagates from air to SF<sub>6</sub> (5 times heavier), the RMI develops leading to the chaotic interpenetration of the gases and a thin turbulent mixing zone (TMZ). The length of SF<sub>6</sub> between interface and shock tube end plate (typically 250 mm) determines the time delays between the passage of incident and reflected waves (a shock wave followed by an expansion wave). When the reflected shock wave impinges on the TMZ, density fluctuations within strongly interact with gradients associated with the shock and the turbulent mixing is amplified resulting in a rapidly thickening of the TMZ. Schlieren flow visualization using a high velocity camera enables to record the trajectory, thickness and structure of the turbulent mixing zone. Two components velocity measurements are performed with a laser-doppler velocimeter at various locations along the axis of the shock tube. They show the amplification of the velocity fluctua-

tions after the reflected shock and the anisotropy of turbulence. The RMI development in the linear and non-linear phase is also investigated using theoretical models, simulation and shock tube experiments carried out at IUSTI in Marseille. In this case, the initial interface is a thin membrane deformed with large wavelength perturbations imposed by stereo-lithography shaped grid and the diagnostics is based on Mie scattering in planar laser sheet.

A second theme involving CEA's collaboration with IUSTI as well as CORIA in Rouen is the interaction of shock waves with aqueous foams [5]. In the modelling by CORIA, the foam is treated as a distribution of drops. In the shock tube experiments carried out at IUSTI, shock waves interact with both sprays or foams.

## References

- [1] J. Griffond, O. Soulard and D. Souffland, "A turbulent mixing reynolds stress model fitted to match linear interaction analysis predictions," *Physica Scripta*, vol. T142, p. 014059, 2010.
- [2] O. Soulard, J. Griffond and D. Souffland, "Pseudo-compressible approximation and statistical turbulence modeling: Application to shock tube flows," *Phys. Rev. E*, vol. 85, p. 026307, 2012.
- [3] G. Bouzgarrou, Y. Bury, S. Jamme, J.-F. Haas, D. Counilh and J.-B. Cazalbou, "Experimental characterization of turbulence produced in a shock tube: a preliminary work for the study of turbulent gaseous mixing induced by the Richtmyer-Meshkov instability," *ISSW28, 17-22 July 2011, Manchester, UK*, 2012.
- [4] S. Jamme, Y. Bury, G. Bouzgarrou and J.-F. Haas, 'Evolution of turbulent fluctuations of an air/SF<sub>6</sub> mixing zone induced by Richtmyer-Meshkov instability,' *IWPCTM 13, 16-20 July 2012, Woburn Abbey, UK*, 2012.
- [5] E. Del Prete, A. Chinnayya, L. Domergue, A. Hadjadj and J.-F. Haas, "Blast wave mitigation by dry aqueous foams," *submitted to Shock Waves Journal*, 2012.

## 4 Simulation and modelling activities at the Institute PPRIME (CNRS, University of Poitiers, ENSMA)

The turbulence activity is performed inside the department *Fluids, Thermal Science and Combustion* created with the Institute PPRIME in January 2010. Inside the department, the two research teams *Aerodynamics, Turbulence, Acoustics and Control* and *Structures of flames and turbulent Combustion* are mainly concerned by turbulence issues. For its investigation of turbulence via High Performance Computing (HPC), the Institute PPRIME is granted access each year to the HPC resources of IDRIS/CINES/CCRT under the allocation 20xx-020912 made by GENCI (Grand Equipement National de Calcul Intensif). The activity on fractal-generated turbulence was also supported within the DEISA Extreme Computing Initiative ([www.deisa.eu](http://www.deisa.eu)) through the EU FP6 project RI-031513 and the FP7 project RI-222919. As complementary computational

resources, the researchers have also the access to the PPRIME supercomputer of which the peak performance of 8.5 TFlops was enough for middle size calculations. For the DNS studies of turbulence briefly summarized in sections 4.1, 4.2, 4.3 and 4.4, the high-order code *Incompact3d* was used with an Immersed Boundary Method (IBM) [1, 2, 3, 4, 5]. The DNS/LES studies of sections 4.5 and 4.6 have been carried out with *NIGLO* code, which is based on high-order finite difference schemes designed for the study of high-speed shear flows in compressible regime. For RANS and hybrid RANS/LES studies, the open-source CFD tool *Code\_Saturne* [6], developed by EDF, is used. Computational modelling of turbulent combustion makes also use of available CFD tools such as *Code\_Saturne* or *N3S\_Natur*. A hybrid Monte Carlo PDF - low Mach number flow solver has been also recently developed to perform large eddy simulations of turbulent reactive flows. Finally, a priori analyses are also conducted on direct numerical simulations databases. Some examples of the PPRIME activities on turbulence are illustrated in what follows.

#### 4.1 Fractal-generated turbulence

The first experiments of turbulence generated by fractal grids in wind tunnels have been conducted at Imperial College London [7, 8]. To better understand the interesting and unexpected results observed in these experiments, the Institute PPRIME and Imperial College London has started a collaborative study where Direct Numerical Simulations (DNS) have been performed at very high resolution using massively parallel computing. New insights have been provided to interpret the small-scale generation of turbulence near the fractal grid and the turbulence decay further downstream. As illustrated in Figure 2, a more intermittent dynamics is observed using a fractal grid instead of a regular grid, with an increase of the turbulence intensity in the near-grid region and a persistent geometrical imprint of the fractal grid quite far downstream [9]. The acoustic properties of the fractal-generated turbulence have also been investigated via a hybrid approach based on Lighthill's analogy [10]. By comparison with a regular grid of same porosity and mesh-based Reynolds number, a fractal square grid of three fractal iterations was found to provide a noise reduction on a wide frequency range but with a well-defined peak in the acoustic spectrum. This particular behaviour is interpreted as a consequence of quasi-periodic vortex shedding that can clearly occur only when wakes from the grid bars do not mix too early. It has been shown that this condition can be satisfied using a fractal grid through the wake dynamics from the smallest bars. More details can be found in [10]. A Special Interest Group, SIG 44, devoted to the Multiscale-generated turbulent flows, was created in 2011.

#### 4.2 Separation bubble dynamics

The separation bubble formed over a 2D or 3D half-body has been studied by DNS [11, 12]. How the shape of the body can influence the bubble dynamics has been investigated by considering the effects of the body width and/or the front edge curvature. Using a finite-width body, a highly 3D separation bubble is observed with the presence of a pair of longitudinal counter-pair vortices pumping the fluid from the side of the body to the top of the flow. The structure of the separation bubble is in agreement with experiments [13], especially the combination of singular points associated with the surface

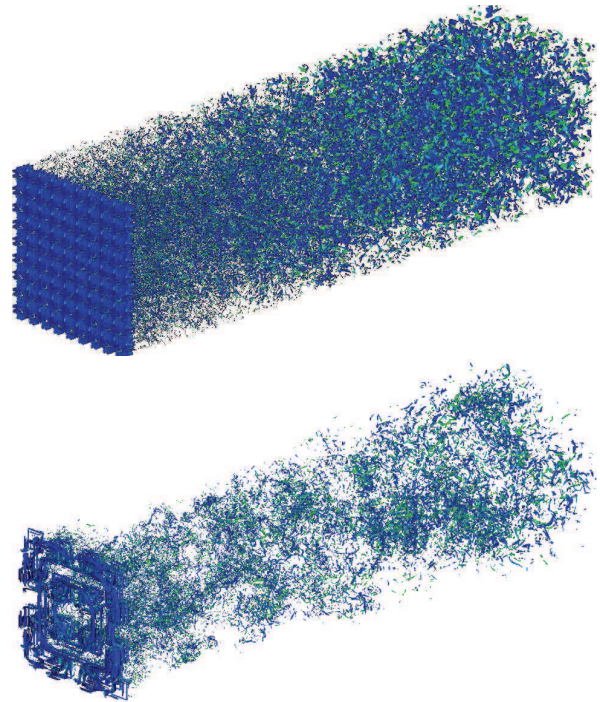


Figure 2: Isosurfaces of normalised enstrophy (in blue) and longitudinal vorticity (in green). Regular grid (top), fractal grid (bottom), see [9, 10] for more details

flow on the top-boundary of the body. At small aspect ratios, strong lambda vortices govern the unsteady dynamics, especially the separation bubble flapping [11]. Concerning the curvature effects, as illustrated in Figure 3, the use of a sharper front edge is found to expand the bubble size through an increase of the separation angle combined with the reinforcement of turbulence [12]. Considering the deterministic response of the bubble dynamics with respect to cyclic inlet excitation, strong curvature was found to deeply change the bubble sensitivity with respect to upstream/downstream perturbations.

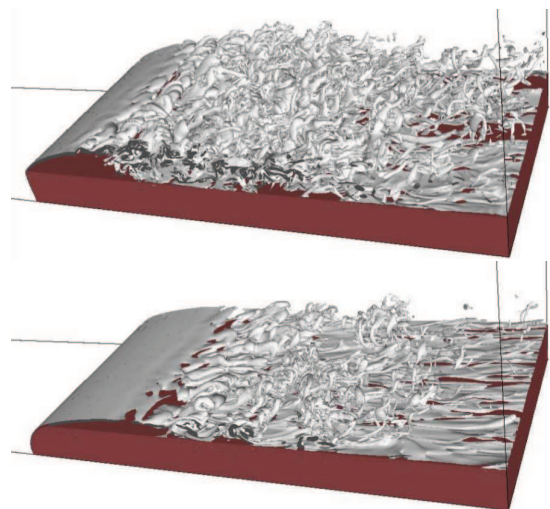


Figure 3: Perspective views of enstrophy isosurface. High curvature (top), low curvature (bottom), see [11, 12] for more details

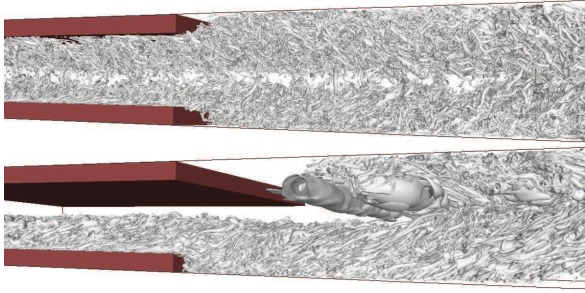


Figure 4: Q criterion isosurface for non-rotating (top) and highly-rotating (bottom) diffusers, see [14] for more details

### 4.3 Rotating turbulent diffuser

The effects of a spanwise rotation on the channel flow across a sudden expansion have been investigated by DNS [14]. Upstream from the expansion, inflow turbulent conditions are generated realistically for each rotation rate through a very simple and efficient technique of recycling without the need of any precursor calculation. As the rotation is increased, the flow becomes progressively asymmetric with stabilization/destabilization effects on the cyclonic/anticyclonic sides respectively. These rotation effects, already present in the upstream channel consistently with previous studies [15, 16], lead further downstream to a reduction/increase of the separation size behind the anticyclonic/cyclonic step. In the cyclonic separation, the free-shear layer created behind the step corner leads to the formation of large-scale spanwise vortices that are found more and more 2D as the rotation is increased. Conversely, in the anticyclonic region, the turbulent structures in the separated layer are more 3D and also more active to promote the reattachment. These behaviours are illustrated in Figure 4. In the present flow configuration where Coriolis forces do not work while being passive on a purely 2D dynamics, the phenomenological model of absolute vortex stretching [17] is useful to understand how the rotation influences the flow dynamics.

### 4.4 Mixing layer behind a splitter plate

The flow obtained behind a trailing edge separating two streams of different velocities was studied by means of DNS [18]. The influence of the trailing-edge shape was considered through the analysis of the destabilizing mechanisms and their resulting effect on the spatial development of the flow, both in terms of mean quantities and flow dynamics, as shown in Figure 5. The wake component, which dominates the flow close to the trailing edge, was found to be also influential further downstream. Using instantaneous visualizations, statistical/stability analysis considerations and proper orthogonal decomposition, some insights have been provided about the transition regime from the wake to the mixing layer and its influence on the self-similarity state where no wake influence can be locally detected.

### 4.5 Shock wave/Boundary layer interaction

In the framework of the ANR SPICEX project, the influence of both wall-cooling and shock interaction on the spatial development of a supersonic boundary layer has

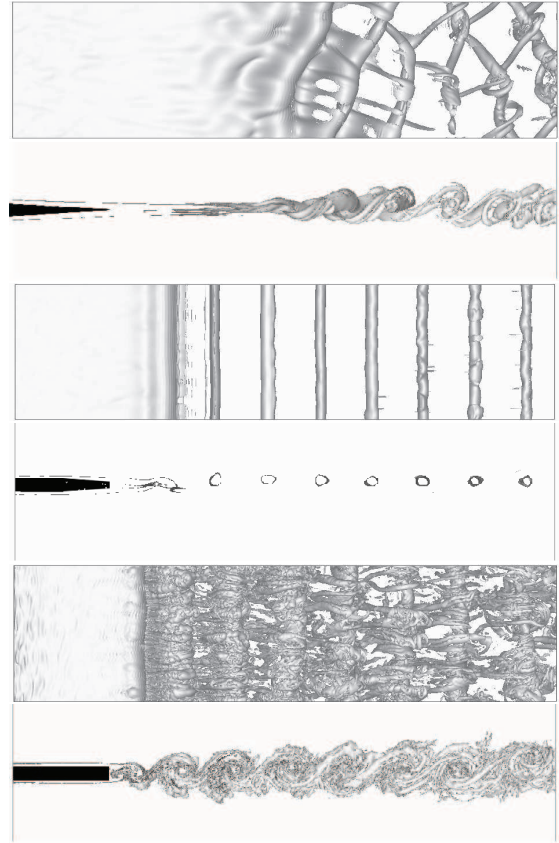


Figure 5: Side and top views of enstrophy isosurface in the near-plate region. Thin splitter plate (top), intermediate trailing edge (middle), blunt trailing edge (bottom), see [18] for more details

been studied by DNS. In the present case, the full spatial development of wall-turbulence has been simulated by means of upstream wall perturbations triggering the most unstable modes. This has enabled to obtain a realistic transition and fully-reliable inflow data upstream of the interaction region of most interest. The mean and turbulent thermal fields have been shown to be strongly modified by the wall cooling which significantly dampens more particularly the turbulent thermal quantities levels across the boundary layer. In addition, the wall-cooling was shown to lead to a reduction of the upstream influence and lengths of shock-induced separation along with a faster recovery process downstream of the shock-system. A thorough description of the evolution of the statistical turbulent properties is described in [19] [20].

Some a priori tests of subgrid-scale models have also been carried out [21] in order to assess the predictive capacities of common subgrid-scale modelling approaches commonly used for such flow configurations. As illustrated in Figure 6 for the pressure/dilatation term, the relative weight of subgrid-scale contributions to the computable energy budget have been found to vary significantly within the flow. The compressible contributions can not be neglected in particular in the upstream region of the recirculation region underneath the shock system. It was also observed that classical hybrid (similarity/dissipative) models a priori enable a correct representation of the subgrid-scale tensor but that a correct closure for these compressible SGS contributions largely remains an open issue, which motivate further developments.

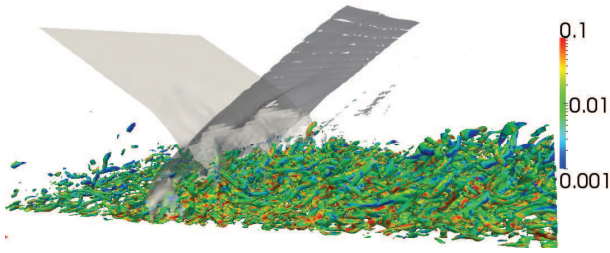


Figure 6: A priori analysis of subgrid scale contributions based on DNS data of shock wave/boundary layer interaction: pressure and  $Q$  criterion iso-surfaces shadowed by the relative contribution of the pressure/dilatation to the transport

#### 4.6 Identification of noise source mechanisms in jets

This research activity has been conducted in collaboration with the RWTH (Aachen) and the Hermann Fattinger Institut (T.U. Berlin) and supported by subprojects of the GDR DFG/CNRS 056 "Numerical Fluid Mechanics", action "Noise generation in turbulent flows". Some LES of simple or coaxial jets have been carried out for cold and heated jets, in order to characterize the influence of thermal and Mach effects on the dynamics and acoustics of turbulent jets [22]. An example of instantaneous snapshot of the simulated flowfield is given in Figure 7. As expected, the jet spreading was found, for example, to be significantly enhanced for hot jets. While the contributions to the turbulent kinetic energy appeared to be enhanced accordingly, their global balance remains qualitatively similar. However, the initial development of the secondary longitudinal instabilities was found to be significantly enhanced by thermal effects. The baroclinic torque has been suspected to play an essential role to trigger this process and to explain the main differences observed in the jet development between cold and hot conditions. In order to explain some essential features of the radiated sound, the LES data obtained have also been used in [23] to identify noise source mechanisms and develop a model based on a modulated wave-packet ansatz.

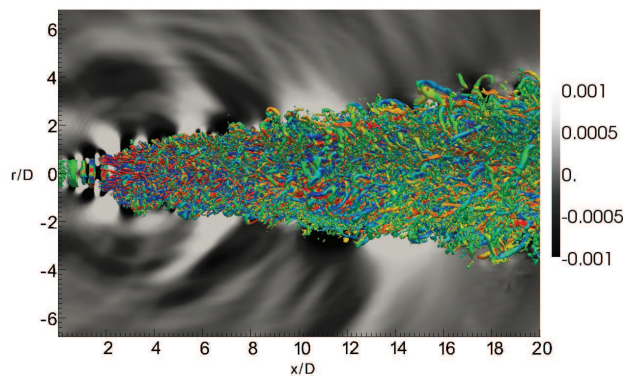


Figure 7: Cold jet at  $Mach = 0.6$  and  $Re = 1.10^6$ :  $Q$  criterion and fluctuating pressure

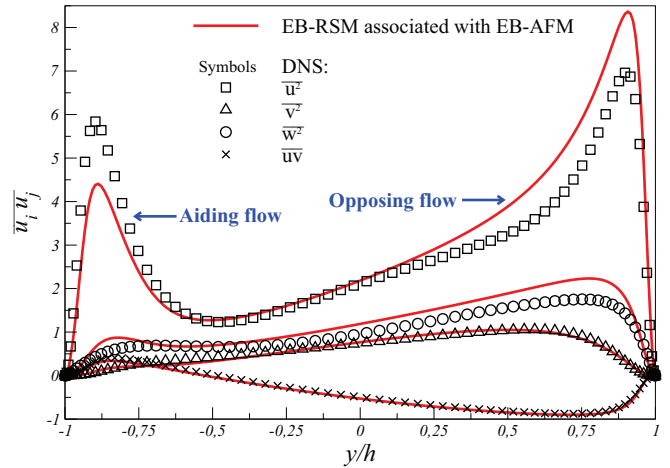


Figure 8: Reynolds stresses in mixed convection regime (differentially heated channel with an imposed pressure gradient). Comparison of the predictions of the EB-RSM [24] associated with the Elliptic-Blending Algebraic Flux Model [28] with the DNS data of Kasagi and Nishimura, 1997

#### 4.7 Statistical modelling of turbulence (RANS)

The main objective of the work on statistical modelling is to introduce complex physical phenomena in the models: wall blockage [24, 25, 26, 27], heat transfer [28, 29], rotation [30, 31, 32]. In order to propose models applicable to industrial configurations, a compromise is sought between an accurate representation of the physics and numerical robustness. The originality of this work lies in the introduction of methods derived from the *elliptic relaxation* of Durbin to account for the non-local, kinematic blockage due to walls. A crucial step toward numerical robustness is the introduction of the *elliptic blending* approach [24], leading to the so-called *EB-RSM*, a second moment closure used worldwide, by at least 10 teams in 8 countries, for applications ranging from aeronautics to nuclear power generation. Moreover, the model can be simplified further (from 8 to 3 equations), without impairing the physics, by applying the theory of invariants [33], leading to an explicit algebraic version [27]. Differential and algebraic heat flux models accounting for wall blockage, see Figure 8, are also developed in collaboration with EDF [28].

#### 4.8 Hybrid RANS/LES modelling

The cost of LES remaining too high for many industrial applications, an intensive research activity was devoted in the last decade to hybrid RANS/LES modelling, in order to be able to use LES in dedicated regions only, where it is necessary, and RANS in the rest of the domain. In so-called *zonal* approaches, in which segregated RANS and LES computations are carried out in fixed sub-domains, the difficulty lies in the coupling at the interfaces. In particular, methods for generating synthetic turbulence at the inlet of the LES domain, making use of information given by the upstream RANS region, are developed. Synthetic fluctuations can be generated by a dynamical system [34], the synthetic eddy method [30], or a new volume forcing method, the so-called ALF (Anisotropic Linear Forcing) [35]. In so-called *seamless* approaches, a unique model is build, able to continuously transition from RANS mode to LES mode in the domain. A theoretical work was conducted in order to provide a

consistent formalism, based on temporal filtering, to this family of methods, leading to the hybrid temporal LES concept (HTLES), see Figure 9 [36, 37, 38]. One of the main difficulties then consists in the modelling of the subfilter stresses. Indeed, when the cutoff frequency lies in the productive region of the turbulent spectrum, it is necessary to account for anisotropic production and redistribution, such that the effort was devoted to transport models for the subfilter stresses [39], in particular in the frame of the French-German program *LES of complex flows* [40].

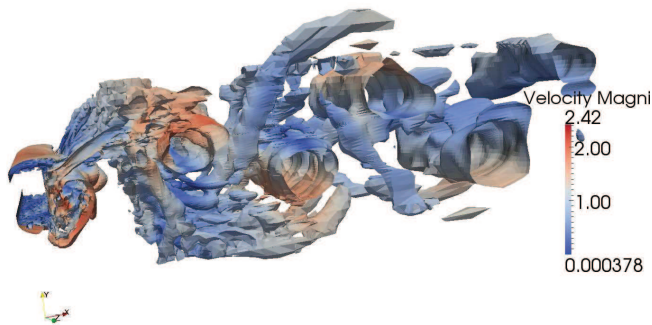


Figure 9: Hybrid temporal LES applied to the case of the flow around a rectangular cylinder of aspect ratio  $R = 0.6$  [38].  $Q$ -isocontour coloured by the velocity magnitude

An in-depth evaluation of the capabilities of these methods for the prediction of pressure fluctuations at the wall is also conducted ([41],[42]). In particular, the ANR program DIB (Dynamic, Unsteadiness, Noise) was devoted to the analysis and the modelling of the spatio-temporal dynamic of coherent structures and their link with the wall pressure fluctuations. In this context, hybrid RANS/LES simulations are performed on two test cases: the flow over a thick plate and the flow over a 3D body generating a A-pillar vortex. Figure 10 shows an instantaneous field of a Detached Eddy Simulation of the flow over a thick plate. This recirculating flow is mainly characterised by a vortex shedding, a flapping of the separated shear layer, and a strong three-dimensionalisation downstream of the mean reattachment. After an evaluation based on classical statistics, an evaluation of the predicted fluctuating motion is necessary before the study of the mechanisms responsible for the wall pressure fluctuations. To this aim, statistical tools devoted to the characterisation of the large scale unsteadiness (mainly based on conditional average, proper orthogonal decomposition, and stochastic estimation) are adapted and developed, and results are directly compared with experimental data. Once the predicted fluctuating motion validated, the access to the full 3D field allows to evaluate the different contributions to the wall pressure fluctuation (linear and non linear contributions). An important result in this case was the dominance of the non linear contributions downstream of the reattachment.

#### 4.9 Turbulent combustion in partially premixed conditions

Under the thin flame hypothesis, the Laboratory keeps an important activity devoted to the analysis and development of refined models to describe and calculate turbulent reactive flows. An important part of the corresponding research activity is devoted to partially pre-

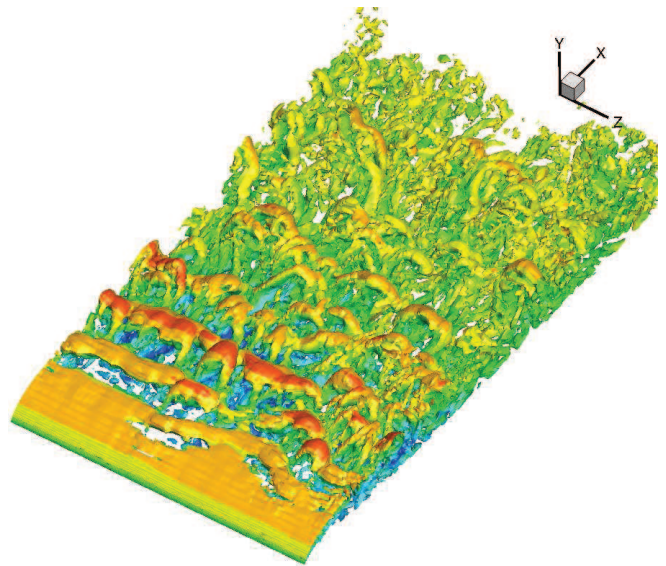


Figure 10: DDES of the flow over a thick plate ( $Re = 80000$ ).  $Q$ -isocontour coloured by the longitudinal component of the velocity

mixed conditions, i.e. situations where the fuel/air ratio is not homogeneous. Some recent results obtained for these conditions include (i) the representation of the fine structure of turbulent flames, i.e. the small scale structure, where molecular mixing between fresh reactants and fully burnt products operates, as well as (ii) the influence of such structures on properties at larger scales including turbulent transport. Special efforts have been devoted to take care of possible departures from the thin flame assumption and to consider other regimes of turbulent combustion, see references [43, 44]. Such regimes of turbulent premixed combustion have received special attention within a hybrid PDF-LES framework where a transport equation for the subgrid scale composition PDF is solved [45, 46], see Figure 11.

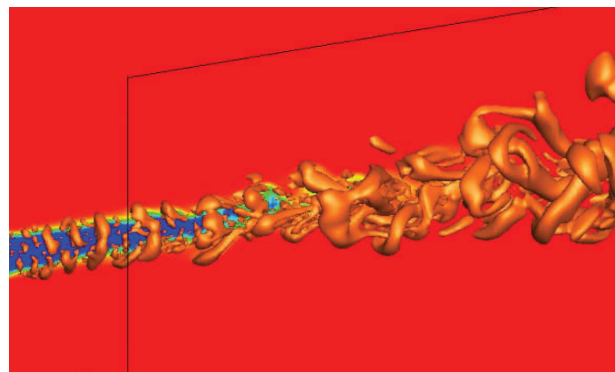


Figure 11: LES-PDF numerical simulation of premixed combustion in a high speed reactive jet. Iso-surface of the second invariant of the velocity gradient tensor, ie  $Q$ , superimposed on the progress variable field

Special emphasis has been placed on the strong couplings that exist between chemical reaction and thermal expansion effects. Such effects are well known to influence the characteristics of turbulent transport *via* the pressure field. For combustion of fully premixed reactants a representation of these effects has been detailed in [47] while partially premixed situations have been addressed in reference [48]. The closure relies on a partitioning of the pressure fluctuations covariance into a

reactive and a non reactive contribution. The corresponding closure was found effective to recover the effects of flame-induced turbulence and non-gradient diffusion as observed in both direct numerical simulation databases (*a priori analyses*) and experiments (*a posteriori analyses*) conducted on the ORACLES test rig [49]. Based on a velocity splitting procedure a recent theoretical analysis allowed to elaborate algebraic closure for turbulent transport [50]. Keeping in mind the difficulties associated with the application of second order closures to practical geometries, the resulting closures provides an interesting alternative to deal with thermal expansion effects [51]. Moreover a recent scaling analysis also leads to a generalization of the Bray criterion and established that the corresponding non dimensional number also delineates the influence of thermal expansion on the smallest length scales of turbulent reactive flows (scalar dissipation rate) [52]. The corresponding effects have stimulated a large amount of work among the combustion community which has been recently reviewed in [53]. The objective of the corresponding works is to improve the representation of the reactive scalar dissipation rate, a key but unknown quantity, which requires to be modelled whatever the retained computational framework (RANS, U-RANS, LES). In this respect, the scalar - turbulence interaction term that correlates velocity gradients to scalar gradients concentrates important modelling difficulties which have been addressed among others in [54, 55]. Along with these physical and computational studies, experimental databases have been collected on the VESTALES and ORACLES test rigs [56, 57]. Conjointly with such experimental investigations, the use of direct numerical simulation now provides a welcome addition to the classical theoretical and modelling tools that have been developed at the Laboratory to analyse turbulent premixed flames.

#### 4.10 Influence of temperature fluctuations on combustion in closed vessels

The influence of heat losses on the development of turbulent combustion within closed vessels has been investigated within the context of ignition in HCCI conditions (Homogeneous Charge Compression Ignition). In such situations, combustion develops under the simultaneous influence of (i) chemical kinetics, (ii) scalar micromixing, and finally (iii) heat losses at the walls. HCCI conditions therefore provide one among the seldom situations where these three different processes are so closely intermingled. A direct consequence is that the control as well as the physical modelling of such conditions is among the most difficult. Some recent investigations that have been conducted in a rapid compression machine (RCM) allowed to confirm and quantify the crucial influence of temperature fluctuations for such conditions, see references [58, 59]. The combined use of experimental measurements: pressure monitoring, direct light visualisation, Planar Laser Induced Fluorescence (P-LIF) techniques together with computational modelling based on the consideration of the joint PDF of the chemical composition allowed to evidence the critical role of temperature fluctuations. In particular, the resort to toluene P-LIF imaging technique provides new insights on the temperature fields and associated gradients at TDC thus allowing for a possible delineation between different propagation modes: auto-ignition fronts or classical deflagration (flame) fronts.

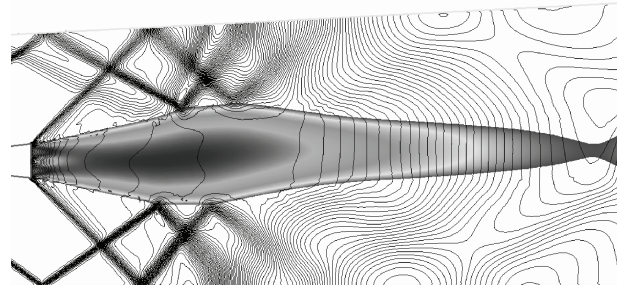


Figure 12: Numerical simulation of a Scramjet combustor model: computational pressure contour plots. The coloured zone delineates the subsonic jet flow

#### 4.11 Combustion in high speed flows

Another situation where ignition and detailed chemistry are crucial mechanisms is the one associated with combustion in high speed flows. In contrast with low mach number situations where propagation effects and associated triple flamelets structures may play an important role, see for instance [43], the thermo-physical and dynamical mechanisms providing the stabilization of combustion in high speed (supersonic) flows are closely related to ignition effects. In such reactive flows ignition processes may be influenced by the conversion of kinetic energy into thermal enthalpy and turbulent combustion models should be generalized to account for such specificities as in the proposal introduced in [60, 61] which has been used to describe high enthalpy supersonic coflowing jets. The same procedure has been also successfully applied to a scramjet combustor model [62], see Figure 12. The influence of compressibility and pressure discontinuities on scalar micro-mixing is now also investigated in details by resorting to direct numerical simulations [63].

### 5 Some experiments on compressible flows at PPRIME

#### 5.1 High-speed flows, turbulence and shock waves

Researchers of PPRIME study the specific effects of compressible turbulent flows. A particular attention is paid on interactions between shock waves and turbulent shear flows (wall bounded or not), by both fundamental and applied approaches.

##### 5.1.1 Shock wave - turbulent boundary layer interactions

Shock wave - turbulent boundary layer interactions separation are studied both experimentally and numerically for flow regimes corresponding to shock separations in over-expanded nozzles.

Experiments comprise simultaneous wall pressure and PIV velocity fields, with the objective to build at term estimated velocity fields from time-resolved wall measurements. Thanks to a POD/LSE complementary technique [64], the estimated velocity fields are used to extract the 3D unsteady flow organisation in the vicinity of the separation zone, as shown in Figure 13 [19, 20].

DNS of shock wave - turbulent boundary separation are performed in order to obtain well-converged turbulent quantities and to extract 3D flow features, see Figure 6.

Future works will aim on cylindrical configuration, so that the transverse curvature will fit real conditions encountered in over-expanded nozzle flows. Also, experiments in cylindrical configurations will reduce side-wall effects.

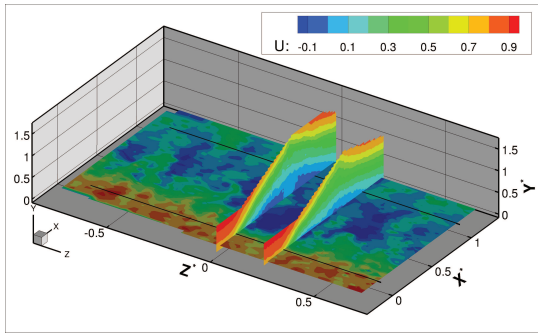


Figure 13: Comparison between instantaneous velocity field (plane parallel to the wall,  $y/\delta_0^* = 0.12$ ), and estimated fields (planes normal to the wall,  $z/L = 0$  and  $0.15$ ) at the same instant

### 5.1.2 Shock wave - turbulent mixing layer interactions

The interaction of a shock wave and a turbulent mixing layer is responsible of emission of intense acoustic waves in the external flow, as well as large variations on the turbulent properties of the mixing layer itself.

Simulations, which are carried out for a simple 2D planar configuration put forward oscillations of the shock wave when it impact Kelvin-Helmholtz vortices. This unsteady behavior generate strong non linear acoustic waves which propagate in the secondary flow, as shown in Figure 14. This phenomenon is known as *shock leakage* [65].

Experiments are performed in an ideally underexpanded jets, with a conical shock generator located on the jet axis. Near-field pressure measurements are associated with spark schlieren and laser-Doppler velocimetry so that mechanisms of shock leakage can be understood in a real, high Reynolds number flow. More complex configurations are also studied, where shock waves are not generated by a physical obstacle, but are inherent in the flow. For instance, in the case of underexpanded jets, shock waves interact also with non-local flow features, see Figure 15.

### 5.1.3 Applied configurations

More complex configurations are also studied.

For instance, a new fluidic device for jet thrust vectorisation has been tested on a supersonic rectangular jet. The device consists in a separation zone located in the vicinity of the jet lip. The separation is driven by a counter flow blowing slot. Beyond the thrust vectoring, the flow manipulation results in a modification of the flapping mode, as shown in Figure 16 [66].

Numerical approaches are also performed for applied flow configurations. For example, DES of overexpanded jet nozzle separation have been performed, for realistic geometry and aerodynamic parameters, (see Figure 17 [67]).

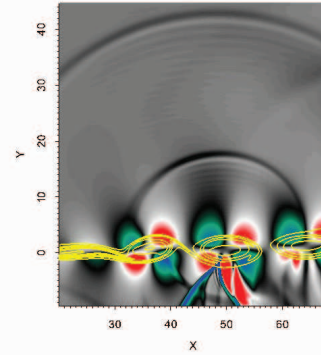


Figure 14: Observation of the shock leakage phenomenon in 2D shock wave/mixing layer interaction at  $M = 1.4$  : isoline of vorticity (yellow contours), divergence (color palette) and pressure field (grey palette)



Figure 15: Schlieren visualization of an underexpanded jet (convergent nozzle,  $NPR = 2.5$ )

## 5.2 Coherent structures in jets

Turbulent jets are the focus of a research effort motivated by the sound they produce. An analysis methodology, based on the combined use of experiment, simulation and theory (in the spirit evoked by [68]), and which is described in detail in [69], is being developed, with an eye towards real-time modelling and control. The methodology is based on the idea that turbulent flows can be meaningfully reduced to simplified kinematic and dynamic descriptions. Coherent structures, whose role in the generation of jet noise has been reviewed by [70], are therefore central.

A first step in understanding the salient features of the time-local fluid-dynamic processes that underpin aerodynamic sound-production by turbulence, and which motivated much of the more recent work, was made by analysing the optimally-controlled mixing layers of [71]. The differences between the uncontrolled and optimally-controlled flows served as a guide to the identification of the ‘loudest’ fluid-dynamics processes present in the simulation. The analysis, by [72], showed how intermittent breakdown of the spatial homogeneity of the axial structure of the mixing layer leads to high-level sound radiation. This behaviour can be modelled by considering the coherent structures to comprise spatiotemporally modulated wavepackets. Such a model was developed in [73] and validated, using data from large eddy simulations (7) and direct numerical simulations in [74].

In all of the above work it was possible to identify the sound-producing flow dynamics through simultaneous use of the turbulence and acoustic fields: the sound field was used to *distill*, from the complexity of the turbulence, the sound-producing flow *skeleton*. In all cases, however, spatiotemporally-extensive data was necessary. As this poses obvious problems in the context of an experiment, an experimentally-viable procedure was devel-

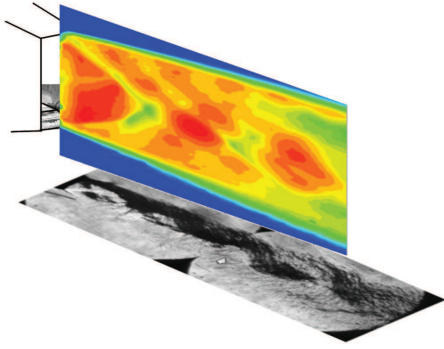


Figure 16: Experimental study of a fluidic device for thrust vectorisation of rectangular supersonic jets: composite image of velocity field ( $xy$  plane), schlieren ( $xz$  plane) and oil flow visualisation

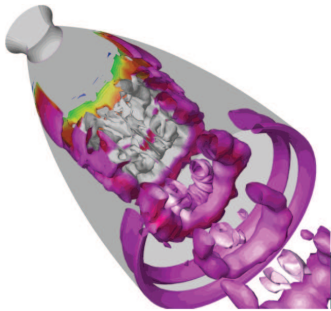


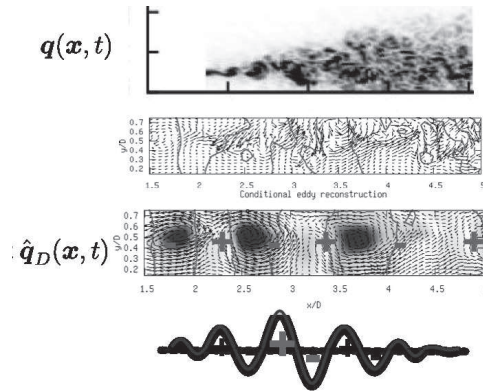
Figure 17: DES of a jet nozzle separation, free separation regime

oped and tested (using an LES database) by [75, 76]. This work, which constitutes a relatively complete exploration and validation of the methodology outlined in [69], involves using the radiated sound field to perform a conditional analysis of the turbulence: the space- and time-resolved kinematic skeleton (both its pressure and velocity components) are educed from the complete flow solution. Figures 18, 19 and 20 provide a synopsis of tFigue main results.

Figure 18 shows the system reduction, from the full flow solution  $\mathbf{q}$ , to the sound-producing skeleton,  $\hat{\mathbf{q}}_D$ , which animates a simplified sound-source *Ansatz*,  $s = T_{11}$  and sound field,  $p$ . The velocity and pressure fields comprised by  $\hat{\mathbf{q}}_D$ , and which are educed independently, are seen to exhibit a behaviour which is consistent with the Navier-Stokes system: low pressure zones correspond to the cores of vortical structures, high pressure regions are found at the saddle points. This motivates the search for a more rigorous link to the flow equations. With this in mind a linear stability analysis is performed based on the mean velocity profile—as detailed in [70], coherent structures in jets are frequently understood as linear instabilities of the mean flow. The results, summarised in Figure 19, show the educed field to match the radial eigenfunctions of linear stability problem; the match is not only in terms of the shapes, *the spatial amplification rates and relative amplitudes of the velocity and pressure fluctuations are also consistent with the linear theory*. A more comprehensive comparison of the coherent structures with linear stability theory is currently underway using time-resolved stereo PIV measurements and Parabolised Stability Equations [77]. A sample result is shown in Figure 20.

As real-time dynamic modelling, for the purpose of control, is the end objective, a stable twenty degree-

of-freedom reduced-order dynamic model has been constructed using  $\hat{\mathbf{q}}_D$  by [78]. This was motivated by the fact that the sound-producing flow skeleton can be much more efficiently compressed by Proper Orthogonal Decomposition than  $\mathbf{q}$ . The result of applying POD to  $\hat{\mathbf{q}}_D$  leads to acoustically-optimised modes, similar to the Observer Inferred Modes of [79]. The reduced order model closely reproduces the dynamics of  $\hat{\mathbf{q}}_D$ , and by means of the same sound-source modelling technique, the sound field can also be reproduced with good accuracy.



$$T_{11}(\mathbf{y}, \tau) = 2\rho_0 U \tilde{u} \frac{\pi D^2}{4} \delta(y_2) \delta(y_3) A(\tau) e^{i(\omega\tau - ky_1)} e^{-\frac{y^2}{L^2(\tau)}}$$

$$p(\mathbf{x}, t) = -A^* \frac{\rho_0 U \tilde{u} M_c^2 (kD)^2 L^* \sqrt{\pi} \cos^2 \theta}{8|\mathbf{x}|} e^{-\frac{(L^*)^2 k^2 (1 - M_c \cos \theta)^2}{4}} e^{i\omega(t - \frac{|\mathbf{x}|}{c})}$$

Figure 18: Résumé of system reduction and analysis. From top to bottom: (a) full flow solution,  $\mathbf{q}$ , showing velocity vectors and isocontours of zero pressure; (b) simplified flow skeleton  $\hat{\mathbf{q}}_D$ , obtained by conditional analysis (linear stochastic estimation); (c) schematic of jittering line source *Ansatz*,  $s(\hat{\mathbf{q}}_D)$ , constructed from  $\hat{\mathbf{q}}_D$ ; (d) mathematical expression for jittering line source; (e) solution for radiated sound obtained using simplified source

## References

- [1] P. Parnaudeau, J. Carlier, D. Heitz, and E. Lamballais, “Experimental and numerical studies of the flow over a circular cylinder at Reynolds number 3900,” *Phys. Fluids*, vol. 20, p. 085101, 2008.
- [2] S. Laizet and E. Lamballais, “High-order compact schemes for incompressible flows: a simple and efficient method with the quasi-spectral accuracy,” *J. Comp. Phys.*, vol. 228, no. 16, pp. 5989–6015, 2009.
- [3] S. Laizet, E. Lamballais, and J. Vassilicos, “A numerical strategy to combine high-order schemes, complex geometry and parallel computing for high resolution DNS of fractal generated turbulence,” *Computers and Fluids*, vol. 39, no. 3, pp. 471–484, 2010.
- [4] S. Laizet and N. Li, “Incompact3d, a powerful tool to tackle turbulence problems with up to  $(10^5)$  computational cores,” *Int. J. Numer. Methods Fluids*, vol. 67, no. 11, pp. 1735–1757, 2011.
- [5] E. Lamballais, V. Fortuné, and S. Laizet, “Straightforward high-order numerical dissipation via the viscous term for direct and large eddy simulation,” *J. Comp. Phys.*, vol. 230, no. 9, pp. 3270–3275, 2011.

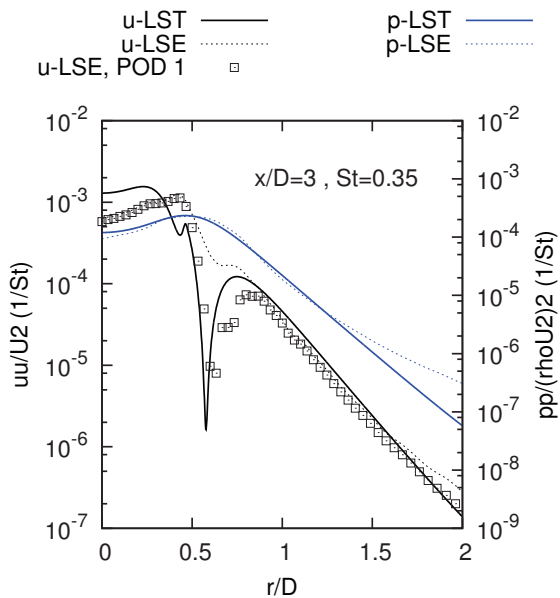


Figure 19: Comparison of educed field (p-LSE and u-LSE) with linear stability theory (p-LST and u-LST)

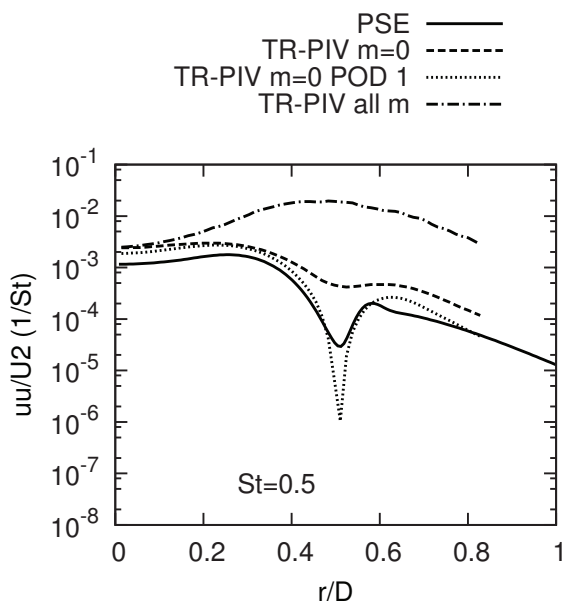


Figure 20: Comparison of experimental data acquired using time-resolved stereo PIV with solutions of Parabolised Stability Equations - [77]

[6] F. Archambeau, N. Méchitoua, and M. Sakiz, “Code Saturne: A Finite Volume Code for the Computation of Turbulent Incompressible flows - Industrial Applications,” *Int. J. on Finite Volume, Electronical edition*: <http://averoes.math.univ-paris13.fr/html>, vol. ISSN 1634, no. 0655, 2004.

[7] D. Hurst and J. C. Vassilicos, “Scalings and decay of fractal-generated turbulence,” *Phys. Fluids*, vol. 19, no. 035103, 2007.

[8] R. E. Seoud and J. C. Vassilicos, “Dissipation and decay of fractal-generated turbulence,” *Phys. Fluids*, vol. 19, no. 105108, 2007.

[9] S. Laizet and J. Vassilicos, “DNS of fractal-generated turbulence,” *Flow, Turbulence and Combustion*, vol. 87, no. 4, pp. 673–705, 2011.

[10] S. Laizet, V. Fortuné, E. Lamballais, and J. C. Vassilicos, “Low mach number prediction of the acoustic signature of fractal-generated turbulence,” *Int. J. Heat and Fluid Flow*, vol. In press, 2012.

[11] E. Lamballais, J. Silvestrini, and S. Laizet, “Direct numerical simulation of a separation bubble on a rounded finite-width leading edge,” *Int. J. Heat and Fluid Flow*, vol. 29, no. 3, pp. 612–625, 2008.

[12] E. Lamballais, J. Silvestrini, and S. Laizet, “Direct numerical simulation of flow separation behind a rounded leading edge: study of curvature effects,” *Int. J. Heat and Fluid Flow*, vol. 31, pp. 295–306, 2010.

[13] S. Courtine, A. Spohn, and J.-P. Bonnet, “Vortex dynamics in the reattaching flow of separation bubbles with variable aspect ratio,” in *Advances in Turbulence XI*, vol. 117, pp. 370–372, Springer Berlin Heidelberg, 2007.

[14] E. Lamballais and M. Lesieur, “Direct numerical simulation of a turbulent channel flow across a sudden expansion: effects of spanwise rotation,” in *Proc. 7th International Symposium on Turbulence and Shear Flow Phenomena*, (Ottawa, Canada), 2011.

[15] R. Kristoffersen and H. I. Andersson, “Direct simulations of low-Reynolds-number turbulent flow in rotating channel,” *J. Fluid Mech.*, vol. 256, pp. 163–197, 1993.

[16] E. Lamballais, O. Métais, and M. Lesieur, “Spectral-dynamic model for large-eddy simulations of turbulent rotating channel flow,” *Theoret. Comput. Fluid Dynamics*, vol. 12, 1998.

[17] M. Lesieur, S. Yanase, and O. Métais, “Stabilizing and destabilizing effects of a solid-body rotation on quasi-two-dimensional shear layers,” *Phys. Fluids A*, vol. 3, pp. 403–407, 1991.

[18] S. Laizet, S. Lardeau, and E. Lamballais, “Direct numerical simulation of a mixing layer downstream a thick splitter plate,” *Phys. Fluids*, vol. 22, no. 015104, 2007.

[19] M. F. Shahab, G. Lehnasch, T. B. Gatski, and P. Comte, “Statistical characteristics of an isothermal, supersonic developing boundary layer flow from dns data,” *Flow Turbulence and Combustion*, vol. 86, pp. 369–397, 2011.

[20] M. Shahab, P. Comte, G. Lehnasch, and T. Gatski, “Analysis of boundary layer structure downstream of a shock impingement,” in *9th International ERCOFTAC Symposium on Engineering Turbulence Modelling and Measurements*, 2012.

[21] G. Lehnasch, M. Shahab, P. Comte, and T. Gatski, “Assesment of compressible turbulence models for large-eddy simulation of shock wave/boundary layer interaction,” in *8th International ERCOFTAC Symposium on Engineering Turbulence Modelling and Measurements*, 2010.

[22] G. Daviller, *Etude numérique des effets de température dans les jets simples et coaxiaux*. PhD thesis, Ecole Nationale Supérieure de Mécanique et d’Aérotechnique, 2010.

- [23] A. Cavalieri, G. Daviller, P. Comte, P. Jordan, G. Tadmor, and Y. Gervais, “Using large eddy simulation to explore sound-source mechanisms in jets,” *J. Sound Vib.*, vol. 330, pp. 4098–4113, 2011.
- [24] R. Manceau and K. Hanjalić, “Elliptic Blending Model: A New Near-Wall Reynolds-Stress Turbulence Closure,” vol. 14, no. 2, pp. 744–754, 2002.
- [25] R. Manceau, J. R. Carlson, and T. B. Gatski, “A rescaled elliptic relaxation approach: neutralizing the effect on the log layer,” vol. 14, no. 11, pp. 3868–3879, 2002.
- [26] A. Fadai-Ghotbi, R. Manceau, and J. Borée, “Revisiting URANS computations of the backward-facing step flow using second moment closures. Influence of the numerics.,” vol. 81, no. 3, pp. 395–414, 2008.
- [27] A. G. Oceni, R. Manceau, and T. Gatski, “Introduction of wall effects in explicit algebraic stress models through elliptic blending,” in *Progress in wall turbulence: Understanding and Modelling* (M. Stanislas, J. Jimenez, and I. Marusic, eds.), Springer, 2010.
- [28] F. Dehoux, Y. Lecocq, S. Benhamadouche, R. Manceau, and L.-E. Brizzi, “Algebraic modeling of the turbulent heat fluxes using the elliptic blending approach. Application to forced and mixed convection regimes,” vol. 88, no. 1, pp. 77–100, 2012.
- [29] T. Gatski, “Second-moment and scalar flux representations in engineering and geophysical flows,” vol. 41, no. 1, 2009.
- [30] B. de Laage de Meux, B. Audebert, and R. Manceau, “Modelling rotating turbulence in hydraulic pumps,” in *Proc. 9th European Conference on Turbomachinery, Fluid Dynamics and Thermodynamics (ETC 9), Istanbul, Turkey, 21-25 March 2011*.
- [31] R. Manceau, R. Perrin, M. Hadžiabdić, P. Fourment, and S. Benhamadouche, “Turbulent jet impinging onto a rotating disc: A collaborative evaluation of RANS models,” 2009.
- [32] J.-F. Qiu, S. Obi, and T. B. Gatski, “Evaluation of Extended Weak-Equilibrium Conditions for Fully Developed Rotating Channel Flow,” vol. 80, pp. 435–454, 2008.
- [33] M. Deville and T. Gatski, *Mathematical Modeling for Complex Fluids and Flows*. Springer, 2012.
- [34] L. Perret, J. Delville, R. Manceau, and J.-P. Bonnet, “Turbulent inflow conditions for large-eddy simulation based on low-order empirical model,” vol. 20, no. 7, pp. 1–17, 2008.
- [35] B. de Laage de Meux, B. Audebert, and R. Manceau, “Anisotropic linear forcing for synthetic turbulence generation in hybrid RANS/LES modelling,” 2012.
- [36] A. Fadai-Ghotbi, C. Friess, R. Manceau, T. Gatski, and J. Borée, “Temporal filtering: a consistent formalism for seamless hybrid RANS-LES modeling in inhomogeneous turbulence,” vol. 31, no. 3, 2010.
- [37] R. Manceau, C. Friess, and T. Gatski, “Toward a Hybrid Temporal LES method,” 2011.
- [38] T. Tran, R. Manceau, R. Perrin, J. Borée, and A. Nguyen, “A hybrid temporal LES approach. Application to flows around rectangular cylinders,” 2012.
- [39] A. Fadai-Ghotbi, C. Friess, R. Manceau, and J. Borée, “A seamless hybrid RANS–LES model based on transport equations for the subgrid stresses and elliptic blending,” vol. 22, no. 055104, 2010.
- [40] S. Jakirlić, R. Manceau, S. Sarić, A. Fadai-Ghotbi, B. Kniesner, S. Carpy, G. Kadavelil, C. Friess, C. Tropea, and J. Borée, *Numerical Simulation of Turbulent Flows and Noise Generation*, ch. LES, Zonal and Seamless Hybrid LES/RANS: Rationale and Application to Free and Wall-Bounded Flows involving Separation and Swirl, pp. 253–282. Notes on Numerical Fluid Mechanics and Multidisciplinary Design, Springer, 2009.
- [41] T. Tran, R. Perrin, R. Manceau, and J. Borée, “Simulation and analysis of the flow over a thick plate at high Reynolds number,” 2010.
- [42] T. Tran, *Modélisation hybride RANS/LES d’écoulements massivement décollés en régime turbulent. Etude des corrélations pression/vitesse et confrontation à l’expérimentation*. PhD thesis, Ecole Nationale Supérieure de Mécanique et Aérotechnique, Poitiers, 2012.
- [43] A. Mura, V. Robin, and M. Champion, “Modeling of scalar dissipation in partially premixed turbulent flames,” *Combustion and Flame*, vol. 149, pp. 217–224, 2007.
- [44] V. Robin, M. Champion, A. Mura, O. Degardin, B. Renou, and M. Boukhalfa, “Experimental and numerical study of stratified turbulent v-shaped flames,” *Combustion and Flame*, vol. 153, pp. 288–315, 2008.
- [45] F. O. de Andrade, L. F. da Silva, and A. Mura, “Large eddy simulation of turbulent premixed combustion at moderate damköhler number stabilized in a high speed flow,” *Combustion Science and Technology*, vol. 183(7), pp. 645–664, 2011.
- [46] J. Vedovoto, A. da Silveira Neto, A. Mura, and L. F. da Silva, “Application of the method of manufactured solutions to the verification of a pressure-based finite volume numerical scheme for variable density flows,” *Computers and Fluids*, vol. 51(1), pp. 85–99, 2011.
- [47] V. Robin, A. Mura, M. Champion, and T. Hasegawa, “A new analysis of the modeling of pressure fluctuations effects on premixed turbulent flames and its validation based on dns data,” *Combustion Science and Technology*, vol. 180, pp. 996–1009, 2008.
- [48] V. Robin, M. Champion, and A. Mura, “A second-order model for turbulent reactive flows with variable equivalence ratio,” *Combustion Science and Technology*, vol. 180, pp. 1707–1732, 2008.
- [49] V. Robin, A. Mura, M. Champion, and P. Plion, “A multi dirac presumed pdf model for turbulent reactive flows with variable equivalence ratio,” *Combustion Science and Technology*, vol. 118, pp. 1843–1870, 2006.

- [50] V. Robin, A. Mura, and M. Champion, "Direct and indirect thermal expansion effects in turbulent premixed flames," *Journal of Fluid Mechanics*, vol. 689, pp. 149–182, 2011.
- [51] V. Robin, A. Mura, and M. Champion, "Algebraic models for turbulent transports in premixed flames," *Combustion Science and Technology*, 2012.
- [52] A. Mura and M. Champion, "Relevance of the bray number in the small-scale modeling of turbulent premixed flames," *Combustion and Flame*, vol. 156, pp. 729–733, 2009.
- [53] N. Chakraborty, M. Champion, A. Mura, and N. Swaminathan, "Scalar dissipation rate approach," in *Turbulent premixed flames* (N. Swaminathan and K. Bray, eds.), pp. 74–102, Cambridge University Press, 2011.
- [54] A. Mura, K. Tsuboi, and T. Hasegawa, "Modelling of the correlation between velocity and reactive scalar gradients in turbulent premixed flames based on dns data," *Combustion Theory and Modelling*, vol. 12, pp. 671–698, 2008.
- [55] A. Mura, V. Robin, M. Champion, and T. Hasegawa, "Small scales features of velocity and scalar fields in turbulent premixed flames," *Flow Turbulence and Combustion*, vol. 82, pp. 339–358, 2009.
- [56] N. Guilbert, A. Mura, B. Boust, and M. Champion, "Study of premixed combustion instabilities using phase-locked tomography piv," in *Fourteenth Int. Symp. on Applications of Laser Techniques to Fluid Mechanics*, Lisboa, Portugal, July 2008.
- [57] V. Robin, A. Mura, M. Champion, and T. Hasegawa, "Modelling the effects of thermal expansion on scalar fluxes in turbulent flames," *Combustion Science and Technology*, vol. 182, pp. 449–464, 2010.
- [58] C. Strozzi, J. Sotton, A. Mura, and M. Bellenoue, "Experimental and numerical study of the influence of temperature heterogeneities on self ignition process of methane air mixtures in a rapid compression machine," *Combustion Science and Technology*, vol. 180, pp. 1829–1857, 2008.
- [59] C. Strozzi, J. Sotton, A. Mura, and M. Bellenoue, "Characterization of two-dimensional temperature fields within a rapid compression machine using planar laser induced fluorescence imaging technique," *Measurement Science and Technology*, vol. 20(12), p. 125403, 2009.
- [60] J.-F. Izard, G. Lehnasch, and A. Mura, "A new analysis of the modeling of pressure fluctuations effects on premixed turbulent flames and its validation based on dns data," *Combustion Science and Technology*, vol. 181(11-12), pp. 1372–1396, 2009.
- [61] L. Gomet, V. Robin, and A. Mura, "Influence of residence and scalar mixing time scales in non premixed combustion in supersonic turbulent flows," *Combustion Science and Technology*, 2012.
- [62] A. Mura and J.-F. Izard, "Numerical simulation of supersonic non premixed turbulent combustion in a scramjet combustor model," *AIAA Journal of Propulsion and Power*, vol. 26(4), pp. 858–868, 2010.
- [63] P. Martinez-Ferrer, G. Lehnasch, and A. Mura, "Direct numerical simulations of high speed reactive mixing layers," in *Eurotherm Conference*, Poitiers, France, September 2012.
- [64] S. Piponnieau, E. Collin, P. Dupont, and J.-F. Debieve, "Reconstruction of velocity fields from wall pressure measurements in a shock wave/turbulent boundary layer interaction," *International Journal of Heat and Fluid Flow*, in press, 2012.
- [65] T. Suzuki and S. Lele, "Shock leakage through an unsteady vortex-laden mixing layer: application to screech jet," *Journal of Fluid Mechanics*, vol. 490, pp. 139–167, 2003.
- [66] V. Jaunet, D. Aymer, E. Collin, J.-P. Bonnet, A. Lebedev, and C. Fourment, "3d effects in a supersonic rectangular jet vectorized by flow separation control," in *40th Fluid Dynamics Conference and Exhibit*, (Chicago, USA), june-july 2010.
- [67] A. Shams, G. Lehnasch, and P. Comte, "Numerical investigation of the side-loads phenomena in overextended nozzles," in *4th European Conference for Aerospace Sciences*, 2011.
- [68] P. Jordan and Y. Gervais, "Subsonic jet aeroacoustics: associating experiment, modelling and simulation," *Experiments in Fluids*, vol. 44, no. 1, pp. 1–21, 2008.
- [69] P. Jordan, "Experimental aeroacoustics and noise source identification," *Lectures on Noise Sources in Turbulent Shear Flows, Int. Center for Mech. Sc., April 18-22, Udine (Italy)*, 2011.
- [70] P. Jordan and T. Colonius, "Wavepackets and turbulent jet noise," *Ann. Rev. Fluid Mech.*, vol. 45, 2013.
- [71] M. Wei and J. B. Freund, "A noise-controlled free shear flow," *Journal of Fluid Mechanics*, vol. 546, pp. 123–152, 2006.
- [72] A. V. G. Cavalieri, P. Jordan, Y. Gervais, M. Wei, and J. B. Freund, "Intermittent sound generation and its control in a free-shear flow," *Physics of Fluids*, vol. 22, no. 11, p. 115113, 2010.
- [73] A. V. G. Cavalieri, P. Jordan, A. Agarwal, and Y. Gervais, "Jittering wave-packet models for subsonic jet noise," *Journal of Sound and Vibration*, vol. 330, no. 18-19, pp. 4474–4492, 2011.
- [74] A. V. G. Cavalieri, G. Daviller, P. Comte, P. Jordan, G. Tadmor, and Y. Gervais, "Using large eddy simulation to explore sound-source mechanisms in jets," *Journal of Sound and Vibration*, vol. 330, no. 17, pp. 4098–4113, 2011.
- [75] F. Kerhervé, P. Jordan, J. Cavalieri, A.V.G.and Delville, C. Bogey, and D. Juvé, "Educing the source mechanism associated with downstream radiation in subsonic jets," *Submitted to Journal of Fluid Mechanics*, 2011.
- [76] F. Kerhervé, P. Jordan, J. Delville, C. Bogey, and D. Juvé, "Jet turbulence characteristics associated with downstream and sideline sound emissio," in *16th AIAA/CEAS Aeroacoustics Conference; Stockholm, Sweden*, American Institute of Aeronautics and Astronautics, 1801 Alexander Bell Drive, Suite 500, Reston, VA, 20191-4344, USA., 2010.

- [77] A. V. G. Cavalieri, D. Rodriguez, P. Jordan, T. Colonius, and Y. Gervais, “Instability waves in unforced turbulent jets detected with time-resolved, stereoscopic piv,” in *SUBMITTED FOR 18th AIAA/CEAS Aeroacoustics Conference and Exhibit*, (Colorado Springs, CL, USA), June 2012.
- [78] F. Kerherve, L. Cordier, P. Jordan, and J. Delville, “A twenty degree-of-freedom model of sound-source dynamics in a turbulent jet,” in *18th AIAA/CEAS Aeroacoustics conference, Colorado Springs, CO, USA*, 2012.
- [79] M. Schlegel, B. Noack, P. Jordan, A. Dillmann, E. Groschel, W. Schroder, M. Wei, J. Freund, O. Lehmann, and G. Tadmor, “On least-order flow representations for aerodynamics and aeroacoustics,” *Accepted for publication in Journal of Fluid Mechanics*, 2011.

## 6 Self-ignition scenarios after rapid compression of a turbulent mixture weakly-stratified in temperature (CORIA)

This work was performed by G. Lodier, C. Merlin, P. Domingo, L. Vervisch, from CORIA - CNRS and INSA de Rouen, Technopole du Madrillet, BP 8 76801 Saint-Etienne-du-Rouvray, France and Renault -Technocentre, 1 avenue du Golf 78 288 GUYANCOURT.

### 6.1 Self-ignition scenarios after rapid compression of a turbulent mixture weakly-stratified in temperature

The physics of ignition at constant pressure or constant volume has been the subject of multiple studies (see Zeldovitch, Comb. Flame 1980, Sreedhara and Lakshmisha, Proc. Comb Inst. 2002, Gu et al, Comb. Flame 2003, Dec, Proc. Comb. Inst. 2009). Recently, numerical simulations of laboratory engines have made great progress addressing cycle-to-cycle variations and other concerns with Large Eddy Simulation (LES) as in Enaux et al, FTaC 2011. Detailed combustion chemistry plays here a major role and Direct Numerical Simulation (DNS) including a refined description of chemistry was also used for understanding the influence of chemical paths on n-heptane/air mixtures ignition, in the case of non-uniform temperature and at constant volume for two-dimensional flows (see Yoo et al, Comb. Flame 2011).

The flow topology is known to have a tremendous impact in ignition after rapid compression, also the objective of the present work is to analyze ignition scenarios in a context as close as possible to an existing experimental system. LES of engine combustion-chambers would lack of resolution to identify the detail of ignition processes. DNS with detailed chemistry is still usually two-dimensional and in canonical geometries for resolution constrains, thereby not including the key features of real flow dynamics, which are responsible for temperature fluctuations appearing within wall boundary layers, along with the complex and specific flow patterns resulting from admission and subsequent rapid compression. A complementary route has been recently tempted

at CORIA; the geometry of a rapid compression machine experimentally investigated by Guibert et al, FTaC 2010 is considered first with LES, to calibrate a three-dimensional simulation procedure with an admission sequence into a cylindrical combustion chamber through a turbulence-grid. Then, keeping the same flow admission velocity sequence, the system is downsized for DNS, with a resolution of about  $20 \mu m$ .

The overall simulation procedure can be compared against experiments and the flow and temperature distributions observed in the DNS are not arbitrary, but result from the experimentally observed admission-compression sequence. However, because of resolution requirements, simple chemistry is used, therefore only the interaction between a generic heat-release ignition process and the turbulent flow is reproduced.

Simulation parameters have been varied for ignition to occur in mixtures featuring various temperature stratification patterns, due to wall cooling and turbulence characteristics. Conditions favoring distributed, spotty- or homogeneous-ignition are evidenced. As anticipated from experiments, depending on characteristic times (coherent structure, residence time, flow engulfment and mixing times) ignition has been shown occur within localized compression zones, between vortical structures, or more homogeneously within large scale flow structures.

Very small differences in local temperature and flow topology appear to lead to different routes toward successful auto-ignition. The underlying mechanisms have been analyzed from an internal energy budget expressed as a temperature balance equation.

Table 1: Cases simulated.  $T_{Ac}$ : activation temperature,  $T_o = 343$  K.  $\tau_{ig}$ : ignition delay.  $t_{TDC} = 29$  ms.  $u'/U_o(t)$ : turbulence intensity at injection ( $U_o(t)$  bulk admission velocity)

Case	$T_{Ac}/T_o$	$\tau_{ig}/t_{TDC}$	$u'/U_o(t)$	Ignition type
(i)	48	0.976	10%	Vortex core
(ii)	52	1.134	10%	Shear layer

The Navier-Stokes equations are solved in their fully compressible form with the structured grid solver SiT-Com (Simulating Turbulent Combustion, Subramanian et al, Comb. Flame 2010), developed at CORIA, using immersed boundaries for wall modeling. The DNS are performed with 70,136,136 grid points in 3D, with a resolution of about  $20 \mu m$ . 4096 processors of an IBM Blue Gene/P machine are used.

Figure 21 shows turbulent structures colored by temperature in case (ii), before ignition. The flow patterns are visualized with the Q-criterion which is a marker of the turbulent vortical structures. Close to top-dead-center, the flow undergoes significant change in its topology. Large scale Kelvin-Helmholtz toroidal vortices, generated downstream of the admission plane, are present at  $0.94 t_{TDC}$  (Figure 21-a), to strongly cascade when the flow reaches the cylinder closing wall, ending in a quite well developed turbulence at  $1.07 t_{TDC}$  (Figure 21-c).

The large scale rollers are visible in the pressure field of Figure 22-a, featuring pressure drop inside the toroidal vortices. At this time, before any chemical ignition, in the center of the cylinder, pressure fluctuations are traveling backwards with turbulence from the end of the chamber, leaving an adiabatic-core almost unaffected by heat losses at walls close to the injection plane, which mainly evolves according to the global compression. This

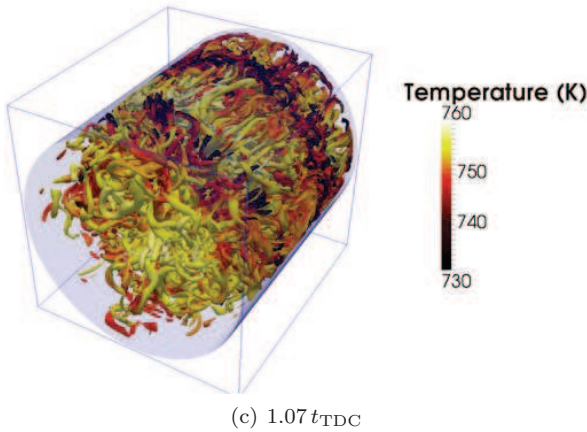
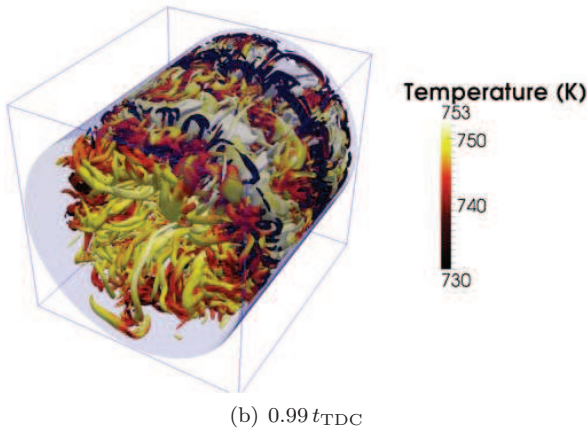
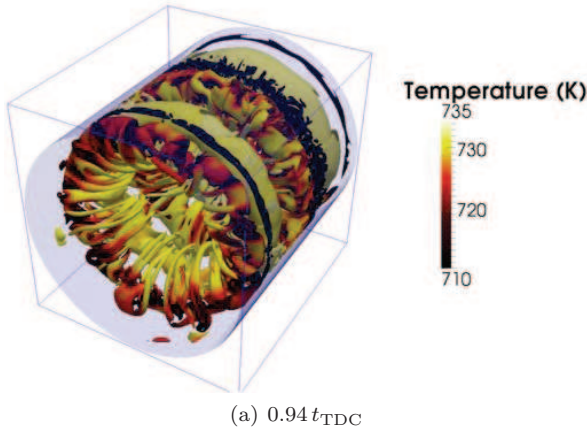


Figure 21: Iso-contour of  $Q$ -criterion ( $Q = 15 \cdot 10^6 \text{ s}^{-2}$ ) colored by temperature, case (ii). Flow goes from left to right

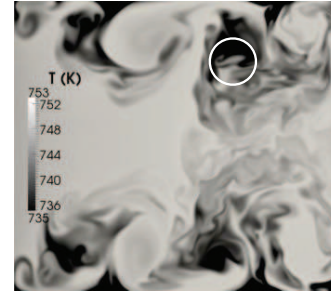
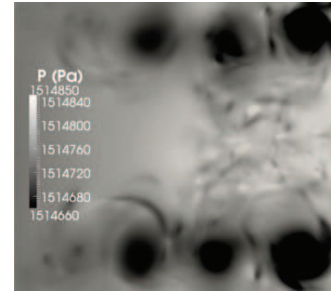


Figure 22: Pressure and temperature centerline plane. Case (ii),  $t = 0.94 t_{TDC}$

is also visible in the temperature snapshot (Figure 22-b), where cold fluid is entrained from the wall to be intensively mixed with the main flow, up to an almost uniform temperature zone, not yet affected by small scale fluctuations.

After the rapid compression, coherent flow structures are generated during the admission of the fuel-lean charge in the combustion chamber (Figure 21). The temperature distribution inside these structures evolves according to three phenomena: adiabatic compression, engulfment and mixing with colder fluid from wall boundary layers. Accordingly, a competition develops between the adiabatic compression, which increases the temperature of the volume of gaseous mixture, and, mixing with colder fluid from wall, which locally decreases fluid internal energy. Under these conditions, two major ignition scenarios have been observed:

I) For an ignition delay smaller than the time required for turbulent mixing to damp out high temperature fluctuations between wall layers and the inside of coherent flow structures, as in case (i), the core of large-scale vortices is almost ‘thermally insulated’ and ignition will primarily appear inside these flow rollers, which are almost homogeneously distributed over the flow domain, leading to a global ignition phenomena.

II) When turbulent mixing has sufficiently influenced the flow before ignition, as in case (ii), the starting of ignition will be controlled by very localized details of the flow topology, as for instance local compression zones between coherent structures, where the flow divergence is an additional source of temperature. Ignition is then found to be non-global, but rather scattered.

## Acknowledgment

This work was granted access to the HPC resources of IDRIS-CNRS under the allocation 2011-020152 made by GENCI (Grand Equipement National de Calcul Intensif) and was funded by ANRT (Agence Nationale de la

Recherche et de la Technologie) and Renault, under the CIFRE N° 382/2009. The authors are grateful to Prof. Philippe Guibert for providing experimental details of the Rapid Compression Machine. This study has been accepted for presentation at the 9th International ERCOFTAC Symposium on Engineering Turbulence Modelling and Measurements, Thessalonique 2012.

## 7 Numerical study of heat transfer in a dielectric liquid inside a cylindrical annulus (LOMC)

This work was performed by Marlene Smieszek, Olivier Crumerolle, Innocent Mutabazi and Christoph Egbers, from LOMC, Le Havre.

We investigate numerically the development of thermoconvective instabilities in a dielectric liquid confined in a vertical cylindrical annulus with a radial dielectrophoretic force and a radial temperature gradient. We show that, with stationary cylinders, the first axisymmetric instability mode appears in form of stationary counter-rotating rolls. These rolls enhance heat transfer between the two cylinders.

### 7.1 Introduction

The problem of the stability of a dielectric liquid confined in a cylindrical annulus submitted to a combined action of a radial temperature gradient and an alternative electric field is of great interest from both fundamental and applied research. The temperature gradient applied to the dielectric liquid induces a gradient in the fluid properties (the dielectric constant and the electrical conductivity). The application of an alternative electrical field to the liquid produces a dielectrophoretic force that can induce convective motion in the fluid. From the fundamental standpoint, the problem of the onset of convective instability in a dielectric liquid under a simultaneous action of a radial ac electric field and a radial temperature gradient is of particular interest since the electric field generates an effective radial gravitation field. The electrical gravitation depends on the distance according  $r^{-5}$  for the spherical geometry and  $r^{-3}$  for the cylindrical configuration. For strong enough electric field, the electrical gravity can overcome the Earth gravity and then it is possible to realize the microgravity conditions. The application of the electric and temperature gradient to a liquid is used for heat transfer enhancement and may yield large reductions in weight and volume of heat transfer systems. This technique may become attractive for aerospace cooling systems [1].

In case of zero Earth gravity, the stability of a dielectric liquid inside a cylindrical annulus without rotation has been investigated both theoretically and experimentally by Chandra and Smylie [2] and theoretically by Takashima [3]. In these studies, the flow system was assumed to be infinite, the effect of the electric field was not well highlighted. In the present study, we consider a finite length annulus and compute the base flow and determine the onset of 2-d stationary electro-hydrodynamic convection for different values of the temperature difference applied to the cylinders.

## 7.2 Problem Formulation

### 7.2.1 Flow Equations

The flow system consists of two stationary coaxial cylinders with the radii  $a$  and  $b$  and the length  $L$ . It is characterized by the following geometrical non dimensional parameters : the radius ratio  $\eta = a/b$  and the aspect ratio  $\Gamma = L/d$  where  $d = b - a$  is the gap-width between the inner and outer cylinder.

The Navier-Stokes equations for an incompressible fluid are:

$$\vec{\nabla} \cdot \vec{v} = 0 \quad (1)$$

$$\rho \frac{\partial \vec{v}}{\partial t} + \rho(\vec{v} \cdot \vec{\nabla})\vec{v} = -\vec{\nabla}p + \mu \nabla^2 \vec{v} + \rho \vec{g} + \vec{f}_E \quad (2)$$

with  $\rho$  is the liquid density,  $\vec{g}$  the gravitational acceleration,  $p$  the pressure,  $\mu$  is the dynamic viscosity of the fluid and  $\vec{f}_E$  is the electric body force given by Landau and Lifshitz [4]:

$$\vec{f}_E = \rho_e \vec{E} - \frac{1}{2} \vec{E}^2 \vec{\nabla} \epsilon + \frac{1}{2} \vec{\nabla} \left( \rho \frac{\partial \epsilon}{\partial \rho} \vec{E}^2 \right) \quad (3)$$

where  $\rho_e$  is the free electric charge density,  $\vec{E}$  is the electric field,  $\epsilon$  is the dielectric permittivity of the liquid. The last term can be inserted into the pressure term in equation (2). In our case we are interested only in the effect of the dielectrophoretic force:

$$\vec{f}_{DEP} = -\frac{1}{2} \vec{E}^2 \vec{\nabla} \epsilon \quad (4)$$

Neglecting the viscous and electric dissipation terms, we write the equation of energy conservation as :

$$\frac{\partial T}{\partial t} + (\vec{v} \cdot \vec{\nabla}) T = \kappa \nabla^2 T \quad (5)$$

where  $\kappa$  is the thermal diffusivity of the fluid. The equations for the electric field are

$$\begin{aligned} \vec{\nabla} \cdot (\epsilon \vec{E}) &= 0, \\ \vec{\nabla} \times \vec{E} &= 0, \\ \vec{E} &= -\vec{\nabla} V \end{aligned} \quad (6)$$

where  $V$  is the rms of the electric high voltage. The Boussinesq approximation is used for the fluid density in the gravity term in equation (2):

$$\rho = \rho_0(1 - \alpha(T - T_0)), \rho_0 = \rho(T_0) \quad (7)$$

where  $\alpha$  represents the thermal expansion coefficient. The dielectric constant is assumed to depend linearly on the temperature:

$$\epsilon = \epsilon_1(1 - \gamma(T - T_1)), \epsilon_1 = \epsilon(T_1). \quad (8)$$

The boundary conditions are no-slip and perfect conduction on the lateral walls (constrained temperatures and electric potential),

$$\begin{aligned} \vec{v} &= \vec{0} \quad \text{at } r=a, r=b \\ T &= T_a \quad \text{at } r=a, \quad T = T_b \quad \text{at } r=b \\ V &= 0 \quad \text{at } r=a, \quad V = V_b \quad \text{at } r=b \end{aligned}$$

and no-slip, thermal and electrical insulation at top and bottom.

### 7.2.2 The Dielectrophoretic effect

A dielectrophoretic force field can be established in the gap between the inner and outer cylinder. From 1 the equation for the vorticity  $\vec{\omega} = \vec{\nabla} \times \vec{v}$  is easily obtained:

$$\frac{\partial \vec{\omega}}{\partial t} + (\vec{v} \cdot \vec{\nabla}) \vec{\omega} = (\vec{\omega} \cdot \vec{\nabla}) \vec{v} + \nu \Delta \vec{\omega} + \alpha (\vec{g} + \vec{g}_e) \times \vec{\nabla} T \quad (9)$$

where  $\vec{g}_E$  is the electric gravity induced by the electric field. For the base state, the electric gravity reads

$$\vec{g}_e = \frac{\epsilon_1 \gamma}{\rho_0 \alpha} \left( \frac{V_b}{\ln(a/b)} \right)^2 \cdot \frac{\vec{e}_r}{r^3} \quad (10)$$

and is directed towards the inner cylinder. We now restrict ourselves to the microgravity case i.e.  $g \simeq 0$ . When a temperature gradient is applied between the inner and outer cylinder, where  $T_a > T_b$ , a Rayleigh number can be defined

$$Ra = \frac{\alpha g_e \Delta T d^3}{\nu \kappa} \quad (11)$$

Here  $\nu = \mu/\rho$  is the kinematic viscosity of the liquid and  $\Delta T = T_b - T_a$  is the temperature difference between the inner and outer cylinder. Since the electrically induced gravity  $g_e$  is a function of the radius, the values of the Rayleigh number refer to  $Ra(b)$  at the outer cylinder.

### 7.2.3 Numerical method

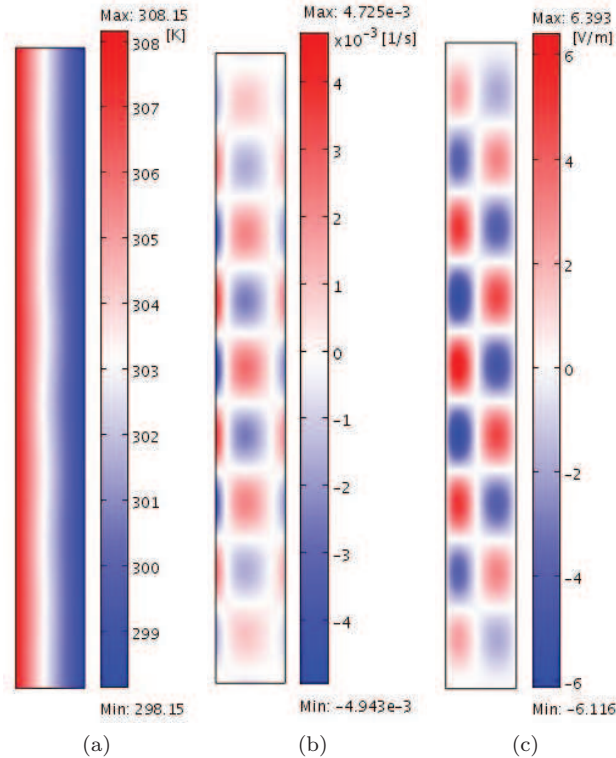


Figure 23: (a) Temperature, (b) vorticity and (c) Axial electric field in axial direction at the onset for  $B = 0.0107$

The numerical simulations are performed with the finite element method implemented in the Comsol Multiphysics package. First we assume axisymmetric behavior and perform 2D simulations. In that case we use Lagrange P2P1 elements for the Navier-Stokes equations.

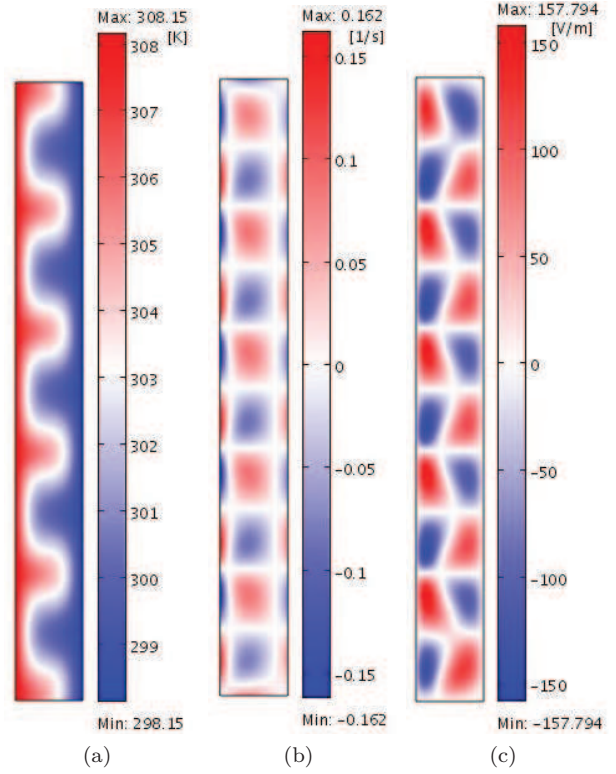


Figure 24: (a) Temperature, (b) vorticity and (c) Axial electric field at  $Ra = 1.31Ra,c$  for  $B = 0.0107$

For the energy equation and the equation of electrostatics Lagrange quadratic elements are chosen. The simulations are performed with a quadrilateral mesh consisting of 6600 elements.

Preliminary 3D simulations are run with P3P2 elements and a mesh consisting of 140 hexahedral elements. Cubic Lagrange elements are used for the energy equation and the equation of electrostatics. The annular gap is represented by a cartesian volume with periodic boundary conditions in the "azimuthal" direction. Curvature effects are explicitly included in the equations. The boundary conditions are the same as in 2D case.

## 7.3 Results

### 7.3.1 2D Simulations

The first instability mode occurs in form of counter-rotating rolls. 23 shows examples the temperature field, the vorticity and the axial component of electric field in the  $(r,z)$  cross section at the onset of the first instability mode for  $B = 0.0107$ . Whereas the temperature field (Figure 23(a)) exhibits only weak perturbations, the electric field in axial direction (Figure 23(c)) is strongly influenced by the occurring flow. With increasing the electric tension the temperature field is affected by the flow as shown in 24.

To investigate the influence of the geometry on the onset of the first instability mode, the radius ratio of the cylindrical annulus is varied. In 25 the variation of the critical Rayleigh number shows a very weak dependence on  $B = \gamma \Delta T$ . For  $\eta = 0.9$  the onset was found at significant higher values of  $Ra$  compared to the simulations with wide-gap ( $\eta = 0.5$ ).

26 shows the Nusselt number  $Nu$  computed at the outer cylinder above the onset of the counter-rotating vortices for three values of  $B$ . The heat transfer increases with the Rayleigh number.

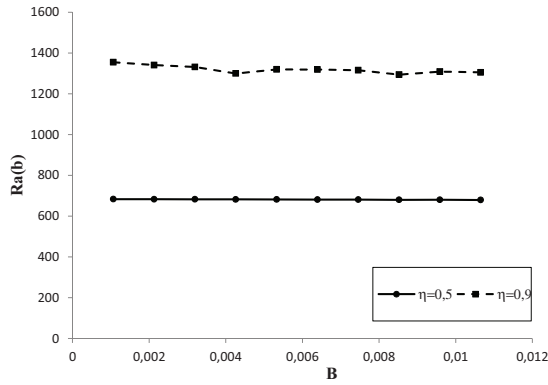


Figure 25: Onset of the axisymmetric instability mode for different values of  $B$  and for  $\eta = 0.5$  (circles) and  $\eta = 0.9$  (squares).

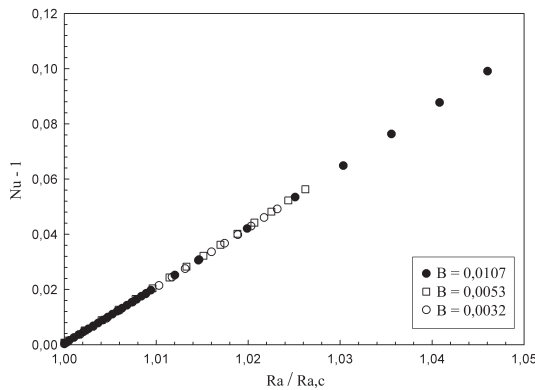


Figure 26: Variation of  $Nu$  at  $r = b$  with reduced Rayleigh number.  $Ra, c$  is the critical Rayleigh number.

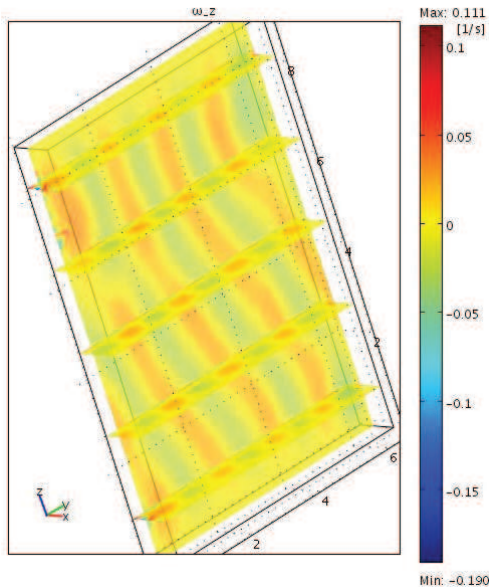


Figure 27: Axial vorticity component at  $t = 1000 \cdot d^2/\kappa$  for  $Ra = 1.01Ra, c$ ,  $B = 0.0107$ .

### 7.3.2 3D Simulations

For short times  $t \sim d^2/\kappa$ , 3D simulations retrieved the axisymmetric counter-rotating rolls. The corresponding azimuthal vorticity is weak but actually dominates the flow pattern. However the long time simulations ( $t = 1000 \cdot d^2/\kappa$ ), the flow is dominated by inclined rolls as shown in 27.

## 7.4 Discussion and Conclusion

Our simulations investigated the heat transfer associated with axisymmetric instability modes in a dielectric fluid in a vertical annulus in microgravity condition. 25 indicates that a flow within a wide gap is more unstable to axisymmetric modes than a flow within a small gap. This emphasizes the importance of curvature. We found that the electric field increases the heat transfer thanks to the counter-rotating rolls. This result is also reported in theoretical and experimental investigations of electrohydrodynamically (EHD) induced heat transfer in liquids [1, 5]. However, in these works, the thermal convection is of less interest and the dielectrophoretic effect is of minor importance due to focussing on homogeneous/DC fields.

We have performed long time 3D simulations (27) which show that rolls are non-axisymmetric and inclined. This last result is in qualitative agreement with experimental investigation by Sitte et al. [6] in a parabolic flight campaign, who reported a broken azimuthal symmetry, in agreement with recent results of linear stability analysis [7].

## Acknowledgment

This work was supported by the CPER Haute-Normandie and the CNES. M.S. benefitted from a post-doctoral fellowship from the Regional Council of Haute-Normandie.

## References

- [1] J. Paschkewitz and D. Pratt *Exp. Therm. Fluid Sci.*, vol. 21, p. 187, 2000.
- [2] D. S. B. Chandra *Geophys. Fluid Dyn.*, vol. 3, p. 211, 1972.
- [3] M. Takashima *Q. J. Mech. appl. Math.*, vol. 33, p. 93, 1980.
- [4] L. Landau and E. Lifshitz, *Electrodynamics of continuous media*. Pergamon Press, New York, 1960.
- [5] T. Jones *Adv. Heat Trans.*, vol. 14, p. 107, 1978.
- [6] B. Sitte, J. Immohr, O. Hinrichs, R. Maier, C. Egbers, and H. Rath in *12<sup>th</sup> ICTW*, 2001.
- [7] S. Malik, O. Crumeyrolle, H. Yoshikawa, and I. Mutabazi *Acta Astronautica*, 2012.

## 8 Effect of a radial temperature gradient on a vertical circular Couette flow (LOMC)

This work was performed by R. Guillerm, A. Prigent, D.-H. Yoon, C.-W. Kang, K.-S., Yang, S. Malik, H. Yoshikawa and I. Mutabazi, from the LOMC Laboratory and Department of Mechanical Engineering, INHA University, Incheon 402-020, Republic of Korea.

## Abstract

We have performed experimental and numerical investigations of the instabilities of a fluid confined in a vertical cylindrical annulus with a radial temperature gradient. The inner surface is rotating while the outer is fixed.

The primary instability occurs via a Hopf bifurcation to a travelling inclined vortices. The velocity and temperature distributions in the gap have been measured using thermochromic liquid crystals. Numerical simulations both in infinite and finite flow systems confirm the experimental data at least near the onset of the first instability.

## 8.1 Introduction

Flow in a differentially rotating cylindrical annulus with a radial temperature gradient is encountered in many industrial applications, such as cooling systems of electric motors or electronic circuitries, in turbomachines and pumps [1]. It has been investigated experimentally and numerically by few authors [2, 3, 4, 5, 6]. For small values of the control parameter, away from the top and bottom boundaries, the base flow has two velocity profiles each of which is unstable. The rotation induces circular Couette flow which is potentially unstable to centrifugally driven perturbations leading to longitudinal vortices. The radial temperature gradient induces a baroclinic vertical flow (ascending near the hot surface and descending near the cold one). This flow has a velocity profile with an inflexion point and it is potentially unstable to transverse oscillatory perturbations. The present study is concerned with experimental and numerical simulations of this flow when the driving forces (control parameters) are increased in magnitude.

## 8.2 Experimental setup

The experimental setup consists of two coaxial cylinders of height  $L = 55.9\text{ cm}$  and a gap  $d = 0.5\text{ cm}$ . The aspect ratio of the system is  $\Gamma = 111.8$  and the radius ratio  $\eta = 0.8$ . The inner cylinder is rotating at angular frequency  $\Omega$  while the outer cylinder is fixed. Inside the inner cylindrical tube was circulating a water maintained at controlled temperature  $T_1$  and the outer cylinder was immersed into a large thermal bath maintained at controlled temperature  $T_2$ . The working fluid is a deionized water with a kinematic viscosity  $\nu = 10^{-2}\text{ cm}^2/\text{s}$  at  $T = 295\text{ K}$ . The flow was visualized by adding a suspension of Kalliroscope AQ1000 in 2% by volume. To visualize the temperature fields, we seeded the flow with SR25C5W thermochromic liquid crystals from Hallcrest of about by 0.05%. They occur in form of encapsulated spheres of mean diameter  $75\mu\text{m}$  and their response time to a temperature change is about  $3\text{ ms}$ . The black to red (first observed color) transition occurs at  $T = 25^\circ\text{C}$  and the width of the active range is  $5^\circ\text{C}$ . To realize quantitative measurements, the temperature of the crystals is associated with the hue angle,  $h$ , defined in a polar chromaticity space determined by the intensities of the Red, Green and Blue primaries (the RGB values) recorded by the image acquisition equipment [3]. These particles have also been used to determine the velocity components, using a Basler IEEE-1394 camera, by tracking pictures of the cross section with a time delay of 82 ms.

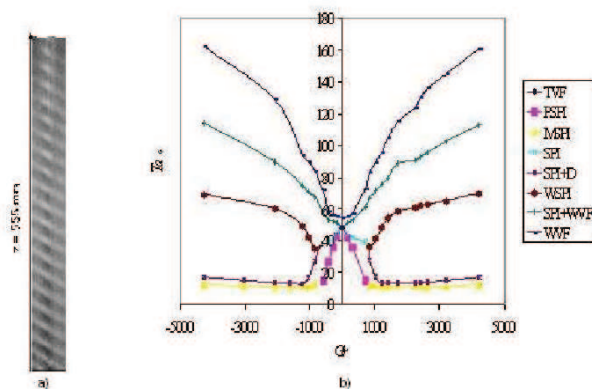


Figure 28: a) Pattern observed for  $Ta = 24$  and  $Gr=706$ . b) Diagram of bifurcations in the plane  $Gr, Ta$

## 8.3 Numerical simulations

The flow is governed by the Navier-Stokes equations, energy equation and mass conservation equations written in cylindrical coordinates together with no-slip boundary conditions and isothermal cylindrical surfaces. Neglecting the end effects near the top and bottom plates, the base flow velocity profile is  $\vec{v} = V(r)\vec{e}_\theta + W(r)\vec{e}_z$  where  $V(r)$  and  $W(r)$  are the circular Couette profile and the baroclinic axial velocity component respectively; their expressions can be found in [5]. We have performed linear stability of this flow assuming an infinite length of the system.

We have performed direct numerical simulations of the governing equations. These equations are discretized using a finite-volume method in a cylindrical coordinate system. For the velocity field, a second-order accurate central differencing is utilized for spatial discretization. For the temperature field, the QUICK (Quadratic Upstream Interpolation for Convective Kinematics) scheme is employed for convective terms. A hybrid scheme is used for time advancement; non-linear terms and cross diffusion terms are explicitly advanced by a third-order Runge-Kutta scheme, and the other terms are implicitly advanced by the Crank-Nicolson scheme. A fractional step method is employed to decouple the continuity and momentum equations. The resulting Poisson equation is solved by a multigrid method.

### 8.3.1 Results

The flow regimes in the chosen configuration can be described by three dimensionless control parameters : the Prandtl number  $Pr = \nu/\kappa$ , the Grashof number  $Gr = \alpha\delta Tgd^3/\nu^2$  which measures the magnitude of the temperature gradient on the flow and the Taylor number  $Ta = (\Omega ad/\nu)(d/a)^{1/2}$  related to rotation and therefore counting for centrifugal effects.

A radial temperature gradient imposed on the cylindrical surfaces of the flow annulus induces a large convective cell with particles ascending near the hot wall and moving downwards near the cold one. The  $z$ -averaged radial temperature profile and  $z$ -averaged radial profile of axial velocity show good agreement with the theoretical profiles obtained by solving the governing equations of the base flow. For a fixed value of Grashof number, we have increased the rotation rate until we obtained a bifurcation to a new state formed of pattern of helicoidal vortices (Figure 1-a). All critical states are represented

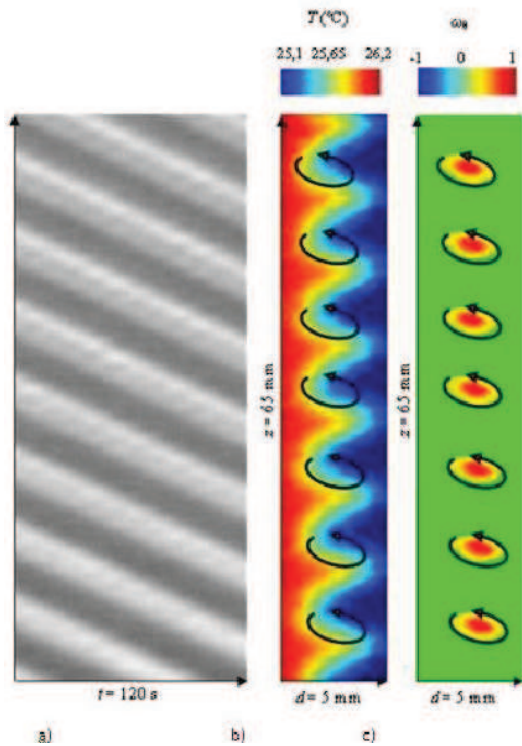


Figure 29: a) Space-time diagram of the pattern observed for  $Ta= 24$  and  $Gr=706$ . b) Temperature distribution in the gap, c) Vorticity distribution in the gap

in the diagram  $(Gr, Ta)$  in Figure 1-b. For chosen state, we have measured the velocity field and the temperature in the cross section (Figure 2).

We have performed linear stability analysis and found that critical modes are non-axisymmetric oscillating vortices, stream functions and isotherms of which are shown in Figure 30 a-b. The variation of critical values of  $Ta$  with  $Gr$  are in a very good agreement with experimental ones. The corresponding state diagrams are well superimposed. Simulated states using DNS are shown in Figure 30 c-d for  $Ta = 40$  and for two values of  $Gr$ . For  $Gr = 500$ , the pattern is formed of co-rotating traveling vortices, while for  $Gr = 1000$  the pattern is formed by counter-rotating vortices with defects.

## 8.4 Conclusion

We have performed thorough investigation of stability of the flow between differentially rotating annulus with a radial temperature gradient. We have found a good agreement between experimental results, those from linear stability analysis and from numerical simulations [7].

## Acknowledgment

This work has benefited from financial support of European Regional Development Fund (FEDER), the CPER, a grant from the Regional Council of Haute-Normandie and bilateral exchange programs STAR and CNRS-KOSEF between France and Korea.

## References

[1] F. Kreith, in *Advances in Heat Transfer* **5**, Academic Press NY, 129 (1968).

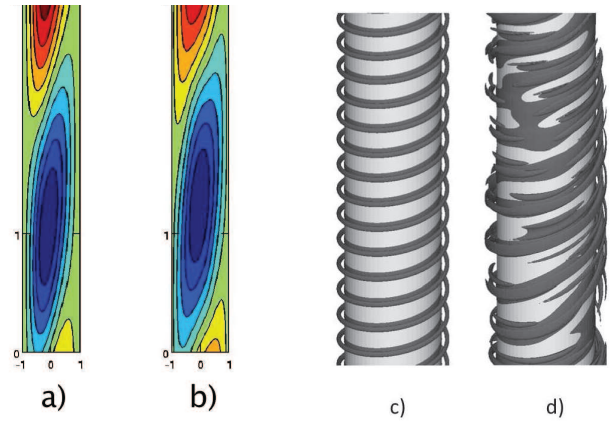


Figure 30: Patterns obtained from linear stability analysis: a) streamfunctions, b) isotherms and from DNS: c) co-rotating vortices, d) counter-rotating vortices

[2] H.A. Snyder, S.K.F. Karlsson, *Phys. Fluids*. **7**(10), 1696 (1964).  
 [3] P.D. Weidman and M. E. Ali, *J. Fluid Mech.***220**, 53 (1990).  
 [4] D.C. Kuo, K.S. Ball, *Phys. Fluids* **9**, 2872 (1997).  
 [5] V. Lepiller, A. Goharzadeh, A. Prigent and I. Mutabazi, *Euro.Phys. J. B* **61**, 445 (2008).  
 [6] R. Guillermin, *Thèse de doctorat de l'Université du Havre* (2010).  
 [7] D.H. Yoon, C.W.Kang, K.S. Yang and I. Mutabazi, *16<sup>th</sup> Int. Couette Taylor Workshop*, Princeton 9-11 September 2009

## 9 Flows and Aerodynamic Systems, PRISME, University of Orléans (Azeddine Kourta)

The group (Flows and Aerodynamic Systems) "Ecoulements et Systèmes Aérodynamiques" (ESA) is one of the groups involved in PRISME laboratory (Pluridisciplinaire de Recherche en Ingénierie des Systèmes, Mécanique et Energétique), research laboratory of University of Orléans. ESA develops physical analysis, modelling and control of free or bounded shear turbulent flows. Theoretical, experimental and numerical approaches are used to:

- Investigate and control shear flows (active flow control and development of actuators),
- Analyse vortex dynamic and vortex interaction,
- Analyse and characterize transition and non equilibrium turbulence,
- Analyse and characterize atmospheric boundary layer flows,
- Study rotating aerodynamic systems (Wind turbine, rotors, ...).

The applicative domains are aerodynamics, aeroacoustics and energy.

The laboratory owns highly performante experimental facilities: large closed-loop wind tunnel (PRANDTL type) and small open-loop EIFFEL type wind tunnel. These facilities are equipped with classical and optical tools (PIV, LDA, hot wires, steady and unsteady pressure sensors, aerodynamic balance), appropriate data acquisition and dedicated post-processing. It also operates numerical codes able to treat complex multi-physics configurations, which can be DNS, LES, URANS and RANS simulations.

The group works in collaboration with automotive and aeronautic transport industry as well as energy and environment institutions. It has many national and international research laboratory collaborations. It is involved in European (PlasmAero, WAUDIT) and national projects (ANR SPICEX SePaCoDe). It is member of GDR Separation Control, GDR Turbulence, GDRE Numerical Computation.

## 9.1 Flow Control and Development of Actuators

The objectives of the ESA group in relation with these topics are to characterize predominant mechanisms undergoing flow separation by developing experimental and numerical studies, and improve the prediction of physical phenomena. Besides, classical passive control, the group develops active flow control strategy and supplies with efficient actuators. It also develops innovative adaptive control.

### 9.1.1 Vortices and unsteady flow analysis

The first step is to characterize separated flows, wakes and vortical structures. The group examined geometrical shape effects on predominant mechanisms and related vortex interaction. Experimental study is done to analyse a 3D separation on bluff body. The geometrical model is an Ahmed body with rear window tilted at  $25^\circ$ . In this case smooth and sharp connexion between the roof and the rear window have been used. If separation exists when geometry is sharp, this one is no more true with smooth one. This allowed to the characterisation of the interaction between longitudinal vortices and separation (Thacker 2010 [1] Gilliéron et al [2]). Studies have been done with various rear Ahmed body part. Wakes after Ahmed body with rear window tilted at  $35^\circ$  or with square back have been analysed. This last configuration continue to be studied and active control will be applied to this case in order to reduce aerodynamic drag.

Identification of organized motion responsible for flow unsteadiness is a key issue in designning efficient control. The ESA group develops the Proper Orthogonal Decomposition (POD) (Thacker 2010 [1] and currently works on an original post-processing method, namely The Empirical Mode Decomposition (EMD) which is relevant to analyse non stationnary and nonlinear systems. In order to discriminate between coherent and turbulent random fluctuations, a "resemblance" criterion has been introduced and assessed on turbulent signals pertubed with low frequency sine or chirp (Mazellier and Foucher 2011 [3])

### 9.1.2 Flow control: development of actuators

To improve performance with low cost, it is important to develop efficient actuators to control separation. The group uses fluidic actuators (steady and unsteady jets) and plasmas actuators. In collaboration with Florida State University, micro jets have been tested (Aubrun et

al 2011 [4]). Also with GREMI laboratory at Orléans, plasma actuators have been developed and tested to control aerodynamic flows (Audier et al 2011 [5], Benard et al 2011 [6]). These actuators will be applied for the drag reduction or the lift enhancement as developed in the paragraph related to the active control with plasma actuators.

Fluidic actuator has been developed in collaboration with IMFT and ICA laboratories at Toulouse to generate continuous, pulsed or synthetic jet. It consists of a cylindrical cavity closed on one side by a metallic plate in which a rectangular slot has been machined and connected on the other side to the exit of a loudspeaker (Batikh et al 2010 [7]). The latter is controlled (in frequency and amplitude) by an electric signals generator associated to a variable volume chamber. The width and the length of the slot are  $500 \mu\text{m}$  and  $10 \text{ mm}$ , respectively. Its thickness is  $500 \mu\text{m}$ . The synthetic jet can be generated in a frequency range from 50 to 1,500 Hz and for each frequency with a pressure peak-to-peak amplitude in the cavity between  $2.5 \times 10^2$  and  $2 \times 10^3$  Pa. For generating the pulsed jet, an additional continuous flow rate is supplied in the cavity. Finally the continuous jet is obtained by keeping only the continuous component without actuating the loudspeaker. When applied to control flow separation, the three types of jets permit to remove the separation bubble. However, the synthetic jet seems to be more efficient insofar as it induces a higher increase in velocity in the near wall zone of the cross-flow downstream from the wall bend.

### 9.1.3 Flow control: Passive and active control

Flow separation control is of major interest in fundamental fluid dynamics as well as in various engineering applications. Numerous techniques have been explored to control the flow separation either by preventing it or by reducing its effects. These methods range from the use of passive devices to the use of active control devices either steady or unsteady (synthetic jets, acoustic excitation, plasma). Among the various strategies employed in aerodynamic control, conventional passive control techniques, consisting in modifying the shape of the vehicle to reduce the aerodynamic drag, appear as the easiest to implement. Unfortunately, this simplicity is also the main drawback of such devices which are often irrelevant when the flow configuration changes. Indeed, the modification of the shape that produces better aerodynamic properties requires a thorough understanding of turbulent flows around vehicles. Current research efforts are now focusing on active flow control techniques as an alternative to conventional design-modification solutions.

#### Passive flow control

Flow control on road vehicle geometry, especially on an Ahmed body was studied in the past by experimental and numerical means. Passive control was performed experimentally by using vertical splitter plates (Gilliéron and Kourta 2010 [8]). The capacity of vertical splitter plates placed at the front or the rear of a simplified car geometry to reduce drag, with and without skew angle, was investigated for Reynolds numbers between  $1.0 \times 10^6$  and  $1.6 \times 10^6$ . Drag reductions of nearly 28% were obtained for a zero skew angle with splitter plates placed at the front of models of MPV or utility vehicles. The results demonstrate the advantage of adapting the position and orientation of the splitter plates in the presence of a lateral wind.

### Passive adaptive flow control

The performances of an original passive control system based on a biomimetic approach are assessed by investigating the flow over a bluff-body (Mazellier et al 2012[9]). This control device consists of a couple of flaps made from the combination of a rigid plastic skeleton coated with a porous fabric mimicking the shaft and the vane of the bird's feathers, respectively. The sides of a square cylinder have been fitted with this system so that each flap can freely rotate around its leading edge. This feature allows the movable flaps to self-adapt to the flow conditions. Comparing both the uncontrolled and the controlled flow, a significant drag reduction ( $\approx 22\%$  in average) has been obtained over a broad range of Reynolds number. This improvement is related to the increase of the base pressure in the controlled case. The investigation of the mean flow reveals a noticeable modification of the flow topology at large scale in the vicinity of the controlled cylinder. Meanwhile, the study of the relative motion of both flaps highlights that their dynamics are sensitive to the Reynolds number. Furthermore, the analysis of the flow dynamics at large scale suggests a lock-in coupling between the flap motion and the vortex shedding.

### Active flow control with plasma actuators

Active flow control has also been performed experimentally by using plasma actuator (Boucinha 2009 [10], Boucinha et al. 2011 [11]). The aim of this study is to reduce the drag of a simplified car geometry using surface dielectric barrier discharge actuators. Experiments were conducted in a wind tunnel for a low Reynolds number ( $6.7 \times 10^5$ ) with the Ahmed body reference (rear slant angle of  $25^\circ$ , zero yaw angle). The effect of steady and unsteady actuation on the flow topology was investigated carrying out 2C-PIV and 1D hot wire measurements. The efficiency of the actuators was characterized by stationary balance measurements. Drag reductions up to 8% were obtained by suppressing the separation bubble above the rear window. The results suggest that plasma actuators are simple to implement on a model and can provide useful information for automotive aerodynamics through parametric studies with parameters relevant for flow control (position, surface, frequency and duty cycle of the pulsed actuation).

The plasma actuator was used to control the turbulent/laminar transition (Magnier et al 2007 and 2009 [12, 13, 14]). The aim was to modify, by using surface plasma actuators, the laminar-to-turbulent transition location of a Blasius boundary layer developing on a flat plate mounted in a wind tunnel. Measurements of flow velocities were performed by hot wire anemometry. Results show that an actuator placed upstream the natural transition zone enables the promotion or the delay of the transition onset, depending on the location, the voltage amplitude, and the frequency of the high voltage electrical parameters.

The flow control has been also applied to airfoil lift enhancement and drag reduction. The enhancement of a NACA0012 aerodynamic airfoil performance by using a thin DBD actuator to control flow separation occurring around the leading-edge has been studied [15, 16]. The goal of this work is to improve the understanding of the actuator effects by selecting appropriate actuation forcing frequencies according to the uncontrolled flow natural frequencies. In order to consider Reynolds effects and to exhibit mechanisms of performance enhancement, tests were carried out in a deep-stall configuration corresponding either to the separation of

the natural boundary layer or of a tripped boundary layer. Mean aerodynamic force measurements, PIV and hot-wire anemometry in the vicinity of the shear layer and in the far wake were performed to characterize the benefits of the control. According to the forcing frequencies different modulation of the shear layer rollup and wake vortex shedding are observed. It is found that forcing frequencies closer to the wake vortex shedding frequency lead to the best response in terms of an improvement in aerodynamic performance.

### Active flow control with fluidic actuators

Continuous suction or blowing from a slot, jets, continuous (Aubrun et al 2011[4]) or pulsed jets (Bideaux et al[17]) were used to control separation. An active flow control solution by continuous suction was tested to reduce the aerodynamic drag on a simplified fastback geometry (Rouméas et al 2009 [18]). The continuous suction was set up according to a preliminary 2D numerical study, and the analysis of the flow topology with and without control was carried out according to the 3D numerical Lattice Boltzmann method. The suction influence on each of the vortices interacting in the near-wake flow was studied and the drag reductions obtained were discussed. Suction is conducive to creating significant local depression on the separation line identified without control, which has the effect of re-attaching the flow on the wall. A parametric analysis indicates that the re-attachment occurs at a suction velocity of  $0.6V_0$ . The elimination of the rear windows separated zone therefore prompts a reduction of the total pressure loss in the wake, a reduction in the wake cross section and an increase of the wall static pressure on the rear part of the geometry (rear window and base). The drag reductions associated with these modifications are close to 17% and the suction velocity increase, at  $V_{asp} > 0.6V_0$ , does not improve such a reduction significantly. Likewise, the drag reductions rapidly decrease when the suction velocity diminishes below  $0.6V_0$ . Considering the power consumed to generate suction, the suction velocity which maximizes the efficiency of control is however  $0.375V_0$ . At this velocity, the suction remains efficient with significant total pressure loss on the slot. This study also analyzes the influence of suction on the longitudinal vortices which significantly interact with the rear window separated zone. The vorticity and total pressure loss associated with the longitudinal vortex core increases as the suction is applied. This increase is reflected by a reduction of the viscous radius in the vortex core which prompts a wall static pressure increase under the vortex axis, on the rear window. Suction however does not significantly modify the structure of the vortices.

The Ahmed body with a  $25^\circ$  slant, was also equipped with an array of blowing steady microjets 6mm downstream of the separation line between the roof and the slanted rear window [4]. The goal here is to evaluate the effectiveness of this actuation method in reducing the aerodynamic drag, by reducing or suppressing the 3D closed separation bubble located on the slanted surface. The efficiency of this control approach is quantified with the help of aerodynamic load measurements. The changes in the flow field when control is applied were examined using PIV and wall pressure measurements and skin friction visualizations. By activating the steady microjet array, the drag coefficient is reduced by 9 to 11% and the lift coefficient up to 42%, depending on the Reynolds number. The strong modification of the flow topology under progressive flow control is particularly studied.

The synthetic jet has been also used both experimentally and numerically (Leclerc 2008 [19]). In this study prior to the flow control analysis, the main features of the reference case, i.e. without control, are deeply investigated in terms of topology and dynamics as well. The optimal parameters of the synthetic jet are found and their influences onto the flow are emphasized by spectral analysis the near-wake unsteadiness and the complex interaction between the actuation and the flow. For this case, the numerical simulations are based on a Lattice Boltzmann Method implemented in the commercial software Powerflow. In this numerical study, the drag reduction reaches 5% and 13% when the actuator is set upstream and downstream the corner between the roof and the rear window, respectively. Concerning the experimental study, a synthetic jet actuator has been developed. It is based on piezoelectric membrane. Its aerodynamic performances have been characterized experimentally. The dynamical response to the membrane power signal (frequency and voltage) is compared to the reduced model (Lumped Element Modeling) of the synthetic jet used to scale the actuator. Spatial and temporal evolution of the jet is compared to the existing results and its operating regime is validated to be used for the control. The flow downstream of the Ahmed body without control is described. The topology of the longitudinal vortices of the wake and their evolution with the Reynolds number is examined. Spectral analysis is also performed. For different Reynolds numbers, the aerodynamic efficiency of the drag control is analyzed varying synthetic jet parameters: momentum coefficient, reduced jet frequency and jet position. The study with respect to the momentum coefficient  $C_\mu$  variation allows for characterizing the mean topology of the controlled flow. The spectral analysis leads to identify the developed instabilities. With a rear window tilted at  $25^\circ$ , drag reductions of 8.5% ( $Re = 1.2 \times 10^6$ ) and of 6.5% ( $Re = 1.9 \times 10^6$ ) are reached. The control allows to reattach dynamically the rear window separation and to balance the torus vortex structure at the base.

An experimental investigation of the dynamic and the control of a longitudinal vortex emanating from the front pillar of a dihedral bluff body corresponding to a simplified geometry of an automotive vehicle has been conducted (Lehuteur et al 2010 [20]). The control system is based on a thin rectangular slot located along the lateral edge of the windscreen and provides steady suction or blowing normal to the lateral face of the geometry. Qualitative results obtained with dye visualizations and Schlieren photos provide an overview of the impact of the control on the topology of the vortex flow. Quantitative Stereo-PIV measurements and unsteady forces measurements are used to characterize the interaction between the control and the longitudinal vortex. The control with blowing is associated with an increase of the transversal sizes of the vortex envelope, a decrease of the velocity in the center of the vortex, associated with a breakdown of the vortex core, and to an increase of the aerodynamic drag. The results obtained with the suction show that the longitudinal vortex of the windscreen is reduced by a reattachment on the lateral side of the model for velocities equal or higher than the far field velocity. In this configuration, aerodynamic drag reductions of about 6% are obtained.

## 9.2 Time dependent turbulence model and its application

In the case where the turbulent flow is unsteady, it is difficult to apply a right procedure to compute it at low cost. Direct numerical simulation (DNS) or at least large eddy simulation (LES) are proper approaches to resolve small scales motion within a 3D framework. However, they require an enormous amount of resources for even simple geometry. A hybrid RANS/LES approach based on blending the best features of RANS and LES can be also used. Ideally, one could adequately simulate this class of flows with adapted unsteady RANS (URANS) technique. However, these turbulence models are well known to be dissipative and without caution unsteadiness might be damped. Here, the two transport equations model used is adapted to this purpose.

The starting point of the present approach is the decomposition of any instantaneous physical variable into a coherent, organized part and an incoherent, random part. Equations for the coherent part are obtained by performing an ensemble average of the instantaneous flow equations. The effects of the random part are introduced by using a non-linear time dependent turbulent viscosity model.

Assuming that the unknown correlations, resulting from the use of ensemble averaging, depend on the averaged velocity gradients, turbulent length, and velocity scales, a closure relation is derived by using the invariance theory. Using the realizability conditions, the coefficients are found to be functions of the time-scale ratio of the turbulence to the averaged strain rate and the one of the time scale of the turbulence to the averaged rotation rate. Using the turbulent kinetic energy and its dissipation to characterize the turbulent length and velocity scales, the averaged turbulent correlations can be derived. In this model the turbulent viscosity coefficient  $C_\mu$  is not constant but dependent on the deformation and rotation so it is locally flow dependent (kourta et al 2005 [21]).

A numerical study was conducted to investigate the oscillations resulting from a transonic shock wave/boundary layer interaction. To perform this computation OAT15A ONERA airfoil was selected. Using the previous turbulence model, the unsteady mechanism resulting from the shock wave/boundary layer interaction is analysed. First the shock wave position is unsteady and it moves downstream. Separation also moves with this displacement. When the flow is separated, in the wake another unsteady mechanism, the von-Karman instability is observed. Frequencies and levels of this phenomenon are well predicted. (kourta et al 2005 [21], Orlik et al 2011 [22]).

## 9.3 Wind resource assessment

Studying the far wake of a wind turbine which has an actuator diameter of hundred meters requires a domain of interest of at least ten hundreds meters. Furthermore, the wind turbine is located in the atmospheric boundary layer (ABL) which must be taken into account. These both requirements can be encountered by the use of an atmospheric boundary layer wind tunnel, which is an experimental facility where the atmospheric boundary layer properties are reproduced (mean velocity and turbulence intensity profiles, spectral content and length scales of the atmospheric turbulence) at a geometric scale from 1:100 to 1:1000. The return circuit of the Lucien Malavard wind tunnel has been adapted to enable the physical modelling of the ABL by adding a boundary

layer development plate of 16m equipped with roughness elements and some turbulence generators at the entrance of the test section. The combination of the turbulence generators and the roughness elements drive the class of terrain (slightly rough to very rough terrain) that one reproduces in the wind tunnel and so, the properties of the modelled ABL at a geometric scale of 1:400. Laboratory PRISME of The department activities in the context of wind resource assessment with the 3%-vision suggested by the European Wind Energy Technology Platform, and particularly of the wind turbine wake properties. Based on experimental investigations in an atmospheric boundary layer wind tunnel, some information about the diffusion process of the wind turbine far-wake, the minimal degree of modelling of the rotor to study its far-wake, the unsteady behaviour of the wake and the production loss due to wake effects are analysed and discussed (Aubrun 2012 [23]).

In this context, studies deal with the way of modelling a rotor in order to reproduce the main properties of its far-wake. This issue is common to the numerical and experimental modelling and the obtained answers can help both communities. The actuator disc model has been used (Espana et al 2012 [24], Espana 2009[25]). Experimental results on the unsteady behaviour of the wake of a modelled wind turbine in an atmospheric boundary layer (ABL) wind tunnel are presented. Tests were performed by modelling in the wind tunnel an ABL above a neutral moderately rough terrain at a geometric scale of 1 : 400, and a wind turbine with the help of the *actuator disk concept*. In order to characterise the meandering properties of its wake, velocity spectra and space-time correlations were measured through hot wire anemometry, both in the wake of the modelled wind turbine and in the wake of a solid disk. Comparing these two configurations allowed the examination of the differences between the random motion of the whole wind turbine wake characterising the meandering in the first case, and the periodic oscillations of the well-known vortex shedding, which appears behind a bluff-body, in the second case. Finally, the same experiments were performed in homogeneous and isotropic turbulent flows to exhibit the role of the large atmospheric turbulent scales in the meandering process. (Espana et al [24])

The second points out in this context was the unsteady behaviour of the wind turbine wake due to largescale turbulent eddies of atmospheric flows. It is of great importance when one deals with aeroelastic properties of the wind turbine to characterise all sources of unsteadiness contained in upstream flows (Espana et al [26]). The present studies attempt to quantify the degree of passivity of the wake to these turbulent eddies: is the whole wake a passive tracer of turbulent eddies larger than its diameter? The last subject is the most applied one since it enables to quantify the power loss of a wind farm due to interactions. The power losses are very important and needs to be quantified and predictable through the use of models. On the other hand, the experimental limitations and the strong approximations which were used to get a power value from the velocity deficit measured downstream of porous discs are a clear limitation of this modelling concept. It is more valuable to focus on the turbulent flow modifications at a scale of one wind turbine or of a wind farm to contribute to a better understanding of the wind conditions.

## References

- [1] A. Thacker, *Contribution expérimentale à l'analyse stationnaire et instationnaire de l'écoulement à l'arrière d'un corps de faible allongement*. These, Université d'Orléans, Dec. 2010.
- [2] P. Gilliéron, A. Leroy, S. Aubrun, and P. Audier, "Influence of the Slant Angle of 3D Bluff Bodies on Longitudinal Vortex Formation," *Journal of Fluids Engineering*, vol. 132, p. 051104 (9 pages), 2010.
- [3] N. Mazellier and F. Foucher, "Separation between coherent and turbulent fluctuations: what can we learn from the empirical mode decomposition?," *Experiment in Fluids*, vol. 51, no. 2, pp. 527–541, 2011.
- [4] S. Aubrun, J. McNally, F. Alvi, and A. Kourta, "Separation flow control on a generic ground vehicle using steady microjet arrays," *Experiments in Fluids*, vol. 51, pp. 1177–1187, 2011.
- [5] P. Audier, R. Joussot, H. Rabat, D. Hong, and A. Leroy, "ICCD imaging of plasma filament in a circular surface dielectric barrier discharge arrangement," *IEEE Transactions on Plasma Science*, vol. 39, pp. 2180–2182, 2011.
- [6] N. Benard, J. Pons, P. Audier, E. Moreau, D. Hong, and A. Leroy, "Filaments in a surface dielectric barrier discharge operating in altitude conditions," *IEEE Transactions on Plasma Science*, vol. 39, pp. 2222–2223, 2011.
- [7] A. Batikh, L. Baldas, R. Caen, W. Ghazlani, and A. Kourta, "Experimental characterization of sub-millimetric fluidic actuator: application to boundary layer separation control ," *Experimental Heat Transfer*, vol. 23, pp. 4–26, 2010.
- [8] P. Gilliéron and A. Kourta, "Aerodynamic drag reduction by vertical splitter plates," *Experiments in Fluids*, vol. 48, pp. 1–16, 2010.
- [9] N. Mazellier, A. Feuvrier, and A. Kourta, "Biomimetic bluff body drag reduction by self-adaptive porous flaps," *Comptes Rendus de l'Académie des Sciences - Series IIB - Mechanics*, vol. 340, pp. 81–94, 2012.
- [10] V. Boucinha, *Etude de l'écoulement induit par une décharge à barrière diélectrique surfacique : contribution au contrôle des écoulements subsoniques par actionneurs plasmas*. These, Université d'Orléans, Dec. 2009.
- [11] V. Boucinha, R. Weber, and A. Kourta, "Drag reduction of a 3D bluff body using plasma actuators," *International Journal of Aerodynamics*, vol. 1, p. 262, 2011.
- [12] P. Magnier, D. Hong, A. Leroy, J.-M. Pouvesle, and J. Hureau, "A DC corona discharge on a flat plate to induce air movement," *Journal of Electrostatics*, vol. 65, pp. pp. 655–659, 2007.
- [13] P. Magnier, D. Hong, A. Leroy, J.-M. Bauchire, and J. Hureau, "Control of separated flows with the ionic wind generated by a DC corona discharge," *Experiments in fluids*, vol. 42, pp. pp. 815–825, 2007.

- [14] P. Magnier, V. Boucinha, B. Dong, R. Weber, A. Leroy, D. Hong, and J. Hureau, “Experimental study of the flow induced by a sinusoidal Dielectric Barrier Discharge actuator and its effects on a flat natural boundary layer,” *Journal of Fluids Engineering*, vol. 131, Issue 1, p. 011203 (11 pages), 2009.
- [15] A. Leroy, P. Audier, D. Hong, H. Rabat, and R. Weber, “Effects of a surface plasma actuation on leading edge flow separation occurring on an aerodynamic airfoil involving a laminar separation bubble,” in *The 20th International Symposium on Plasma Chemistry*, (Philadelphia, États-Unis), July 2011.
- [16] P. Audier, D. Hong, and A. Leroy, “Unsteady forcing of a post-stall flow over a NACA0012 airfoil by a surface DBD actuator,” in *The 6th AIAA Flow control conference*, (New Orleans, États-Unis), June 2012.
- [17] E. Bideaux, P. Bobillier, E. Fournier, P. Gilliéron, M. El Hajem, J.-Y. Champagne, P. Gilotte, and A. Kourta, “Drag reduction by pulsed jets on strongly unstructured wake: towards the square back control,” *International Journal of Aerodynamics*, vol. 1, pp. 282 – 298, 2011.
- [18] M. Rouméas, P. Gilliéron, and A. Kourta, “Analysis and control of the near-wake flow over a square-back geometry,” *Computers and Fluids*, vol. 38, pp. 60–70, 2009.
- [19] C. Leclerc, *Réduction de la traînée d’un véhicule automobile simplifié à l’aide du contrôle actif par sjet synthétique*. These, Institut National Polytechnique de Toulouse, Jan. 2008.
- [20] B. Lehugeur, P. Gilliéron, and A. Kourta, “Experimental investigation on longitudinal vortex control over dihedral bluff body,” *Experiments in Fluids*, vol. 48, pp. 33–48, 2010.
- [21] A. Kourta, G. Petit, J.-C. Courty, and J.-P. Rosenblum, “Buffeting in transonic flow prediction using time dependent turbulence model,” *International Journal for Numerical Methods in Fluids*, vol. 49, pp. 171–182, 2005.
- [22] E. Orlik, N. Mazellier, and A. Kourta, “Numerical Prediction of transonic buffeting by means of standard and time-dependent turbulent models,” in *The 7th International Symposium on Turbulent and Shear Flow Phenomena (TSP-7)*, (Ottawa, Canada), July 2011.
- [23] S. Aubrun, “Wind turbine wake: a disturbance to wind resource in wind farms,” *International Journal of Engineering Systems Modelling and Simulation*, vol. 4, pp. 2–10, 2012.
- [24] G. Espana, S. Aubrun, S. Loyer, and P. Devinant, “Wind tunnel study of the wake meandering downstream of a modelled wind turbine as an effect of large scale turbulent eddies,” *Journal of Wind Engineering and Industrial Aerodynamics*, vol. 101, pp. 24–33, 2012.
- [25] G. Espana, *Étude expérimentale du sillage lointain des éoliennes à axe horizontal au moyen d’une modélisation simplifiée en couche limite atmosphérique*. These, Université d’Orléans, Dec. 2009.
- [26] G. Espana, S. Aubrun, S. Loyer, and P. Devinant, “Spatial study of the wake meandering using modelled wind turbines in a wind tunnel,” *Wind Energy*, vol. 14, pp. 923–937, 2011.

## 10 Laboratory of Engineering Science for Environment (LaSIE) - University of La Rochelle. Team: Mathematical and Numerical Modelling of Transfer Phenomena (Team Leader: Aziz Hamdouni)

The team is composed of researchers in mathematics and mechanics, working on theoretical and numerical modelling of coupled problems. These last years, the main topics developed by the team include turbulence modelling for non-isothermal flows, fluid-structure interaction, particle dispersion, reduced order model and control, invariant numerical scheme for fluid mechanics, porous media and multi-scale problems.

Some topics developed these last four years are described below.

### 10.1 Lie symmetry group in fluid mechanics

The Lie symmetry group of an equation is a Lie-group-structured set of transformations which leave the set of solutions unchanged. The close link between Lie symmetries and conservation laws made the former a powerful tool for investigating physical properties hidden behind the equation. In fluid mechanics, they are used as a modelling tool, as we will see below.

#### Symmetry and turbulence modelling

In turbulence, we used the symmetry group (containing a 6-dimensional and four  $\infty$ -dimensional Lie subgroups) of the Navier-Stokes equations for the development of a class of LES physics-preserving subgrid models. The symmetry approach gives rise to a fundamental and non classical invariant  $\det \bar{S} / \|\bar{S}\|^3$ , on which the model should depend.  $\bar{S}$  is the subgrid strain rate tensor. In the non-isothermal case, four more invariants appear (Al Sayed *et al*, Symmetry 2010). With these invariants, the functional form of the subgrid strain rate tensor and the subgrid heat flux can be derived naturally. Moreover, with this approach, we do not need the Reynolds analogy which limits the scope of LES models when the temperature plays a significant role in the dynamics of the flow.

One simple model of the class has been tested numerically in (Razafindralandy *et al*, Physica A 2012) for the simulation of an air flow in a ventilated room. 31 reproduced here shows that the symmetry based (called “invariant”) subgrid model predicts the velocity and temperature better than the Smagorinsky model. The near-wall behaviour is especially well reproduced by the symmetry-preserving model. This is, in fact, not surprising since as we will see in the next paragraph, wall laws are contained in the symmetries of the equations.

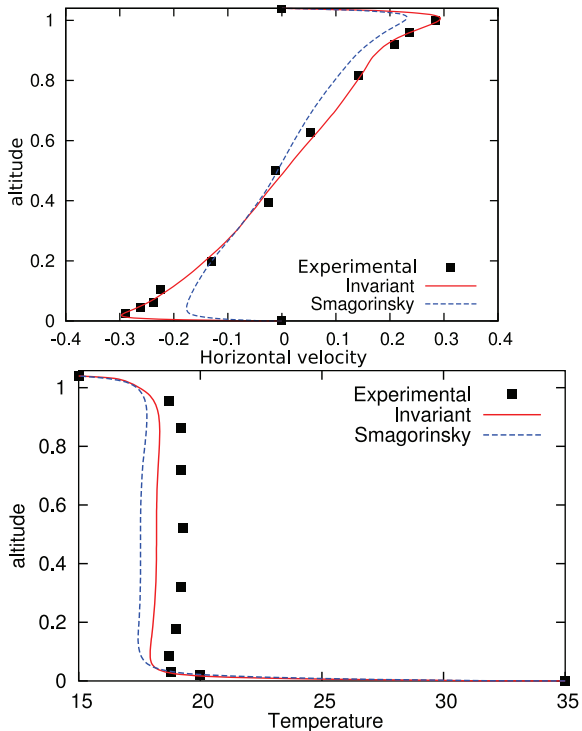


Figure 31: Velocity (top) and temperature (bottom) profiles

### Symmetry and scaling laws

As proved by Oberlack (JFM 2001), symmetries of RANS equations can be used to model the mean behaviour of a flow. They lead to classical scaling laws, but also to new ones such as the exponential law which was confirmed in the mid-wake region of high Reynolds number boundary layers. Extended to the non-isothermal case by Razafindralandy *et al* (Physica A 2012), this law reads

$$U = \exp[c_1(y+c_0)] + c_3, \quad \Theta = \exp[2c_1(y+c_0)] + c_4 \quad (12)$$

where the  $c_i$ 's are constants,  $U$  and  $\Theta$  are the mean velocity and temperature. Another law deduced from the symmetry framework is the algebraic law which can be found in both the center and the near-wall region of a turbulent channel flow. Its non-isothermal extension writes

$$U = c_1(y+c_0)^a + c_3, \quad \Theta = c_2(y+c_0)^{2a-1} + c_4. \quad (13)$$

These expressions show that if the exponent  $a$  of the velocity profile is somehow known, the corresponding exponent of the temperature profile can be deduced. An other and intriguing scaling law is

$$U = c_1 \ln(y+c_0) + c_3, \quad \Theta = c_2(y+c_0)^{-1} + c_4, \quad (14)$$

which suggests the coexistence of a logarithmic velocity profile and an hyperbolic temperature law.

### Symmetry and numerical schemes

On the numerical point of view, we make use of the symmetry approach to build physics-preserving and robust numerical schemes (Chhay *et al*, JCP 2011; Chhay and Hamdouni, Comm. Pure and Applied Anal. 2011). To this aim, one takes a classical scheme and makes it invariant under the symmetries of the equations. Invariantized schemes are a generalization of symplectic schemes, for non-Hamiltonian partial differential equations. They possess similar stability properties as symplectic schemes. In particular, a simulation of a shock

solution of Burger's equation shows that the invariantization process eliminates the non-physical oscillations presented by the numerical solution.

An introductive and synthetic summary of the works on Lie-symmetry groups carried out at the LaSIE can be found in (Razafindralandy, Hamdouni and Chhay, NOVA 2009).

## 10.2 Reduced Order Model (ROM) and control

Despite constantly improving computer capabilities, the search for a solution of a non-linear and complex physical process requires both large computer resources and data memory storage. Classical numerical methods employed in fluid mechanics (DNS, LES, ...) are still out of reach to be used routinely, when a large realizations number is necessary or when a real-time solution is sought. These are the cases for parametric studies or optimization problems. The use of the reduced-order models (ROMs) is therefore an attractive strategy to make these problems tractable both CPU time and memory requirements.

Numerous reduction methods can be found in the literature. Due to its optimal energetical convergence property and its applicability to non-linear systems, Proper Orthogonal Decomposition (POD) method is the most common reduced basis technique used for the particular case of incompressible flows. The reduced dynamical system often involves a Galerkin projection of the Navier-Stokes equations onto a finite number of POD spatial modes,  $\Phi_i$  for  $i = 1, \dots, N$  with  $N$  much smaller than the full model number of degrees of freedom. However two issues are well-known in the litterature with the Galerkin-POD approach : the lack of stability of the resulting ROM and the treatment of the pressure term which appear in the ROM. To overcome theses difficulties, we have proposed to build a reduced order model obtained by minimizing the residual associated to the incompressible Navier Stokes equations (Leblond and Allery, CMAME 2011) . The approach consists in decomposing separately by POD the velocity and the pressure fields. Given a temporal discretization of the Navier-Stokes equations, the projection spaces are here derived thanks to the calculation of variations of the residuals norm. The resulting projection spaces involve both the velocity and pressure modes and differ from a Galerkin projection. The spaces are built such that they minimize exactly the residuals of the Navier Stokes equations residuals.

Another drawback of POD technique is the need for a set of snapshots of the solution in order to construct the reduced basis. A lengthy computing time may be required for the calculation of these snapshots, that is why we have considered to build a reduced basis without a prerequisite knowledge of the solution by using *a priori* model reduction techniques such as the A Priori Reduction (APR) approach or the Proper Generalized Decomposition (PGD). With the APR, the basis is iteratively improved and expanded with the residuals of the full discretized model. This incremental process is done by taking into account the whole time interval where the reduced equation is solved, and can also be used for a fast adaptation of the basis when a parameter changes. We used with success the APR to solve some linear and non linear problems (Allery, Hamdouni, Ryckelynck & Verdon, Applied Math. and Comp. 2011).

The PGD involves looking for a solution to a problem as a product sum of the functions of each space variable. For example, if we search a field  $u$  dependent on  $N$

variables, this can be expressed by  $u(x_1, x_2, \dots, x_N) = \sum_{i=1}^Q F_1(x_1)F_2(x_2) \dots F_N(x_N)$ .  $x_i$  can be any scalar or vector variable involving space, time or any other parameter of the problem). Thus, if  $M$  degrees of freedom are used to discretize each variable, the total number of unknowns involved in the solution is  $Q \times N \times M$  instead of the  $M^N$  degrees of freedom involved in mesh based discretization techniques. In most cases, where the field is sufficiently regular, the number of terms  $Q$  in the finite sum is generally quite small. The functions  $F_j$  are not known a priori. They are adaptively computed by introducing the separated approximation of the representation into the model and then solving the resulting non-linear problem. To our knowledge, we are the pioneer to use the PGD to solve the isothermal and anisothermal Navier Stokes equations (Dumon, Allery & Ammar, JCP 2011). The PGD results are in agreement with those obtained with the full grid solver, with a significant times saving.

We also use the reduced order models to control the temperature or the dispersion of a pollutant in building system (Tallet, Leblond & Allery, ASME ESDA, 2012). The use of ROM within an optimization loop is one of the most efficient approach in the CPU time point of view, and opens the way to real-time control strategy of complex systems.

### 10.3 Particle dispersion in turbulent flows

Two main topics are investigated. The former one focuses on the numerical modelling of heavy particle dispersion in wall bounded flows. The Proper Orthogonal Decomposition approach is employed, in order to model the dynamics of dominant vortical structures at a low computational cost. The Lagrangian technique (point particle approach) enables to track the particles in the turbulent flow, whose instantaneous variables are calculated with a low order dynamical system. Qualitative studies have been applied to heterogeneous flows (Allery, Béghein and Hamdouni, Int. Applied Mech., 2008) and a coherent behavior of heavy particles in such flows has been highlighted. A quantitative study is also performed by research scientists from our team and from Polish Academy of Sciences, for the channel case. In the case of perfect rebound of particles on walls, a full comparison of the results obtained with low order dynamical systems, for particles of varying inertia, and with DNS results (benchmark computation coordinated by Marchioli, Int. J. Multiphase Flow, 2008) is carried out. The case of particle deposition in the channel is also investigated, by comparison with the LES results of Pozorski and Luniewski (Springer 2008).

The latter topic deals with the dispersion of fine particles in the presence of an inhomogeneous electric field. The aim of this work is to contain the dispersion of fine particles by subjecting them to electrostatic precipitation. In addition to the flow field equations, the Poisson equation for the electric field, the charge continuity equation and the particle concentration equation are solved. A drift flux model is used to account for the drift flux of particles induced by the electric field (Ramechecandane and Béghein, Building and Environ. 2010; Int. J. Multiphysics 2011). Comparisons with experimental results of Leonard for the case of a plate plate electrostatic precipitator are done. This model will then be applied to a more complex configuration (cabinet) dedicated to the deviation of ultrafine particles in a flow by an electric field.

## 10.4 Fluid Structure Interaction

Fluid structure interaction modelling covers a large application area of LaSIE domains. We focus on stable and robust coupling algorithms for fluid structure interaction. Abouri *et al.* (J. Pressure Vessel Tech., 2006) have developed stable and robust implicit coupling method for industrial problems in Arbitrary Lagrangian Eulerian (ALE) formulation. Benaouicha and Hamdouni (Int. Applied Mech. 2011) adapted implicit coupling algorithm to a body immersed and anchored in a fluid flow.

Reduced order models for moving domains are developed. In FSI, the fluid and the structure domains are moving, owing to which the POD method cannot be applied directly to reduce the equations of each domain. We have proposed to compute the POD modes for a global velocity field (fluid and solid), and then to construct a low-order dynamical system. This method, called POD-multiphase, consists in treating the entire fluid-solid domain as a fluid (Liberge and Hamdouni, JFS 2010) by introducing a Lagrange multiplier. The snapshots result from a classical fluid structure interaction resolution in ALE, and each snapshot is interpolated from the time variant grid to a fixed one. Next, the POD basis is computed for the global velocity field (fluid and solid) defined on this fixed grid. The difference with a classical approach is that, rather than the fluid equations in ALE, it is the multiphase Navier-Stokes equations which are projected. The simulation of a flow around an oscillating cylinder shows the efficiency of the POD-multiphase (Liberge and Hamdouni, JFS 2010; Liberge *et al.*, Europ. J. Comp. Mech. 2010).

Lattice-Boltzmann simulation method of Fluid Structure Interaction is also carried out in the laboratory. This method, combined with GPU (Graphic cards instead of classical CPU), is a very efficient and fast tool in fluid mechanics and allows a quasi real-time computing.

## 11 An experimental aspect of the research in CORIA. Experimental study of turbulent mixing process in simultaneously reacting and non-reacting confined flow

This work was performed by G. Boutin, B. Renou and L. Danaila (CORIA, Rouen). Dual-tracer planar laser-induced fluorescence (PLIF) and Particle image Velocimetry (PIV) techniques are used to quantify instantaneous distributions of macro and micro-mixing. The investigated flow is a Partially Stirred Reactor (PaSR) composed of 16 pairs of sheared jets. The typical pattern consists in a jet surrounded by 4 jets in counter flow, arranged on a cartesian grid.

The first scalar concentration measurement is performed by PLIF of nitric oxide (NO) seeded in a nitrogen jet, to mark the unmixed jet fluid fraction. PLIF on acetone, seeded in the counter-flowing air jets, marks the total fluid fraction. By combining data from these two simultaneous images, quantitative measurements of micro-mixing between counter-flowing jet fluids can be made on a pixel-by-pixel basis. Simultaneously, two velocity components measurements (by PIV) are used to get information about the velocity field which mixes. The first objective of this experimental work is to provide a reliable database for different flow geometries and Reynolds

numbers. This database is further used to study the influence of such parameters on the micro-mixing properties and in particular on its efficiency. It is shown that micromixing is favored by either increasing injection Reynolds numbers, or injection by small diameter jets in comparison with the flow dimensions (small-scale injection).

## 11.1 Introduction

Quantitative characterization and prediction of micromixing are of significant interest in numerous applications, such as chemical processing, combustion, aerospace propulsion, etc. 'Micro-mixing' is generally used when the mixture of two substances A and B occurs at small scales, or at molecular scales. In this case, the contact surface between the two substances is maximal, and the chemical reaction can occur on a maximum surface to volume ratio. This is why chemical reactions are very good candidates to characterize micro-mixing [2]. PLIF has been used extensively to image the scalar field in both reacting and non-reacting flows, and a variety of laser based techniques have been implemented. In high Reynolds number flows, however, the ratio between the largest and the smallest scales is important and the challenge is therefore to visualize both large and small scales.

To overcome these difficulties, various strategies have been proposed. In reactive configurations, mixing statistics can be obtained by using a 'flip' experiment ([2], [5]). The obvious limitation of this technique is that it cannot be used to obtain instantaneous images of molecular mixing. As an alternative to methods based on fast chemistry, several studies have utilized quenching of fluorescence of tracer species as the product marker, also known as 'cold chemistry' [1]. Hu and Koochesfahani ([4]) used the quenching of acetone phosphorescence as a marker of mixed fluid, as a variant of cold chemistry technique. The first technique for measuring both instantaneous molecularly mixed fluid quantities and the large-scale structures in high turbulent flow was implemented by [7] in a shear layer. This technique uses acetone PLIF as a passive-scalar measurement of the fluid fractions from each fluid stream of a shear layer, and uses NO PLIF simultaneously to obtain the molecularly unmixed fluid fraction. Thus, the instantaneous molecularly mixed fluid fraction, mixing efficiency, and relevant statistics can be obtained in post-processing. Several studies in (high-speed) turbulent jets, planar shear layers etc. have been performed using this approach (e.g. [6], [11]).

However, the existing studies are mainly devoted to free shear flows that entrain and mix freestream (unmixed) fluids. This work is aimed at a quantitative understanding and the development of models for molecular mixing in turbulence. Mixing in a Partially Stirred Reactor (PaSR) is examined over a range of flow conditions. The proposed PaSR geometry has well-characterized boundary conditions facilitating comparisons with modeling, numerical simulations. The turbulent flow is composed of multiple shear jets [10], with a typical pattern consisting in a jet surrounded by 4 jets in counter flows, arranged on a cartesian grid.

First, we provide a reliable experimental data set, for variable flow geometries and Reynolds numbers. Measurements rely on laser diagnostics that simultaneously measure the following:

- The scalar concentration field in cold reacting flow, in which NO is used as a tracer (PLIF on NO). Its fluores-

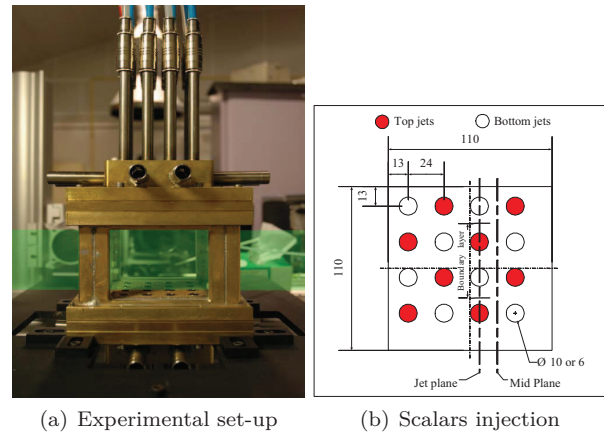


Figure 32: The reactor

cence is strongly quenched by oxygen from the counter-flow jets. This concentration will mark the unmixed scalar.

- The concentration field of a non-reacting scalar (e.g., acetone) transported as is NO (PLIF on Acetone). This latter quantity marks the mixture fraction.

- Two components of the velocity field using PIV.

## 11.2 Experimental set-up and diagnostics

### 11.2.1 The reactor

The reactor is presented in Figure 32(a). The basic design allows for a modular and flexible experiment, generating flows in which velocity and scalar fields can be simultaneously investigated. The reactor interior is a rectangular parallelepiped ( $110 \times 110 \times 60 \text{ mm}^3$ ) equipped with quartz Suprasil windows ( $100 \times 80 \text{ mm}^2$ ). The top/bottom porous boundary plates are backed by plena connected to an exhaust piping network through 8 exhaust ports on each cap (Krawczynski, 2007 [8]). Each plenum provides 8 tubes that supply the top/bottom jets individually. Two types of tubes are employed. These are 200 mm long, with an inner diameter of either  $D = 10 \text{ mm}$  or  $D = 6 \text{ mm}$ , respectively, arranged on a 24 mm spacing cartesian mesh, Figure 32(b). The horizontal distance between two neighboring jet axes is  $2L = 24 \text{ mm}$ . Hence, the geometry of the confined flow is fixed through the scales :  $L = 12 \text{ mm}$ ,  $H = 60 \text{ mm}$  and the injection jets diameter  $d$ . To document internal conditions, one wall is equipped with a 1 mm diameter pressure tap, connected to a digital manometer and a platinum probe for temperature measurement. All the experiments are performed at  $P = 1.6 \text{ bar}$  and at room temperature. In this work, the Reynolds number  $Re_d = U_{inj}d/\nu$  based on  $U_{inj}$ , the fluid injection velocity, varies between 6400 up to 16000. We focus on the influence of the lateral confinement and of the Reynolds number on statistics, thanks to the fluid injection by either 10 or 6 mm tubes diameter.

Since the injection jets diameter takes two values while the lateral distance among each two consecutive opposed jets is fixed, the flow configuration is double: CSJ close sheared jets ( $d = 10$ ) and FSJ far sheared jets ( $d = 6$ ).

### 11.2.2 Experimental measurements

The ensemble-averaged displacement of Di-Ethyl-Hexyl-Sebacat (DEHS,  $\text{C}_{26}\text{H}_{50}\text{O}_4$ ) particles ( $\rho_p = 918 \text{ kg.m}^3$ )

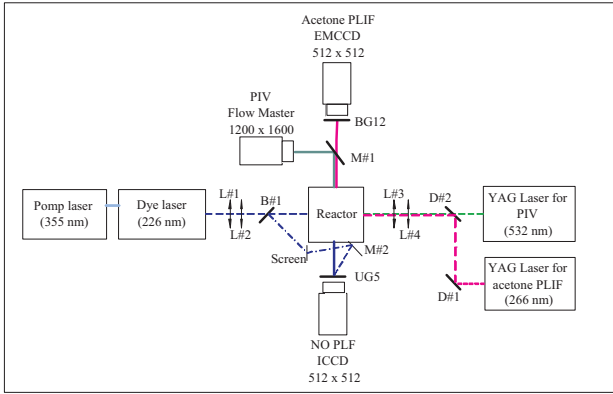


Figure 33: Experimental set-up

between pairs of images is estimated using a PIV cross-correlation technique, 2D-2C velocity field. The particles diameter (calibrated with a Malvern diffractometer) is between 1 and 1.15  $\mu\text{m}$ . Due to the periodic pattern of the fluid injection, we have restricted the investigated fields to a couple of counter-flowing jet, (see Figure 32(b)).

The light source is a Nd-Yag laser (Big Sky laser, 120 mJ/pulse) with a second-harmonic-generating crystal that produces a Q-switched laser output in the green ( $\lambda_{PIV} = 532 \text{ nm}$ ). Light scattered from the particles is collected on a CCD camera (R&D Vision, 12 bits, 1600  $\times$  1200 pix<sup>2</sup>) with a 50 mm f/1.2 Nikkor lens, yielding a magnification of 21.76 pix.mm<sup>-1</sup>. The initial size of the PIV interrogation window is 64 pix<sup>2</sup>. Six iterations are used to obtain a final interrogation window size of 16 pix<sup>2</sup>, with a 50% overlap. The spatial resolution of the measurements is determined according to the PIV transfer function (Foucaut et al. 2004 [3]). This analysis yields a cut-off spatial frequency for the PIV system of  $f_c = 2.8 \cdot 10^{-2} \text{ pix}^{-1}$  corresponding to a scale of  $\approx 1.12 \text{ mm}$ . These spatial resolutions are fixed in a given experimental configuration and do not depend on the flow. The size of velocity field is 55.2  $\times$  73.5 mm<sup>2</sup>.

The passive scalar (air + acetone (3%)) is injected by the lower side jets (illustrated by white jets in Figure 32(b)), while the reactive scalar ( $N_2 + NO$  (300 ppm)) by upper jets (red jets in Figure 32(b)). Passive scalar measurement is investigated by Planar Laser Induced-Fluorescence (PLIF) on acetone molecule. A laser sheet is created by the same optical system as PIV measurement. The light source is a Nd:YAG laser (Spectra Physics) with a fourth-harmonic generating crystal that produces a Q-switched laser output in the UV ( $\lambda_{Ac} = 266 \text{ nm}$ , 170 mJ). Fluorescence signal is collected on a "Princeton Instrument PhotonMax EMCCD" camera, 16 bits, 512  $\times$  512 pixels coupled to a visible Nikkor 50 mm focal length, f/1.2 lens. The exposure time on is 2 ms, that is why parasites lights have to be rejected by color glass, by using a dichroic mirror and a BG12 filter.

Spatial resolution is estimated to 490  $\mu\text{m}$  thanks to the FTM of the optical acquisition system. Camera's FTM is determined by taking an image of "infinite" gradient simulated by a razor blade placed on the target is acquired. FFT is applied on the image gradient. The cut frequency is got when the contrast is less than 10%.

Despite a small part of fluorescence signal available, because of high energy laser, the signal to noise ratio is more than 10. Fluorescence signal is normalized by the mean sheet and the maximum grey level is adjusted by a zone in which mixing fraction of passive scalar is one (jet potential core).

The reactive scalar is simulated by the oxygen and acetone quenching on NO molecule (Paul et al., 1993 [12]; Clemens et al. 1995 [1]), call "Cold chemistry Method". The laser was tuned to  $Q_1(1) \rightarrow Q_1(4)$  line of the  $A^2\Sigma^+ \leftarrow X^2\Pi(0,0)$  NO electronic transition ( $\lambda_{NO} = 226.18 \text{ nm}$ ), using a frequency doubled BBO crystal of a dye laser pump by Nd:YAG laser at 355 nm. The global energy laser output is 3 mJ during 10 ns. PLIF images were acquired using an ICCD camera (Princeton Instrument, 16 bits, 512  $\times$  512 pixels) coupled to a UV Nikkor 48 mm focal length, f/1.2 lens. A UG 5 glass filter 3 mm thickness is used to remove Mie diffusion scattering at 226 nm. The peak signal to noise ratio is about 40. The scalar field is 55  $\times$  55 mm<sup>2</sup> as acetone PLIF field. A huge attention has been devoted to the calibration of the shot-to-shot energy fluctuations in order to correct the spatio-temporal inhomogeneities energy laser distribution. A small part of laser sheet is split using a beamsplitter (see Figure 33, B#1) and projected on the image edge. The aim of this procedure is to provide accurate quantitative evaluation of the reactive scalar concentration. The normalized fluorescence signal  $Sf_{norm}$  can be written as:

$$Sf_{norm}(x,y,t) = \frac{Sf_{raw}(x,y,t) - \langle Noise(x,y) \rangle}{\langle Sheet(x,y) \rangle - \langle Noise(x,y) \rangle} R(x,t)$$

with  $R(x,t) = \frac{\langle U_{v,sheet}(x) \rangle}{U_v(x,t)}$  and  $\langle U_{v,sheet}(x) \rangle$  is the mean split energy profile acquired with homogeneous flow fields and  $U_v(x,t)$  is the instantaneous energy profile acquired on the image edge of the reactive scalar.

The spatial resolution of nitric oxide diagnostic is equal to 640  $\mu\text{m}$ .

All scalar fields are filtered using a Wiener filter type (Krawczynski et al., 2006 [9]), which removes high frequency fluctuations. After normalization and filtering processes, residuals fluctuations of passive scalar measurement are  $\approx \pm 1\%$  and for reactive scalar measurement  $\approx \pm 5\%$ .

A post processing is applied to scalar fields to get the same spatial physical mesh for the the three measured quantities: the 'reactive' scalar NO, the conserved scalar and the velocity field. A linear data interpolation is applied to the scalars at the level of the velocity field mesh, the latter being the least accurate field.

The post processing yields an experimental data set containing at one mesh point: the conserved scalar mixing fraction  $Z$ , the reactive scalar mixing fraction  $Z_{reactive}$ , and two velocity components (u and v) presented on Figures 34 and 35.

## 11.3 Results

While the axisymmetric jet mixing layer has been investigated using many fluid diagnostic techniques, quantitative measurements of the extent of molecular mixing have been elusive. Chemical reaction in fluid flows is not initiated until the fuel and oxidant streams are mixed at the molecular level, a state distinct from that of macroscopically stirred, but unmixed, reactants.

As far as the reactive scalar is concerned, measurements provided simultaneously (a) The scalar concentration field for NO, using NO PLIF, that reacts with  $O_2$ . This scalar is called  $Z_{reactive}$ . (b) The concentration field of a nonreacting scalar (e.g., acetone) transported as is NO. This latter quantity marks the mixture fraction,  $Z$ , and can be considered as inert. The acetone mole fraction field is measured by PLIF on acetone. Therefore,

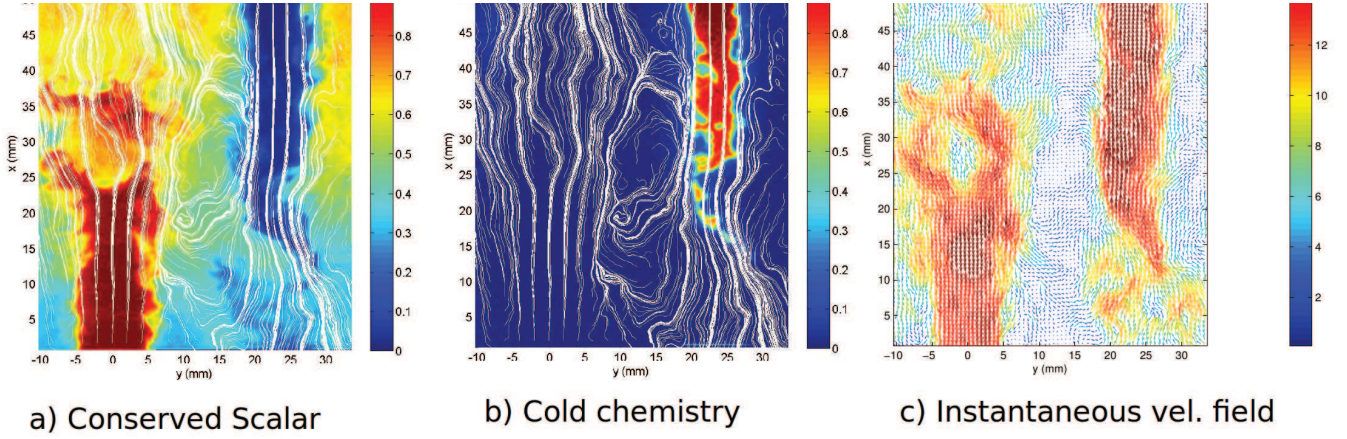


Figure 34: Simultaneous measurements data sets for  $d = 10$  mm. Distributions of the conserved scalar  $Z$  (left), the pure fluid mixing fraction  $Z_{reactive}$  (middle) and instantaneous velocity field (right). Close shear jets,  $Re_d = 10700$

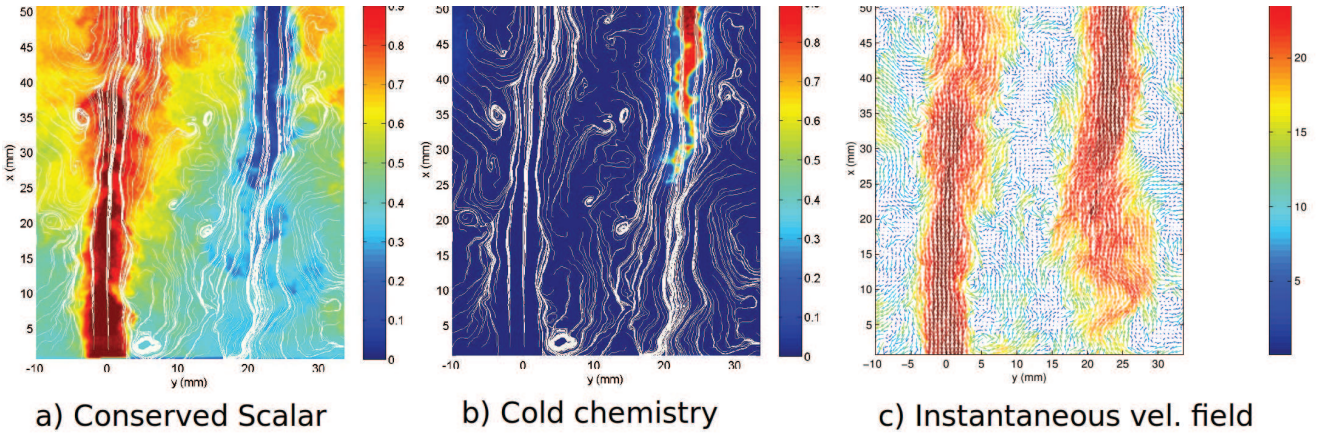


Figure 35: Simultaneous measurements data sets for  $d = 10$  mm. Distributions of the conserved scalar  $Z$  (left), the pure fluid mixing fraction  $Z_{reactive}$  (middle) and instantaneous velocity field (right). Far shear jets,  $Re_d = 10700$

a double species map is produced. A first map, with NO, which will indicate places where NO is pure and unmixed. A second map, simultaneous to the first, with acetone, indicating places where NO would have been present, if it had not been reacted. By subtracting [6], one will then obtain an instantaneous image of molecular mixing  $Z_m$ , and the reacting zone.

In the following, the focus is on the molecular mixing via the scalar  $Z_m$  and the influence of the geometry and of the Reynolds number on instantaneous distribution and of statistics of the molecularly mixed fluid fraction  $Z_m$ . We choose to represent only the field corresponding to one jet, with the vertical  $x$  axis and the horizontal  $r$  axis normalized with respect to the jet diameter  $d$ .

### 11.3.1 Instantaneous and statistical aspect of molecularly mixed fluid fraction for the close sheared jets geometry

We first extensively pay attention to the CSJ geometry. For CSG flow, Figure 36 represents instantaneous images of the passive scalar  $Z$  (left) and of the molecularly mixed fluid fraction  $Z_m$  (right). At the jet injection, a potential core is clearly visible on both figures, where fluid is pure ( $Z = 1$ ) and therefore there is no molecular mixing  $Z_m = 0$ . For regions where  $Z < 1$ , it is not a priori obvious to state which quantity of this fluid concentration is pure and which one is molecularly mixed with the other scalar. In this case, the complementary measurements of pure fluid are necessary. The result is the  $Z_m$  map

(right) in which mixing region are represented. It is to be noted the (approximately) "V" shapes of the mixing regions. The boundaries of this mixing region are marked by the mixing vortical structures (streamlines obtained from PIV are also represented), which are much more pronounced than those (Kelvin-Helmholtz like) present in a free axisymmetric jet (see Fig. 5 of [6]). Here, both the lateral confinement and the short distance over which jets develop, do influence the micromixing region.

It is of interest to represent instantaneous values of micromixing efficiency  $\eta_m = \frac{Z_m}{Z}$ , Figure 37 (left) which is equal to zero in regions where molecular mixing is completely absent, and rapidly grows to high values close to 1 on the boundaries of the potential core. In most of the flow volume,  $\eta_m = 1$ , which signifies that all the scalar present at that point is completely molecularly mixed. Regions where the mixing efficiency rapidly grows are strongly correlated with azimuthal vorticity (large-scale circulation, as solved by PIV) represented on Figure 37 right.

Quantitative characterization of molecular mixing is readily done by using statistics, among which the simplest are mean values and variance of  $Z_m$  fluctuations (Figure 38). On the jet axis ( $r/d = 0$ ),  $\langle Z_m \rangle$  monotonically grows from 0 at  $x/d = 0$  till values close to 0.8 (80% of molecular mixing) near the exit of the reactor. Between  $x/d = 3$  and  $x/d = 6$ , i.e. over approximately half of the reactor height, molecular mixing is quite good from a statistical viewpoint. Most of the fluctuations (i.e. time fluctuations between unmixed and molecularly

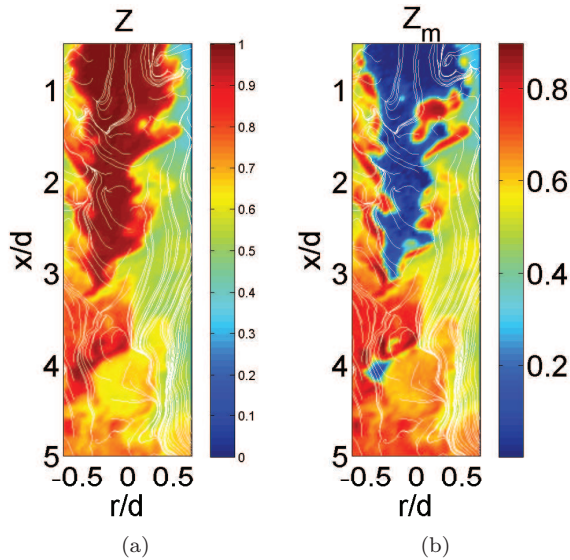


Figure 36: Instantaneous image of passive tracer (left) and of fluid mixed at molecular level (right). Close sheared jets ( $Re = 6400$ )

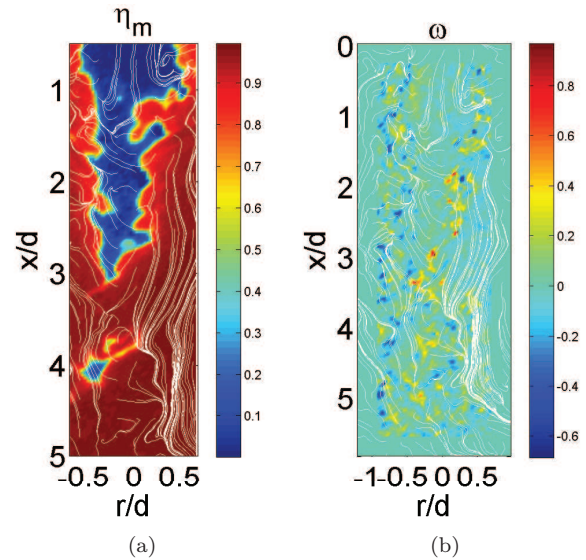


Figure 37: Instantaneous image of micromixing efficiency (left) and PIV-resolved circulation (right). Close sheared jets ( $Re = 6400$ )

mixed fluid) occur on the top half of the reactor, near the injection, as it is illustrated by the  $Z_m$  variance distribution. Near the injection, fluctuations are strong over radial distances going up to  $r/d = 0.5$ .

A more detailed insight in micromixing fluctuations is possible by investigating the probability density functions (Pdfs) of the molecularly mixed fluid fraction, at different axial and radial positions. Figure 39 represents these Pdfs for axial positions varying between  $x/d = 1$  (in the potential core) till the bottom part of the reactor,  $x/d = 4$ . Pdfs are calculated:

- on the jet axis (red), for which very important values of  $Pdf(Z_m)$  are noted for  $Z_m = 0$  (unmixed fluid) at  $x/d = 1$  (top left figure). For further downstream positions, molecular mixing progressively improves and the Pdfs peak more and more towards values of  $Z_m = 1$  (nice aspect of micromixing).
- at a further radial position (violet), for which the shape of the Pdf is approximately the same whatever the axial position, and
- out of the potential core (blue) which reflects an improved mixing, better and better towards high values of  $x/d$ . Finally, while near the injection the Pdfs at different radial positions are strongly different as a sign of strong radial inhomogeneity, at  $x/d = 4$  the three Pdfs are much more similar, thus reflecting the good homogenisation of the molecular mixing.

### 11.3.2 The influence of Reynolds number and of the geometry on the molecularly mixed fluid fraction

One question addressed here is the effect of increasing Reynolds number, up to to  $Re_d = 16000$ , on the micromixing. Figure 40 represents three instantaneous images of molecularly mixed fluid fraction  $Z_m$  for the lowest Reynolds number  $Re_d = 6700$  (three top figures) and for the highest Reynolds number  $Re_d = 16000$  (three bottom figures). Both of them concern the same geometry, that of close shear jets ( $d = 1cm$ ). Two features are to be noted: first, at higher Reynolds number, the potential core (where the jet fluid is pure and micromixing is therefore completely absent) is longer, incursions of pure fluid are present till distances as large as  $x/d = 4$ . Second,

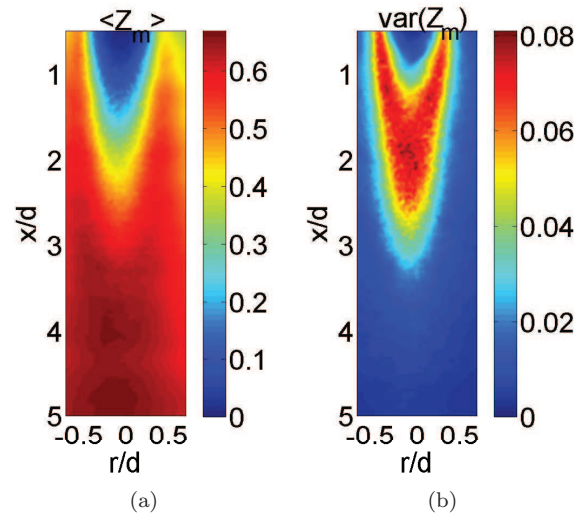
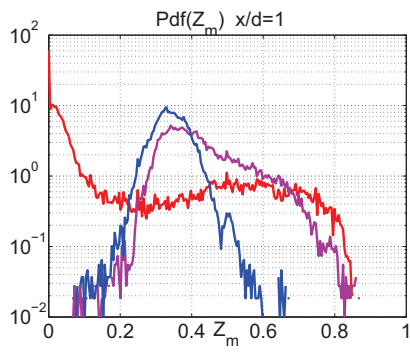


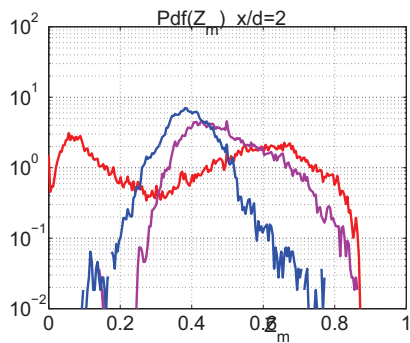
Figure 38: Average of fluid molecularly mixed (left) and variance of its fluctuations (right). Close sheared jets ( $Re = 6400$ )

micromixing on edges of potential core is more efficient and takes place at earlier values of  $x/d$ . This suggest that the volume of micromixed fluid increases for higher and higher Reynolds numbers (not shown here).

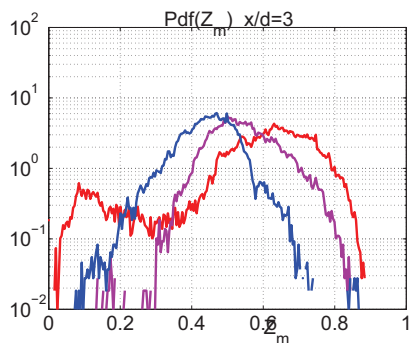
Better micromixing for larger Reynolds is emphasized by mean values of molecularly mixed fluid fraction  $\langle Z_m \rangle$ , which are illustrated on Figure 41 left, on the jet axis (solid lines) and at  $r/d = 0.25$  (dashed lines). The latter radial position corresponds to points within the shear layers, the intensity of the shear ( $\frac{\partial U}{\partial r}$ ) being much stronger for increasing Reynolds numbers. On the jets axis, increasing the Reynolds number corresponds to higher values of  $\langle Z_m \rangle$ , which are reached earlier. As an example, at  $x/d = 1$ ,  $\langle Z_m \rangle = 0.15$  for  $Re_d = 6700$ , while  $\langle Z_m \rangle = 0.2$  for  $Re_d = 16000$ . Moreover, in the shear layers situated on both edges of the potential core at  $r/d = 0.25$ , for a downstream position  $x/d = 0.5$  values of  $\langle Z_m \rangle$  are equal to 0.25 for the lower Reynolds and as high as 0.5 for the largest Reynolds. Qualitatively, the Pdfs of  $Z_m$  are similar to that earlier discussed for



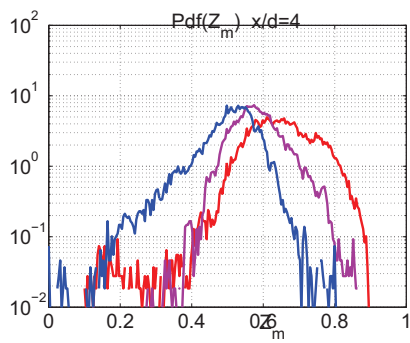
(a)



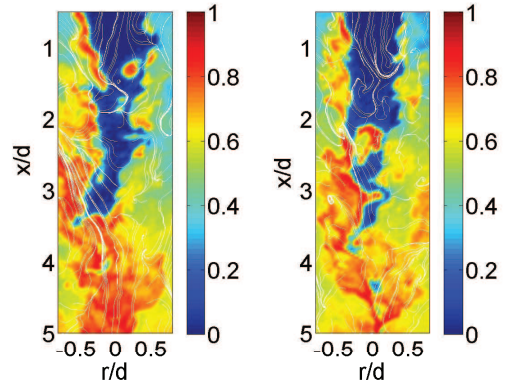
(b)



(c)

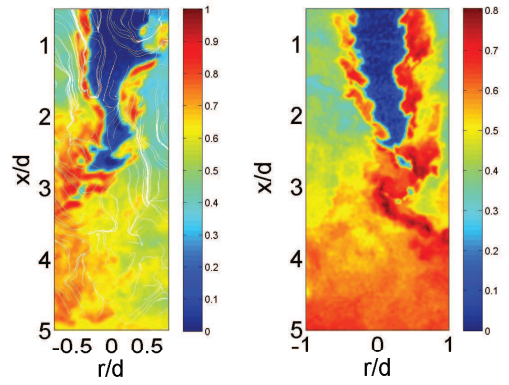


(d)



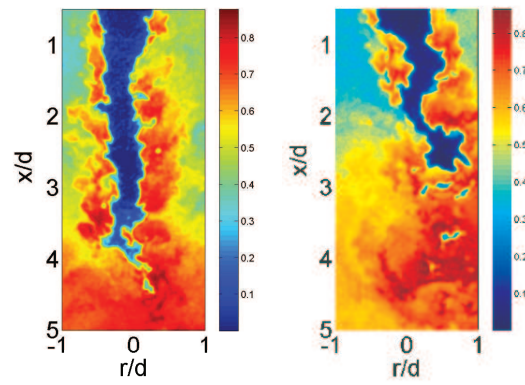
(a)

(b)



(c)

(d)



(e)

(f)

Figure 40: Instantaneous images of  $Z_m$  for close sheared jets for  $Re_d = 6400$  (three top) and  $Re_d = 16000$  (three bottom)

Figure 39:  $PDF(Z_m)$  for  $x/d = 1$  (top left),  $x/d = 2$  (top right),  $x/d = 3$  (bottom left) and  $x/d = 4$  (bottom right). Lines represent  $PDF(Z_m)$  at  $r/d = 0$  (red),  $r/d = 0.25$  (violet) and  $r/d = 0.5$  (blue). Close sheared jets ( $Re = 6400$ )

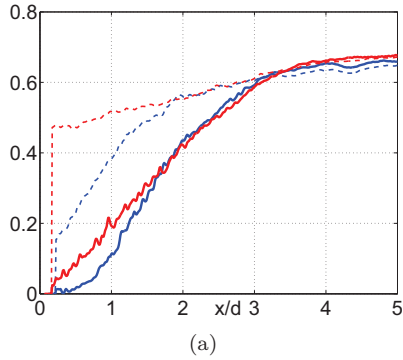


Figure 41: Evolution of  $\langle Z_m \rangle$  (left) and of  $var(Z_m)$  (right) as functions of the downstream position  $y/d$  on the jet axis (solid lines) and at  $r/d = 0.25$  (dashed lines).  $Re_d = 6400$  (blue) and  $Re_d = 16000$  (red)

$Re_d = 6700$ , with the clear distinction that higher values of  $Z_m$  are clearly privileged, and this is true for downstream positions as small as  $x/d = 0.5$ , for radial positions placed in the lateral shear layers. The connection between these properties and the local structure of the velocity field is certainly a subject to be presented in a near future. Note that an improved micromixing with increasing Reynolds, in the shear layers of a single round jet, was also emphasized by [6], over a wider range of Reynolds numbers.

Last, we test the influence of a slightly variable geometry on the micromixing efficiency. We choose to compare, at the same injection Reynolds number  $Re_d = 10700$ , values and characteristics of  $Z_m$ , for  $d = 1\text{cm}$  (close shear jets, illustrated on the top three instantaneous images on Figure 42) and for  $d = 0.6\text{cm}$  (far shear jets, see the last three instantaneous images on Figure 42). For far shear jets, the dimensions of the potential core are reduced, leaving more space to the molecularly mixed fluid. Therefore, micromixing is improved when the pure scalar is injected at smaller scales.

## 11.4 Conclusions

We investigated flow and micromixing in a Partially Stirred Reactor (PaSR) composed of 16 pairs of sheared jets. The typical pattern consists in a jet with counterflow. Dual-tracer planar laser-induced fluorescence (PLIF) and Particle image Velocimetry (PIV) techniques are used to quantify instantaneous distributions of macro and micro-mixing. The total fluid fraction  $Z$  was quantified by PLIF on acetone, whereas the pure fluid fraction was detected by PLIF on NO, quenched by oxygen ('cold chemistry'). Instantaneous images of  $Z$ ,  $Z_m$  and two-velocity field  $u$  and  $v$  were used to investigate mixing and in particular micromixing.

It was shown that micromixing is favored by either increasing injection Reynolds numbers, or injection by small diameters jets in comparison with the flow dimensions (small-scale injection).

We are grateful for the support of ANR 'Agence Nationale de Recherche' under the activity 'Micromélange' and 'ANISO'. Professor P.E. Dimotakis is warmly thanked for his contribution in the initial phase of this research.

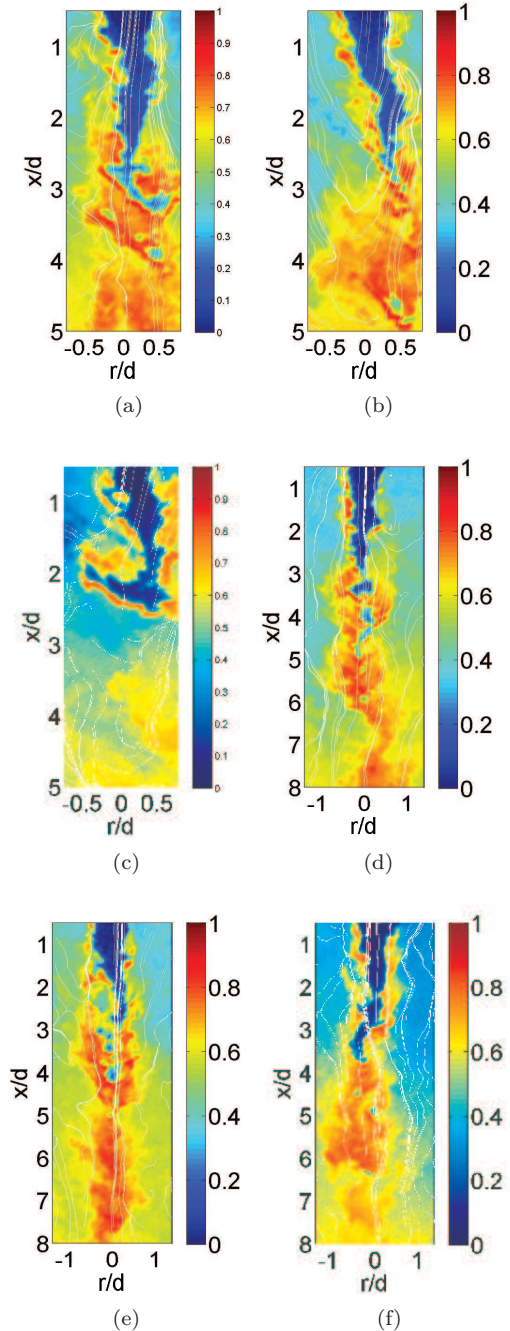


Figure 42: Instantaneous images of  $Z_m$  for far sheared jets, and  $Re_d = 10700$ . Injecting jet diameter  $d = 1\text{cm}$  (top three images) and  $d = 0.6\text{cm}$  (three bottom images)

## References

- [1] N.T. Clemens and P.H. Paul, "Scalar measurements in compressible axisymmetric mixing layers", *Phys. Fluids*, **Vol. 7**, No 5, pp. 1071-1081, (1995).
- [2] P.E. Dimotakis, "Turbulent mixing", *Ann. Rev. Fl. Mech.*, **Vol. 37**, pp. 329-356, (2005).
- [3] J. M. Foucaut, J. Carlier and M. Stanislas, "PIV optimization for the study of turbulent flow using spectral analysis", *Meas. Sci. Tech.*, **Vol. 8**, pp. 1427-1440, (2004).
- [4] H. Hu and M.M. Koochesfahani, "A novel method for instantaneous, quantitative measurement of molecular mixing in gaseous flows", *Exp. Fluids*, **Vol. 33**, No 1, pp. 202-209, (2002).
- [5] T.C. Island, W.D. Urban and M.G. Mungal, "Quantitative scalar measurements in compressible mixing layers", *34-th Aerospace Sciences Meeting and Exhibit, AIAA Paper*, Vol. 96, p. 0685, (1996).
- [6] G.F. King, J.C. Dutton and R.P. Lucht "Instantaneous, quantitative measurements of molecular mixing in the axisymmetric jet near field", *Opt. Letters*, **Vol. 22**, No 5, p. 633, (1997).
- [7] G.F. King, R.P. Lucht and J.C. Dutton, "Quantitative dual-tracer planar laser-induced fluorescence measurements of molecular mixing", *Opt. Letters*, **Vol. 22**, No. 5, p. 633, (1997).
- [8] J.F. Krawczynski, "La structure du champ de vitesse dans un réacteur jets opposés. Caractérisation du mélange turbulent", PhD Thesis, Université de Rouen, France, (2007).
- [9] J.F. Krawczynski, B. Renou, L. Danaïla and F. X. Demoulin, "Small-scale measurements in a Partially Stirred Reactor (PaSR)", *Exp. Fluids*, **Vol. 40**, pp. 667-682, (2006).
- [10] J.F. Krawczynski, B. Renou and L. Danaïla, "The structure of the velocity field in a confined flow driven by an array of opposed jets", *Phys. Fluids*, **Vol. 22**, pp. 045104, (2010).
- [11] T.R. Meyer, J.C. Dutton and R.P. Lucht, "Experimental study of the mixing transition in a gaseous axisymmetric jet", *Phys. Fluids*, **Vol. 13**, Vol. 11, pp. 3411-3424, (2001).
- [12] P.H. Paul and N.T. Clemens, "Sub-resolution flow-field measurements of unmixedness using electronic quenching of NO  $A^2\Sigma^+$ .", *Opt. Lett*, **Vol. 18**, pp. 161-163, (1993).

# THE GERMANY SOUTH PILOT CENTER REPORT

Stefan Becker : Coordinator of PC

*University Erlangen-Nuremberg*

*Inst. of Process Machinery and Systems Engineering, Cauerstr. 4, 91058 Erlangen*

*email : sb@ipat.uni-erlangen.de*

## 1 Introduction

The ERCOFTAC Pilot Centre Germany South was founded in 1991. It currently composes of twenty five members from university institutes, six members from industry, and two members from research centres.

The centre is coordinated by PD Dr. Stefan Becker from University Erlangen-Nuremberg since January 2011.

PD Stefan Becker represents the Pilot Centre in the Scientific Programme Committee and Dr. Florian Menter (ANSYS) represents the Pilot Centre in the Industrial Committee. Both are members of the Managing Board. Prof. Wolfgang Rodi (KIT), Prof. Suad Jakirlic (TU Darmstadt) and Dominic v. Terci (GE) are elected Members of the Executive Committee. In the committee Prof. Rodi is the responsible editor for the ERCOFTAC Knowledge Base Wikis. He is still one of the four editors of the ERCOFTAC Journal “Flow, Turbulence and Combustion” and also, together with Prof. Geurts, Series Editor of the ERCOFTAC Book Series. In the Executive Committee Prof. Jakirlic (TU Darmstadt) is the chairman of Horizon 10 and Dr. v. Terci (GE) is the Deputy Chairman of the Scientific Programme Committee. Also Dr. Menter (ANSYS) and Prof. Dreizler (TU Darmstadt) are advisory editors of the Journal “Flow, Turbulence and Combustion”.

## 2 Organizational structure

The Pilot Centre is organized in the following way. There is an annual meeting of the members which is called by the coordinator. All organizational issues of the PC are discussed and if needed voted on during these meetings. Typical participation in such meetings is about 20 member representatives.

## 3 Members

The members of the Pilot Centre are:

- Universities:

- Institute of Process Machinery and Systems Engineering, University of Erlangen-Nuremberg.
- Institute of Fluid Mechanics, University of Erlangen-Nuremberg.
- Institute of Thermodynamics, University of Erlangen-Nuremberg.
- Institute of Fluid Mechanics and Aerodynamics, Technical University Darmstadt.
- Institute of Energy and Power Plant Technology, Technical University Darmstadt.

- Institute of Numerical Methods in Mechanical Engineering, Technical University Darmstadt.
- Institute for Fluid Mechanics, Technical University Dresden.
- Interdisciplinary Center for Scientific Computing, University of Heidelberg.
- Goethe-Centre of Scientific Computing, Goethe University Frankfurt.
- Institute of Fluid Machinery, Karlsruhe Institute of Technology.
- Institute of Piston Machines, Karlsruhe Institute of Technology.
- Institute for Hydromechanics, Karlsruhe Institute of Technology.
- Institute of Thermal Turbomachines, Karlsruhe Institute of Technology.
- Institute for Fluid Mechanics, Karlsruhe Institute of Technology.
- Engler-Bunte Institute, Karlsruhe Institute of Technology.
- Institute for Nuclear and Energy Technologies, Karlsruhe Institute of Technology.
- Institute for Neutron Physics and Reactor Technology, Karlsruhe Institute of Technology.
- Institute of Nuclear Engineering and Energy Systems, University of Stuttgart.
- Institute of Thermal Turbomachinery and Machinery Laboratory, University of Stuttgart.
- Institute of Aero- and Gas Dynamics, University of Stuttgart.
- Institute for Hydromechanics, Technical University Munich.
- Institute of Thermodynamics, Technical University Munich.
- Institute of Aerodynamics and Fluid Mechanics, Technical University Munich.
- Institute of Thermodynamics, University of the Federal Armed Forces Munich.
- Institute of Fluid Mechanics and Aerodynamics, University of the Federal Armed Forces Munich.

- Research Centres:

- Institute of Combustion Technology, German Aerospace Centre DLR, Stuttgart.
- Institute of Technical Thermodynamics / Solar, German Aerospace Centre DLR, Stuttgart.

- Industry:

- ANSYS Germany GmbH, Otterfing.
- BASF AG, Ludwigshafen.
- Bosch GmbH, Stuttgart.
- GE Global Research, Munich.
- Festo AG, Esslingen
- Voith Hydro GmbH, Heidenheim.

## 4 Activities of the centre

### 4.1 Technology day

The main scientific event of the Pilot Centre is a Technology Day, which will take place this year on the 19th of October 2012 in Stuttgart for the eighth time. The meeting is organized together with Germany Pilot Centre North. During the event, members of the PC present their newest research results. The Technology Day is an open event and is widely advertised in Germany. It is also announced in the ERCOFTAC bulletin. The event finds wide-spread interest and attracted approx. 80 participants/year for the last seven years. Many of the participants are non-ERCOFTAC members, who are interested in this compact forum, which provides them with information on the many different research topics covered by our members. Most of the participants come from industry. In that respect, the Technology Day is a valuable opportunity for generating interest in ERCOFTAC beyond the well established contacts.

The success of the Technology Day depends crucially on the willingness of the PC members to participate with high-quality scientific presentations given mostly by institute leaders and senior staff members. For the last eight years, the members have contributed 10 presentations each year. The feedback from the participants has been very positive and it is planned to continue with the event.

### 4.2 Activities of the members

The members of the PC are actively engaged in a wide range of topics:

- General Fluid Mechanics / Aerodynamics / Hypersonics.
- Transition and Turbulence.
- Aeroacoustics.
- Fluid Structure Interaction
- Combustion Research.
- Gasdynamics.
- Multiphase Flows.
- Chemical Processes.
- Propulsion. .

### 4.3 Participation in special interest groups

Members of the centre coordinate and participate in the following Special Interest Groups:

- Large Eddy Simulation.
- Transition Modelling.

- Turbulence Modelling.
- Reactive Flows.
- Transition Mechanisms, Prediction and Control.
- Design Optimization.
- Aeroacoustics.
- Smoothed Particle Hydrodynamics.
- Fluid Structure Interaction.
- Uncertainty Quantification in Industrial Analysis and Design.

## 5 Research activities

The following selection of examples gives a short overview of the current research activities of the members in Pilot Centre Germany South.

### 5.1 Institute of Aerodynamics and Fluid Mechanics, Technical University Munich

The unsteady behavior in shockwave turbulent boundary layer interaction is investigated by analyzing results from a large eddy simulation of a supersonic turbulent boundary layer over a compression-expansion ramp. The interaction leads to a very-low-frequency motion near the foot of the shock, with a characteristic frequency that is three orders of magnitude lower than the typical frequency of the incoming boundary layer. Wall pressure data are first analyzed by means of Fourier analysis, highlighting the low-frequency phenomenon in the interaction region. Furthermore, the flow dynamics are analyzed by a dynamic mode decomposition which shows the presence of a low-frequency mode associated with the pulsation of the separation bubble and accompanied by a forward-backward motion of the shock (Figure 1).

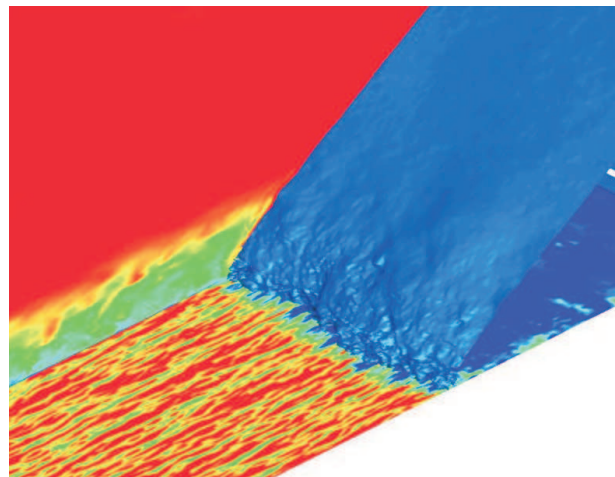


Figure 1: Instantaneous shock structure

More information: [christian.stemmer@tum.de](mailto:christian.stemmer@tum.de)

## 5.2 Institute of Fluid Mechanics, Technical University Dresden

The research activities of the institute are hence extremely vast, covering experimental as well as numerical approaches on different levels. A representative project, conducted at the Chair of Fluid Mechanics, is concerned with the modeling and simulation of particle-laden flows by immersed boundary methods. After recognizing that existing collision models do not yield satisfactory results in collision-dominated cases, it was developed an own approach, termed Adaptive Collision Model. It covers normal as well as oblique collisions of particles with walls as well as between two particles and assembles several components: a stretching factor in time together with an optimization procedure that maintains the restitution coefficient, a lubrication model for gap sizes below the grid spacing, and an adaptive determination of tangential forces so as to yield the appropriate tangential motion for given surface properties and collision angles. The figure below shows a result for the normal collision of a Teflon bead on glass. The new model is currently used in large scale simulations of dense particle-laden flows where it yields improved results compared to other models (Figure 2).

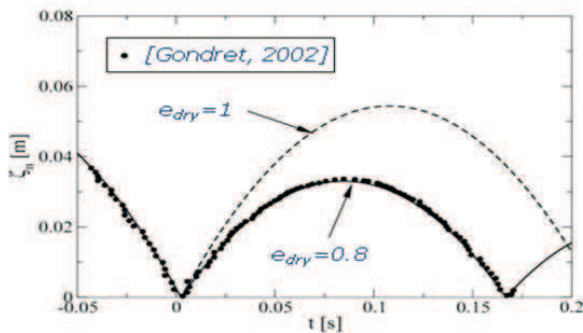


Figure 2: Teflon bead impacting on glass wall

More information: [jochen.froehlich@tu-dresden.de](mailto:jochen.froehlich@tu-dresden.de)

## 5.3 Institute of Aero- and Gasdynamics, University of Stuttgart

So-called jet-in-crossflow configurations, where an isolated jet is injected into the boundary layer close to a flat plate, are fundamental for a better understanding of flow control. Researchers at the Institute of Aero- and Gasdynamics of the Stuttgart University are performing DNS of various cases for low to moderate Mach numbers and several jet angles with respect to the cross flow. Proper Orthogonal Decomposition (POD) and Dynamic Mode Decomposition (DMD) are used to extract and understand the relevant flow motions depending on configuration. The aim of this research is to contribute to a better understanding and prediction of the different unsteady dynamics depending on the configuration. The latter influences the route to turbulence in the free stream and the separation-, mixing-, and re-attachment-characteristics at the wall. A better understanding will help to improve different applications where either a better mixing, e.g. of fuel with the crossflow, or a delay of boundary-layer separation or film cooling is required (Figure 3).

More information: [rist@iag.uni-stuttgart.de](mailto:rist@iag.uni-stuttgart.de)

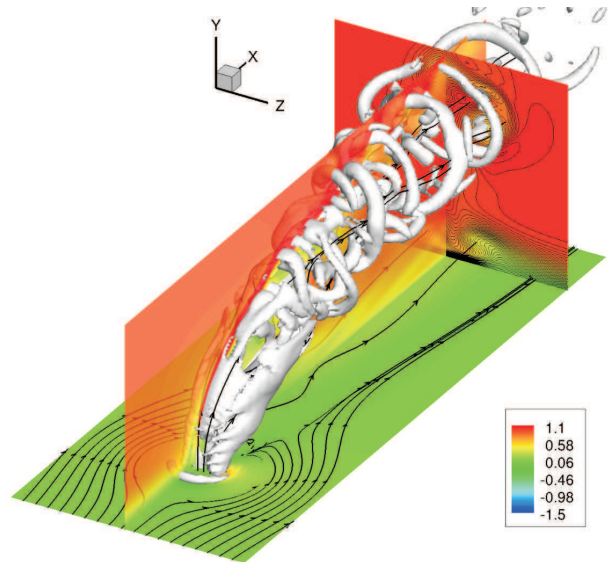


Figure 3: Jet-in-crossflow configurations

## 5.4 Institute of Thermal Turbomachinery and Machinery Laboratory, University of Stuttgart

Today steam turbine power plants produce about for 70% of the world wide electrical power. Beside fossil fuels other heat sources such as biomass, geothermal or solar-thermal energy can also be used to vaporize the working fluid, so that steam turbines will retain their important role even in an environment with renewable energy sources. Already in the low pressure part of the turbine the steam reaches saturated conditions and water droplets are formed, even before the condenser is reached. At the outlet of the turbine 8% to 16% wetness exists which leads to enhanced corrosion, droplet erosion of the blades and additional energy dissipation. A research project at the Institute of Thermal Turbomachinery and Machinery Laboratory focuses on the simulation of this complex 3D transonic two-phase flow. The aim is to provide a reliable numerical method which can be used to improve condensing turbine flows. An estimation of the important thermodynamic dissipation during phase change has already been reached within the project. The influence of friction between the droplets and the vapor phase is a future research topic as well as the prediction of droplet deposition on steam turbine blades.

More information: [starzmann@itsm.uni-stuttgart.de](mailto:starzmann@itsm.uni-stuttgart.de)

## 5.5 Institute of Hydrodynamics, Karlsruhe Institute of Technology

Fluid flow with suspended solid particles is encountered in a multitude of natural and industrial processes. Examples include the motion of sediment particles in rivers, fluidized beds and blood flow. Despite the great technological importance of these systems our understanding of the dynamics of fluid-particle interaction is still incomplete at the present date. Recently, however, significant progress has been made based on data provided by new experimental methods as well as numerical simulations. While most past investigations of numerical type have been performed in the context of the point-particle approach, it has now become possible to simulate the motion of a considerable number of finite-size particles

including an accurate description of the surrounding flow field on the particle scale. Although the complexity of recent particle-resolved simulations (in terms of Reynolds number, number of particles and computational domain size) is still limited, new insight into the physics of fluid-particle systems is beginning to emerge from such studies. We have simulated turbulent flow in a vertically-oriented plane channel seeded with heavy spherical particles with a diameter corresponding to approximately 11 viscous (near-wall) turbulent length scales at a solid volume fraction of 0.4%. The pressure-driven upward flow (at constant flow rate) is found to be strongly modified due to the particle presence, with increased wall-shear stress and strongly enhanced turbulence intensity. The average relative flow, corresponding to a Reynolds number (based on particle diameter) of approximately 135, leads to the establishment of wakes behind individual particles. The accumulated data-base has been analyzed w.r.t. a number of derived statistical quantities. Some of these are: Voronoi analysis of the spatial structure of the dispersed phase; the statistics of particle acceleration; particle-conditioned averaging of the fluid flow field. We expect the data to be of further value for modeling purposes in the future (Figure 4).

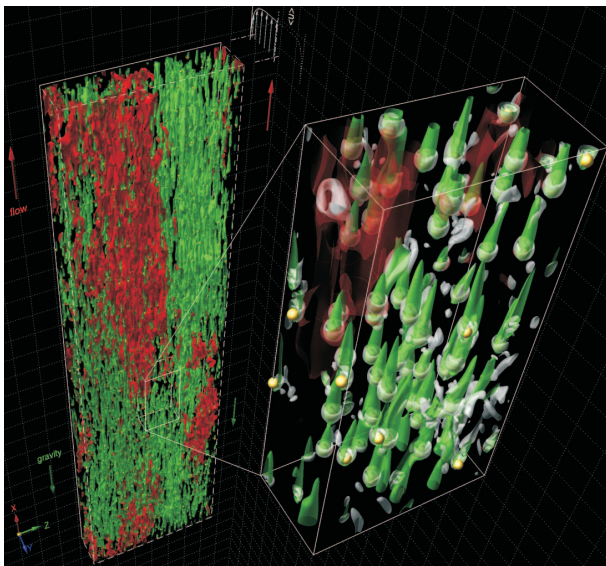


Figure 4: Particle-laden vertical channel flow simulation with interface resolution. Shown are flow structures of high (red) and low (green) streamwise velocity, intense vortex structures (grey) and particle locations (yellow)

More information: [markus.uhlmann@kit.edu](mailto:markus.uhlmann@kit.edu)

## 5.6 Engler-Bunte-Institute, Combustion Division, Karlsruhe Institute of Technology

Three-dimensional Direct Numerical Simulations of lean premixed methane and hydrogen flames and their interaction with turbulent eddies are investigated. The reaction mechanism for methane contains 16 species and 35 elementary reactions, and the mechanism for hydrogen contains 9 species and 37 reactions. The computer code is PARCOMB-3D, obtained in cooperation with Prof. D. Thévenin, University of Magdeburg. It solves the Navier-Stokes equations together with energy- and species conservation equations for a compressible reacting gas mixture. The method uses explicit fourth order Runge-Kutta time stepping on orthogonal grids

and a sixth order central difference scheme in space. The physical cases investigated comprise flame-vortex interactions of different vortex structures (variable number, shape, size and vorticity) with differently curved flame surfaces. Results are evaluated in terms of speed decomposition, curvature, strain rate, surface density function and reaction rates. Verification with experimental data shows good agreement. Modeling assumptions regarding various data correlations are tested and developed.

More information: [Jordan.Denev@kit.edu](mailto:Jordan.Denev@kit.edu)

## 5.7 Institute of Thermodynamics, Technical University Munich

Thermo-acoustic instabilities with significant amplitudes may arise in combustion chambers of gas turbines or aero-engines. Their presence may lead to limitations of operating conditions or, in severe cases, to damage of combustion chamber hardware. To prevent combustion chamber operations from unstable conditions, predictive methodologies are sought for. The Institute of Thermodynamics, Technical University Munich works in a number of projects on predictive methods, which take into account the complex coupling mechanisms between acoustics, flow and flame dynamics. In addition, acoustic dissipation or amplification, occurring through interaction processes with the mean flow and thermodynamic conditions, are either not captured at all or modeled rather coarsely. State of the art methods, which consider details of combustion chamber geometry, are based on linearized Navier-Stokes or Euler equations. After transformation into frequency space, an eigenvalue problem results, which is solved numerically via a Semi-implicit restarted Arnoldi algorithm. To gain knowledge about the robustness and predictive capabilities of the linearized equations, these are first solved for generic configurations, e.g. an area-expansion or orifice. In a next step, the complexity is increased. An experimental test case is constructed in the present project, including an aero-engine flame. The numerical method is validated on this test case with respect to the frequencies of instabilities and their respective growth rates.

More information: [polifke@td.mw.tum.de](mailto:polifke@td.mw.tum.de)

## 5.8 Institute for Nuclear Technology and Energy Systems, University of Stuttgart

For the analysis and design of efficient energy systems the accurate prediction of the wall-shear stress and the heat-transfer coefficient for pipe and channel flows at super-critical pressure ( $>22.1$  MPa) is needed. In circular pipe flows a numerical model based on the one-dimensional conservation equations of mass, momentum and energy has been developed, based on the algebraic approach of Prandtl/van-Karman, including a model for the buffer layer. The influence of wall roughness is taken into account by a new modified numerical damping function of the turbulence model. The thermo-hydraulic properties of super-critical water are implemented according to the international standard. An extensive validation of the method with comparison of model results with experiments in a wide range of flow parameters has been performed. It can accurately predict the wall temperature even under deterioration

conditions, where the heat transfer coefficient depends nonlinearly on the wall heat flux. The wall-roughness height is identified as an important model parameter. The model will be extended to flow of super-critical CO<sub>2</sub>.

More information: [laurien@ike.uni-stuttgart.de](mailto:laurien@ike.uni-stuttgart.de)

## 5.9 Institute of Engineering Thermodynamics, University Erlangen-Nuremberg

For many years the interaction of electric fields with flames is well known and many investigations on electric field assisted combustion have been carried out to understand the ongoing processes. For technical applications flame stabilization and the reduction of the pollutant emissions such as carbon monoxide (CO) and nitrogen oxides (NO<sub>x</sub>) are the most convenient effects of weak electric fields. Especially for premixed flames, a significant increase in flame stability can be achieved by applying a longitudinal electric field towards the burner. In a current Deutsche Forschungsgemeinschaft (DFG) funded project, fundamental studies were performed in laminar premixed flames to clarify the underlying mechanisms. For a detailed insight into the ongoing processes laser based measurement techniques were applied such as laser-induced fluorescence (LIF) for flame front tracking and particle image velocimetry to analyze the resulting flow field. The measurements show a strong flow deceleration in the order of 0.8 to 1.6 m/s in the postoxidation zone at supply voltages of 6 kV which is responsible for the flame deformation especially at the flame root point. This confirms the dominance of electro-hydrodynamic effects, i.e. a momentum transfer by charge carriers produced in the flame front (ionic wind) whereas no significant change in the flame chemistry was observed. In transient electric fields the flame behavior was measured showing response time of few milliseconds (2-4 ms) which also makes electric fields applicable for suppressing thermo-acoustic oscillations in technical burner systems (Figure 5).

More information: [alfred.leipertz@lft.uni-erlangen.de](mailto:alfred.leipertz@lft.uni-erlangen.de)

## 5.10 Institute of Process Machinery and Systems Engineering, University of Erlangen-Nuremberg

Aeroacoustically generated sound is a common phenomenon in engineering applications. Examples range from noise generated by turbo machinery, over automotive aerodynamically noise to sound production in pipe systems. Numerical simulation can help to provide a deeper understanding of the physics involved. Today a wide range of numerical approaches exists to simulate turbulent flows and the propagation of sound. Especially in low Mach-number flows, hybrid approaches are very often used to compute the flow in a first step. Based on the flow information aeroacoustic source terms are calculated. In a second step the propagation of the sound is computed based on acoustic analogies or linearized transport equations. Since the acoustic calculation can be seen as a post-processing step within this hybrid approach, the quality of the flow field and the aeroacoustic source terms is crucial to the process. Numerical simulation of the flow over a forward-facing step with a Reynolds number of 8000 based on the step height has

been carried out (Figure 6). Calculations were performed using second order finite volume discretization in space on co-located meshes. The simulation results are used

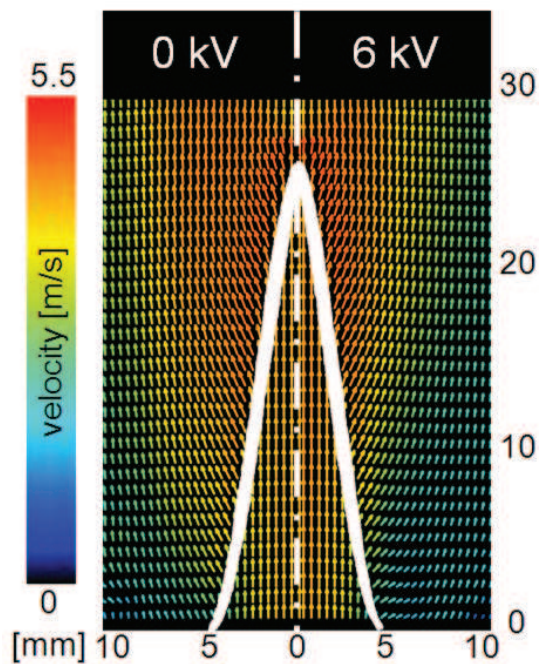


Figure 5: Premixed Bunsen Flame without (0 kV, left half image) and with electric field (6 kV, right), positively charged electrode is positioned above the flame; flame front (white colour) is calculated from CH<sub>2</sub>O and OH-LIF distributions

as a basis for the validation of different discretization schemes and simulation approaches for the calculation of sound using a hybrid approach. Turbulent statistics were predicted along with acoustic source regions. Also the data management for this simulation on a highly parallel system is carried out together with the hybrid calculation approach based on Lighthill's acoustic analogy implemented in a finite element framework. In summary the investigations deliver a data basis for the assessment of the quality of simulated flow induced acoustic sources.

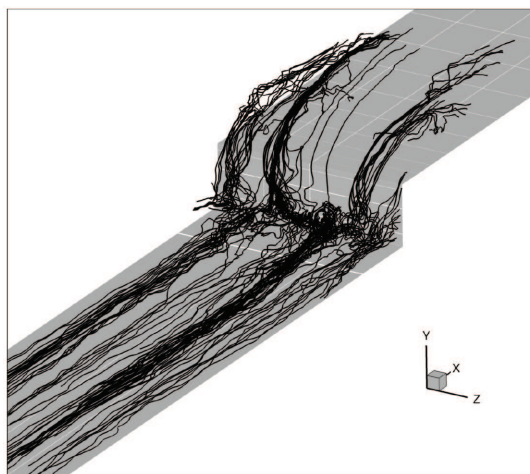


Figure 6: Streamtrace for flow over forward facing step

More information: [christoph.scheit@ipat.uni-erlangen.de](mailto:christoph.scheit@ipat.uni-erlangen.de)

## *ERCOFTAC Workshops and Summer Schools*

<b>Title</b>	<b>Location</b>	<b>Date</b>	<b>Organisers</b>	<b>Email addresses</b>
CFD for dispersed multi-phase flows (course)	Graz, Austria	18/07/2012 - 19/07/2012	Sommerfeld, M.	Stephane.Bongaerts@ercofac.org AdmMgr-ercofac@live.com richard.seoud-ieo@ercofac.org
15th meeting of ERCOFTAC's Nordic Pilot Centre	Porvoo, Finland	28/08/2012 - 29/08/2012	Hämäläinen, J.	jari.hamalainen@lut.fi
3rd International workshop on the turbulent combustion of sprays	Rottmannsaal, Heidelberg-Handschuhsheim, Germany	2/09/2012	Gutheil, E. Masri, A. R. Mastorakos, E. Merci, B. Raman, V. Roekaerts, D. Sadiki, A.	gutheil@iwr.uni-heidelberg.de assaad.masri@sydney.edu.au em257@eng.cam.ac.uk bart.merci@ugent.be v.raman@mail.utexas.edu d.j.e.m.roekaerts@tudelft.nl sadiki@ekt.tu-darmstadt.de
9 <sup>th</sup> European fluid mechanics conference	Rome, Italy	9/09/2012 - 13/09/2012	Verzicco, R.	verzicco@uniroma2.it
13 <sup>th</sup> Workshop on two-phase flow predictions	Halle, Germany	17/09/2012 - 20/09/2012	Sommerfeld, M.	martin.sommerfeld@iw.uni-halle.de
20 <sup>th</sup> Polish national fluid dynamics conference	Gliwice, Poland	17/09/2012 - 20/09/2012	Wroblewski, W. Drobniaak, S.	wlodzimierz.wroblewski@polsl.pl drobniaak@imc.pcz.czest.pl
Coronary arterial and microvascular fluid-structure interactions: evolving concepts and investigative approaches	London, UK	17/09/2012	Kilner, P.	richard.seoud-ieo@ercofac.org AdmMgr-ercofac@live.com
Computational aeroacoustics (course)	Munich, Germany	30/10/2012 - 31/10/2012	Bailly, C.	richard.seoud-ieo@ercofac.org
Unsteady Separation in Fluid-Structure Interaction	Mykonos, Greece	17/06/2013 - 22/06/2013	Braza, M. Bottaro, A.	marianna.braza@imft.fr alessandro.bottaro@unige.it

---

# ERCOFTAC Special Interest Groups

---

## 1. Large Eddy Simulation

Geurts, B.J.  
University of Twente, Holland.  
Tel: +31 53 489 4125  
[b.j.geurts@math.utwente.nl](mailto:b.j.geurts@math.utwente.nl)

## 4. Turbulence in Compressible Flows

Comte, P.  
University of Poitiers, France.  
Tel: +33 5 49 36 60 11  
Fax: +33 5 49 36 60 01  
[Pierre.comte@tea.univ-poitiers.fr](mailto:Pierre.comte@tea.univ-poitiers.fr)

## 5. Environmental CFD

Armenio, V.  
Università di Trieste, Italy.  
Tel: +39 040 558 3472  
Fax: +39 040 572 082  
[vi.armenio@gmail.com](mailto:vi.armenio@gmail.com)

## 10. Transition Modelling

Dick, E.,  
University of Gent, Belgium.  
Tel: +32 9 264 3301  
Fax: +32 9 264 3586  
[erik.dick@ugent.be](mailto:erik.dick@ugent.be)

## 12. Dispersed Turbulent Two Phase Flows

Sommerfeld, M.  
Martin-Luther University, Germany.  
Tel: +49 3461 462 879  
Fax: +49 3461 462 878  
[martin.sommerfeld@iw.uni-halle.de](mailto:martin.sommerfeld@iw.uni-halle.de)

## 14. Stably Stratified and Rotating Flows

Redondo, J.M.  
UPC, Spain.  
Tel: +34 93 401 7984  
Fax: +34 93 401 6090  
[Redondo@fa.upc.es](mailto:Redondo@fa.upc.es)

## 15. Turbulence Modelling

Jakirlic, S.  
Darmstadt University of Technology,  
Germany.  
Tel: +49 6151 16 3554  
Fax: +49 6151 16 4754  
[s.jakirlic@sla.tu-darmstadt.de](mailto:s.jakirlic@sla.tu-darmstadt.de)

## 20. Drag Reduction and Flow Control

Choi, K-S.  
University of Nottingham, England.  
Tel: +44 115 9513 792  
Fax: +44 115 9513 800  
[kwing-so-choi@nottingham.ac.uk](mailto:kwing-so-choi@nottingham.ac.uk)

## 24. Variable Density Turbulent Flows

Anselmet, F.  
IMST, France.  
Tel: +33 4 91 505 439  
Fax: +33 4 91 081 637  
[fabian.anselmet@irphe.univ-mrs.fr](mailto:fabian.anselmet@irphe.univ-mrs.fr)

## 28. Reactive Flows

Tomboulides, A.  
Aristotle University of Thessaloniki,  
Greece.  
Tel: +30 2310 991 306  
Fax: +30 2310 991 304  
[ananiast@enman.auth.gr](mailto:ananiast@enman.auth.gr)

## 32. Particle Image Velocimetry

Stanislas, M.  
Ecole Centrale de Lille, France.  
Tel: +33 3 20 337 170  
Fax: +33 3 20 337 169  
[stanislas@ec-lille.fr](mailto:stanislas@ec-lille.fr)

## 33. Transition Mechanisms, Prediction and Control

Hanifi, A.  
FOI, Sweden.  
Tel: +46 8 5550 4334  
Fax: +46 8 5550 3481  
[ardeshir.hanifi@foi.se](mailto:ardeshir.hanifi@foi.se)

## 34. Design Optimisation

Giannakoglou, K.  
NTUA, Greece.  
Tel: +30 210 772 1636  
Fax: +30 210 772 3789  
[kgianna@central.ntua.gr](mailto:kgianna@central.ntua.gr)

## 35. Multipoint Turbulence Structure and Modelling

Cambon, C.  
ECL Ecully, France.  
Tel: +33 4 72 186 161  
Fax: +33 4 78 647 145  
[claude.cambon@ec-lyon.fr](mailto:claude.cambon@ec-lyon.fr)

## 36. Swirling Flows

Braza, M.  
IMFT, France.  
Tel: +33 5 61 285 839  
Fax: +33 5 61 285 899  
[braza@imft.fr](mailto:braza@imft.fr)

## 37. Bio-Fluid Mechanics

Poelma, C.  
Delft University of Technology, Holland.  
Tel: +31 15 278 2620  
Fax: +31 15 278 2947  
[c.poelma@tudelft.nl](mailto:c.poelma@tudelft.nl)

## 38. Micro-thermofluidics

Borhani, N.  
EPFL, Switzerland.  
Tel: +41 21 693 3503  
Fax: +41 21 693 5960  
[navid.borhani@epfl.ch](mailto:navid.borhani@epfl.ch)

## 39. Aeroacoustics

Bailly, C.  
Ecole Centrale de Lyon, France.  
Tel: +33 4 72 186 014  
Fax: +33 4 72 189 143  
[christophe.bailly@ec-lyon.fr](mailto:christophe.bailly@ec-lyon.fr)

## 40. Smoothed Particle Hydrodynamics

Le Touzé, D.  
Ecole Centrale de Nantes, France.  
Tel: +33 2 40 37 15 12  
[david.letouze@ec-nantes.fr](mailto:david.letouze@ec-nantes.fr)

## 41. Fluid Structure Interaction

Longatte, E.  
EDF, France.  
Tel: +33 1 30 87 80 87  
Fax: +33 1 30 87 77 27  
[elisabeth.longatte@edf.fr](mailto:elisabeth.longatte@edf.fr)

## 42. Synthetic Models in Turbulence

Nicolleau, F.  
University of Sheffield, England.  
Tel: +44 114 22 27867  
Fax: +44 114 22 27890  
[f.nicolleau@sheffield.ac.uk](mailto:f.nicolleau@sheffield.ac.uk)

## 43. Fibre Suspension Flows

Hämäläinen, J.  
Lappeenranta University of Technology,  
Finland.  
Tel: +358 40 596 1999  
[jari.hamalainen@lut.fi](mailto:jari.hamalainen@lut.fi)

## 44. Fundamentals and Applications of Fractal Turbulence

Fortune, V.  
Université de Poitiers, France.  
Tel: +33 5 49 45 40 44  
Fax: +33 5 49 45 36 63  
[veronique.fortune@lea.univ-poitiers.fr](mailto:veronique.fortune@lea.univ-poitiers.fr)

## 45. Uncertainty Quantification in Industrial Analysis and Design

Meyers, J.  
Katholieke Universiteit Leuven, Belgium.  
Tel: +32 16 322 502  
Fax: +32 16 322 985  
[johan.meyers@mech.kuleuven.be](mailto:johan.meyers@mech.kuleuven.be)

---

---

## ERCOFTAC Pilot Centres

---

### Alpe – Danube – Adria

Reichl, C.  
Austrian Institute of Technology,  
Giefinggasse 2,  
A-1210 Wien,  
Austria.  
Tel: +43 1 50550 6605  
Fax: +43 1 50550 6439  
[christoph.reichl@arsenal.ac.at](mailto:christoph.reichl@arsenal.ac.at)

### Belgium

Geuzaine, P.  
Cenaero,  
CFD Multi-physics Group,  
Rue des Frères Wright 29,  
B-6041 Gosselies,  
Belgium.  
Tel: +32 71 919 334  
[philippe.geuzaine@cenaero.be](mailto:philippe.geuzaine@cenaero.be)

### Czech Republic

Bodnar, T.  
Institute of Thermomechanics AS CR,  
5 Dolejskova,  
CZ-18200 Praha 8,  
Czech Republic.  
Tel: +420 224 357 548  
Fax: +420 224 920 677  
[bodnar@marian.fsik.cvut.cz](mailto:bodnar@marian.fsik.cvut.cz)

### France – Henri Bénard

Cambon, C.  
Ecole Centrale de Lyon.  
LMFA,  
B.P. 163,  
F-69131 Ecully Cedex,  
France.  
Tel: +33 4 72 18 6161  
Fax: +33 4 78 64 7145  
[claude.cambon@ec-lyon.fr](mailto:claude.cambon@ec-lyon.fr)

### France South

Braza, M.  
IMF Toulouse,  
CNRS UMR – 5502,  
Allée du Prof. Camille Soula 1,  
F-31400 Toulouse Cedex,  
France.  
Tel: +33 5 61 28 5839  
Fax: +33 5 61 28 5899  
[marianna.braza@imft.fr](mailto:marianna.braza@imft.fr)

### France West

Comte, P.  
Université de Poitiers,  
CEAT/LEA  
F-86036 Poitiers Cedex,  
France.  
Tel: +33 5 49 36 60 11  
Fax: +33 5 49 36 60 01  
[Pierre.comte@tea.univ-poitiers.fr](mailto:Pierre.comte@tea.univ-poitiers.fr)

### Germany North

Gauger, N.R.  
CCES,  
RWTH Aachen University,  
Schinkelstr. 2,  
D-52062 Aachen,  
Germany.  
Tel: +49 241 80 98 660  
Fax: +49 241 80 92 600  
[gauger@mathcces.rwth-aachen.de](mailto:gauger@mathcces.rwth-aachen.de)

### Germany South

von Terzi, D.  
Inst. Thermische Strömungsmaschinen,  
Universität Karlsruhe (TH),  
Kaiserstr. 12 (Geb. 10.91, Zi. 201)  
D-76131 Karlsruhe,  
Germany.  
Tel: +49 721 608 6829  
[vonterzi@its.uni-karlsruhe.de](mailto:vonterzi@its.uni-karlsruhe.de)

### Greece

Papailiou, K.D.  
National Tech. University of Athens,  
Laboratory of Thermal Turbomachines,  
9 Iroon Polytechniou,  
P.O. Box 64069,  
Gr-15710 Athens,  
Greece.  
Tel: +30 210 772 1634  
Fax: +30 210 772 1658  
[kpapail@lnt.ntua.gr](mailto:kpapail@lnt.ntua.gr)

### Iberian East

Onate, E.  
Universitat Politecnica de Catalunya,  
Edificio C-1, Campus Norte,  
Gran Capitan s/n,  
E-08034 Barcelona,  
Spain.  
Tel: +34 93 401 6035  
Fax: +34 93 401 6517  
[onate@cimne.upc.es](mailto:onate@cimne.upc.es)

### Iberian West

Theofilis, V.  
Universidad Politécnica de Madrid,  
Plaza Cardenal Cisneros 3,  
E-28040 Madrid,  
Spain.  
Tel: +34 91 336 3291  
Fax: +34 91 336 6371  
[vassilis@torroja.dmt.upm.es](mailto:vassilis@torroja.dmt.upm.es)

### Italy

Martelli, F.  
University of Florence,  
Department of Energy,  
Via Santa Marta 3,  
I-50139 Firenze, Italy.  
Tel: +39 055 479 6237  
Fax: +39 055 479 6342  
[francesco.martelli@unifi.it](mailto:francesco.martelli@unifi.it)

### Netherlands

Ooms, G.  
J.M. Burgerscentrum,  
Research School for Fluid Mechanics,  
Mekelweg 2,  
NL-2628 CD Delft,  
Netherlands.  
Tel: +31 15 278 1176  
Fax: +31 15 278 2979  
[g.ooms@wbmt.tudelft.nl](mailto:g.ooms@wbmt.tudelft.nl)

### Nordic

Wallin, S.  
Swedish Defence Research Agency FOI,  
Computational Physics,  
S-16490 Stockholm,  
Sweden.  
Tel: +46 8 5550 3184  
Fax: +46 8 5550 3062  
[stefan.wallin@foi.se](mailto:stefan.wallin@foi.se)

### Poland

Rokicki, J.  
Warsaw University of Technology,  
Inst. of Aeronautics & Applied Mechanics,  
ul. Nowowiejska 24,  
PL-00665 Warsaw,  
Poland.  
Tel: +48 22 234 7444  
Fax: +48 22 622 0901  
[jack@meil.pw.edu.pl](mailto:jack@meil.pw.edu.pl)

### Switzerland

Jenny, P.  
ETH Zürich,  
Institute of Fluid Dynamics,  
Sonneggstrasse 3, ML H 38,  
CH-8092 Zürich,  
Switzerland.  
Tel: +41 44 632 6987  
Fax: +41 44 632 1147  
[jenny@ifd.mavt.ethz.ch](mailto:jenny@ifd.mavt.ethz.ch)

### United Kingdom

Barton, I.  
BAE Systems,  
ATC – Sowerby, FPC 267,  
P.O. Box 5,  
Bristol BS34 7QW,  
England.  
Tel: +44 117 302 8251  
Fax: +44 117 302 8007  
[iain.barton@baesystems.com](mailto:iain.barton@baesystems.com)

---



# Best Practice Guidelines for Computational Fluid Dynamics of Dispersed Multi-Phase Flows

## Editors

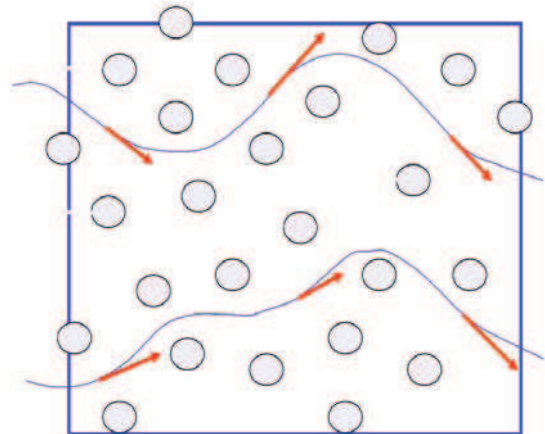
Martin Sommerfeld, Berend van Wachem  
&  
René Oliemans

The simultaneous presence of several different phases in external or internal flows such as gas, liquid and solid is found in daily life, environment and numerous industrial processes. These types of flows are termed multiphase flows, which may exist in different forms depending on the phase distribution. Examples are gas-liquid transportation, crude oil recovery, circulating fluidized beds, sediment transport in rivers, pollutant transport in the atmosphere, cloud formation, fuel injection in engines, bubble column reactors and spray driers for food processing, to name only a few. As a result of the interaction between the different phases such flows are rather complicated and very difficult to describe theoretically. For the design and optimisation of such multiphase systems a detailed understanding of the interfacial transport phenomena is essential. For single-phase flows Computational Fluid Dynamics (CFD) has already a long history and it is nowadays standard in the development of air-planes and cars using different commercially available CFD-tools.

Due to the complex physics involved in multiphase flow the application of CFD in this area is rather young. These guidelines give a survey of the different methods being used for the numerical calculation of turbulent dispersed multiphase flows. The Best Practice Guideline (BPG) on Computational Dispersed Multiphase Flows is a follow-up of the previous ERCOFTAC BPG for Industrial CFD and should be used in combination with it. The potential users are researchers and engineers involved in projects requiring CFD of (wall-bounded) turbulent dispersed multiphase flows with bubbles, drops or particles.

## Table of Contents

1. Introduction
2. Fundamentals
3. Forces acting on particles, droplets and bubbles
4. Computational multiphase fluid dynamics of dispersed flows
5. Specific phenomena and modelling approaches
6. Sources of errors
7. Industrial examples for multiphase flows
8. Checklist of 'Best Practice Advice'
9. Suggestions for future developments



Copies of the Best Practice Guidelines can be acquired electronically from the ERCOFTAC website:

[www.ercoftac.org](http://www.ercoftac.org)

Or from:

ERCOFTAC CADO  
Crown House  
72 Hammersmith Road  
London W14 8TH, United Kingdom

Tel: +44 207 559 1429

Fax: +44 207 559 1428

Email: [Richard.Seoud-ieo@ercoftac.org](mailto:Richard.Seoud-ieo@ercoftac.org)

The price per copy (not including postage) is:

### ERCOFTAC members

First copy	Free
Subsequent copies	45 Euros
Students	30 Euros

Non-ERCOFTAC academics	90 Euros
Non-ERCOFTAC industrial	180 Euros